THE UNIVERSITY OF CALGARY

A Six Degree of Freedom Goniometer for the Rabbit Knee

by

Daren Paul Tremaine

A THESIS

SUBMITTED TO THE FACULTY OF GRADUATE STUDIES

IN PARTIAL FULFILLMENT OF THE REQUIREMENTS FOR THE

DEGREE OF MASTER OF SCIENCE

DEPARTMENT OF CIVIL ENGINEERING

CALGARY, ALBERTA

JANUARY, 1997

The author has granted a non-exclusive licence allowing the National Library of Canada to reproduce, loan, distribute or sell copies of his/her thesis by any means and in any form or format, making this thesis available to interested persons.

L'auteur a accordé une licence non exclusive permettant à la Bibliothèque nationale du Canada de reproduire, prêter, distribuer ou vendre des copies de sa thèse de quelque manière et sous quelque forme que ce soit pour mettre des exemplaires de cette thèse à la disposition des personnes intéressées.

The author retains ownership of the copyright in his/her thesis. Neither the thesis nor substantial extracts from it may be printed or otherwise reproduced with the author's permission.

L'auteur conserve la propriété du droit d'auteur qui protège sa thèse. Ni la thèse ni des extraits substantiels de celle-ci ne doivent être imprimés ou autrement reproduits sans son autorisation.

0-612-20887-7

Canada

ABSTRACT

This thesis involves the design, construction, and testing of a six degree of freedom goniometer for the rabbit knee. This device will allow researchers to gather *in vivo* kinematic data regarding the position of the bones in the knee. The project included the calibration of the goniometer, and the development of a system of transformation equations for converting the output data into a useful form.

To evaluate the goniometer's potential for biomechanical testing, a preliminary investigation was conducted into the force on the medial collateral ligament (MCL), versus tibial rotation. The force was measured using a load cell developed at the University of Calgary. The testing was able to generate consistent load versus tibial rotation data for the individual rabbits. This data indicates that the loading on the MCL varies with joint angle in terms of the laxity of the ligament, and the slope of the force versus rotation curve.

ACKNOWLEDGMENTS

TABLE OF CONTENTS

vi

LIST OF TABLES

LIST OF FIGURES

CHAPTER ONE: Background

1.1 Introduction

The knee is a very complex joint whose movement and stability is determined by a large number of ligaments, tendons and their attached muscles. A complete understanding of joint kinematics is important: in the diagnosis of joint disorders resulting from injury or disease, in the quantitative assessment of treatment, in the design of better prosthetic devices, and in the general study of locomotion.

During normal motion, the bones in the knee move relative to each other in a complex three dimensional pattern. Many researchers studying the knee have used joint models which simplify this motion. These models include the simple hinge joint (one degree of freedom), and the planar joint (three degrees of freedom). However, to understand the knee joint completely it must not be simplified, but instead, studied in terms of all six degrees of freedom. The six degrees of freedom are defined as the rotation and translation of a moving body about the three axes of a Cartesian coordinate system. A six degree of freedom goniometer is a kinematic linkage which attaches to the femur and tibia, and records the three dimensional relative motion of the bones.

1.2 The Mechanics of the Knee

A functional view of the joint structure is given by Goodfellow and O'Connor (1978). "The animal limb can be thought of as a chain of rigid bars joined together by soft tissues, which include the muscles and their tendons no less than the ligaments." The function of all elements in the skeleton is to transmit load. The primary means by which load is transferred across a joint is a combination of tensile and compressive forces within the joint. The tensile forces are generated within the soft tissues; which, due to

their cable-like structure, are thought to be only capable of carrying loads in the line of their fibers. The compressive forces are carried by the articular joint surfaces. They are always perpendicular to the articular surfaces as synovial joints are very smooth and well lubricated so as to offer a minimal resistance to sliding. Figure 1.1 shows an example of how this combination of tensile and compressive forces within the joint work to prevent sliding. Rotations about the joint are resisted in a similar fashion.

Within the knee, a large number of hard and soft tissues work together to provide mobility and stability. Mobility is conferred by the low-friction bearing surfaces of the joint. Stability is a measure of the degree to which the relative movement at the bearing surfaces is limited or resisted. The product of all the tissues within the knee is a functional yet complex joint.

The complexity of the knee's motion can be demonstrated using the two dimensional model of flexion shown in Figures 1.2a-c. As shown in the figure, flexion of the knee involves both a sliding, and a rolling motion, of the femoral condyles upon the tibial plateau. These motions translate the point of contact backward during flexion and forward during extension. The model shown in the figure allows three degrees of freedom. If a six degree of freedom model is used more translations and rotations between the bones are evident. This shows the complexity of the knee joint, and the need to study the joint in terms of all six degrees of freedom.

Due to the complexity of the motion, and the large number of force-carrying members, the knee is highly indeterminate. Quantifying the motions of the members, and the loads that they carry, is highly complex.

1.3 Motion in Three-Dimensional Space

The most common method used to describe the relative motion between two bodies in three dimensional space is to attach a set of coordinate axes to each body as shown in Figure 1.3. One body is considered fixed in space relative to the other body
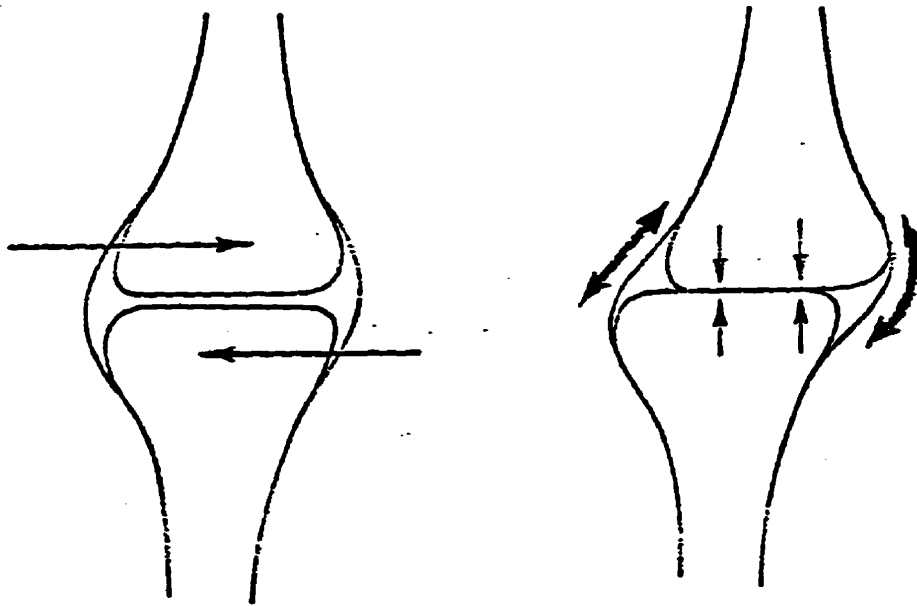
Figure 1.1: A general example of how a combination of tensile and compressive forces prevent sliding in the knee (from Goodfellow and O'Connor, 1978).
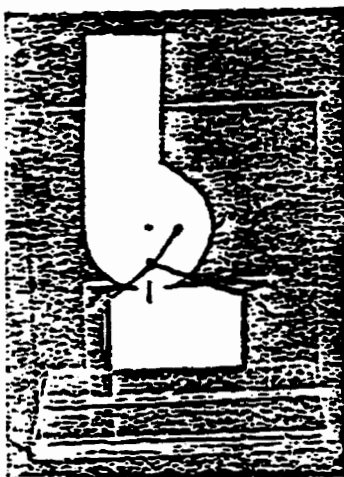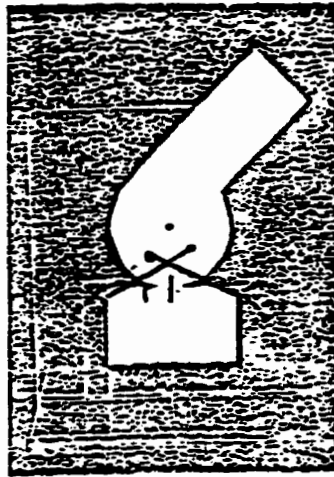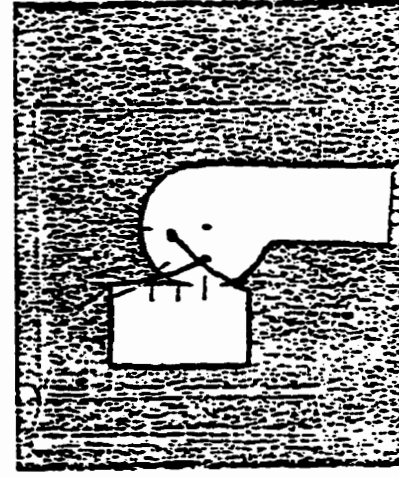
Fig. 1.2a   Fig. 1.2b   Fig. 1.2c

Figure 1.2a, b, and c: A two dimensional example of the complex nature of the motion in the knee joint. Note that the discrepant distances between the ticks on the femur and tibia indicate that flexion of the knee involves both rolling and sliding contact (from Goodfellow and O'Connor, 1978).
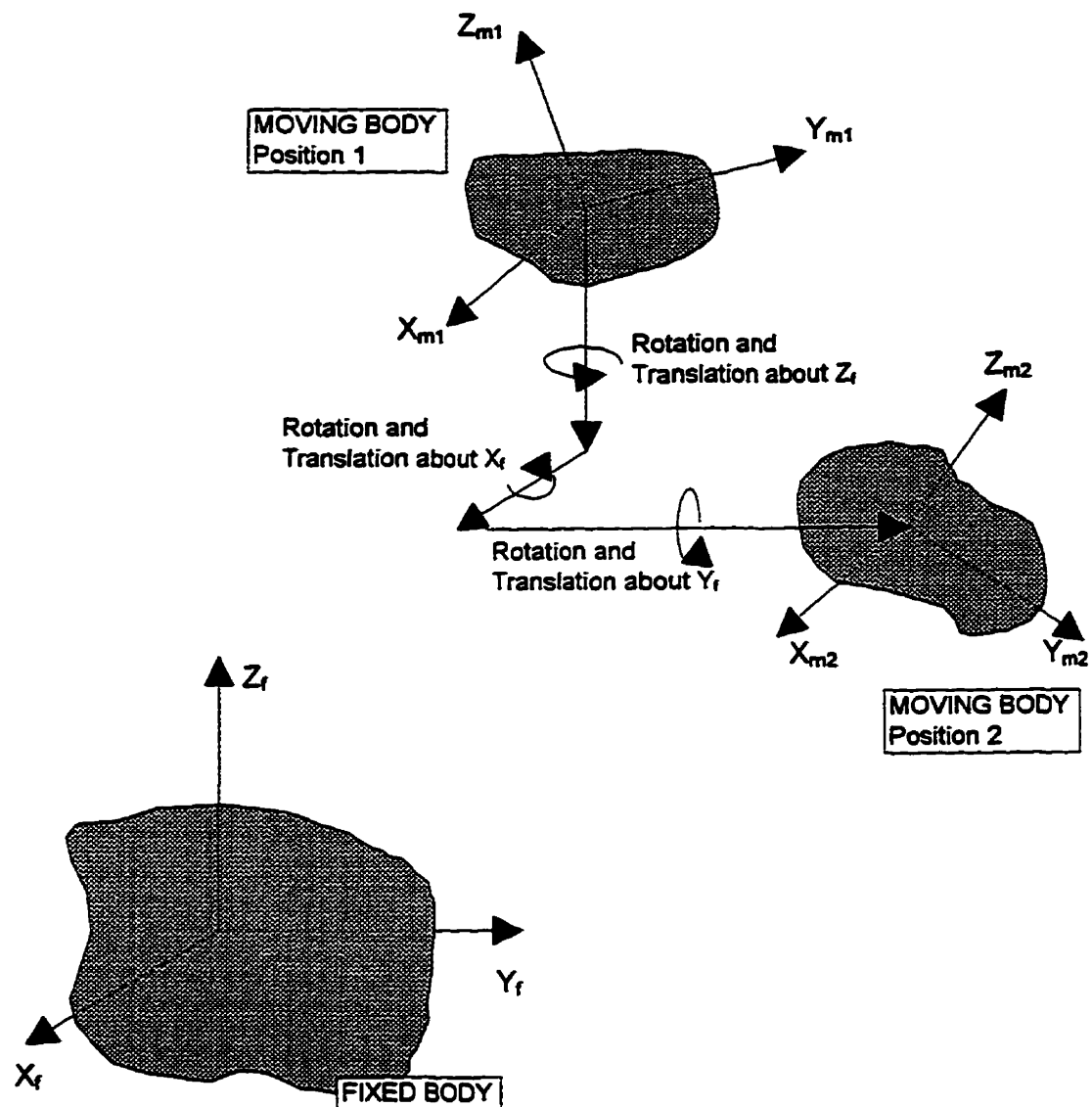
FIGURE 1.3: Each new location of the moving body is stated as the translation and rotation of the moving body's coordinate system (subscript m), relative to the fixed body's coordinate system (subscript f). Note: the order of the rotations is important.

which is moving. The location of the moving body, relative to the fixed body, at any moment in time, is determined by the rotation and translation of the coordinate system of the moving body, relative to that of the fixed body. This theory can be applied to measuring the motion of the tibia relative to the femur by attaching a set of coordinate axes to each bone.

The medical community also has an established system for describing the motion of the knee joint. This is a system of terminology used to describe the various motions such as varus-valgus and medial-lateral. For the data from any six degree of freedom goniometer to be of maximum value, it must be presented in a fashion that is both mathematically precise, such as the coordinate system used by engineers, and compatible with the established terminology of the medical community. The ISB Standardization and Terminology Committee's Recommendations for the reporting of kinematic data suggest the joint coordinate system shown in Figure 1.4. This system is based on the work of Grood and Suntay (1983). In the figure, the subscript p denotes the proximal coordinate system and the subscript d denotes the distal coordinate system. For both coordinate systems the x-axis is anterior, the y-axis is proximal, and the z-axis is defined by the right hand rule. The relative location of the coordinate systems is described by the translation and rotation about the Z_p, F, and Y_d axis. The three rotations α, β, and γ, and their positive directions, are shown in the figure. The translations are positive in the same direction as the axis along which they are measured. Using these axes it is possible to state the absolute motion of one bone relative to the other in a form that is both mathematically precise and easily understood by biomechanicians and physicians. Table 1.1 shows the correlation between the three rotations and three translations, used to describe joint motion with the coordinate system shown in Figure 1.4, and the clinical terms for describing joint motion.
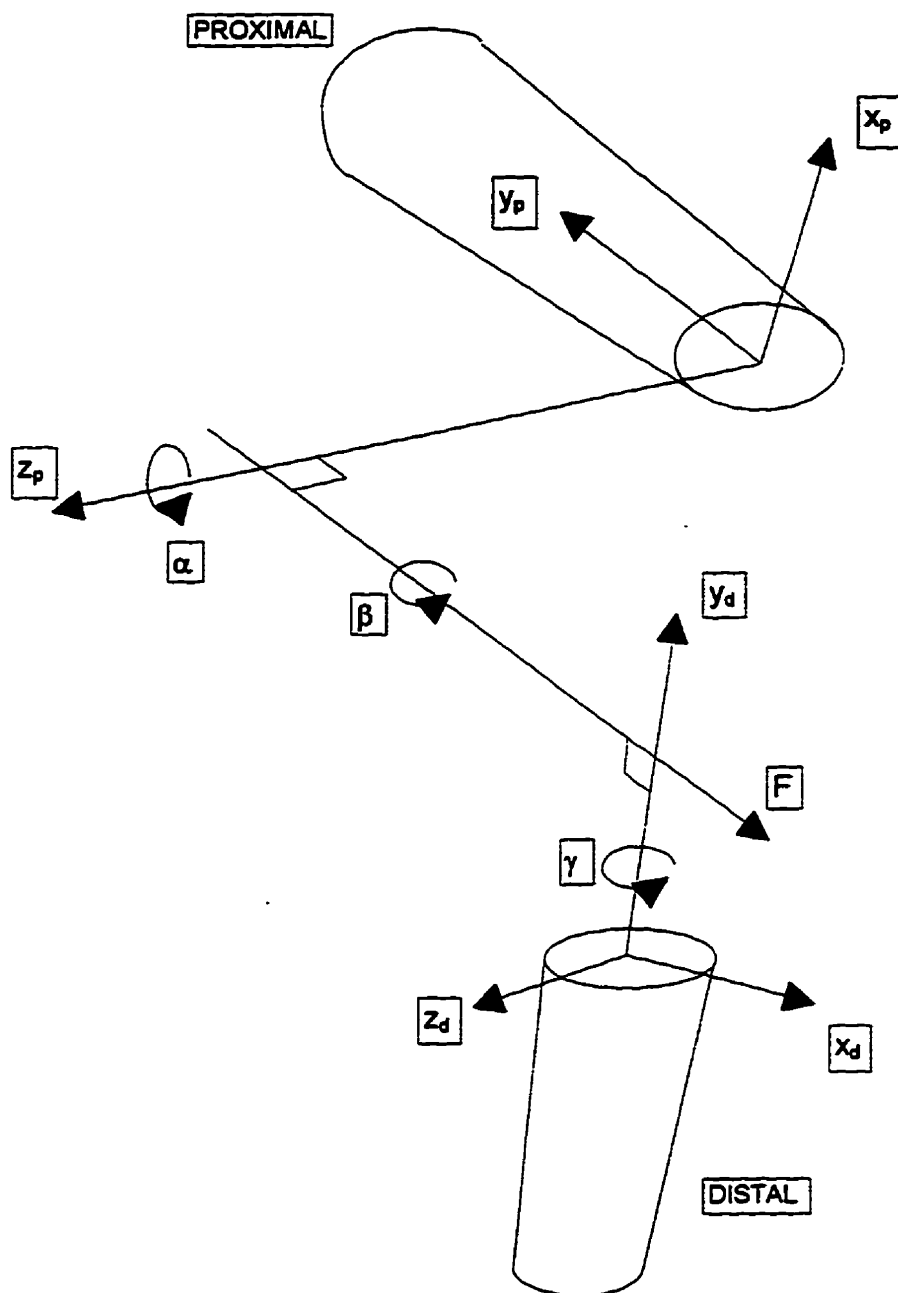
FIGURE 1.4: ISB coordinate system for reporting kinematic data.

Table 1.1: Comparison of ISB Coordinate System to the Clinical Descriptions of Knee Joint Motion.

Joint Coordinate System	Clinical Description
α	flexion-extension
β	varus-valgus
γ	tibial rotation
Translation along F	anterior-posterior
Translation along Z_p	medial-lateral
Translation along Y_d	proximal-distal

The choice of which coordinate system to use when reporting kinematic data will affect the results. This can cause the comparison of data sets to be very difficult. The goal of the ISB Standardization Committee is to eliminate the problem of comparing data sets by creating a standard coordinate system for reporting all kinematic data.

In order to utilize the ISB's coordinate system, the tibial and femoral coordinate systems must be precisely located on the bones. However, the complex shape of the bones suggests no obvious location at which to attach the coordinate systems. Therefore they are located in relation to three boney landmarks on each bone. These landmarks are chosen such that their relative location can be determined using traditional surveying techniques, such as a theodolite, or a coordinate measuring machine. The location of the origin for each of these coordinate systems will drastically affect the results. The ISB makes no specific recommendations as to which boney landmarks should be used to locate the coordinate systems, but does suggest using the work of Grood and Suntay (1983) as a model. Grood and Suntay's system of boney landmarks for locating the coordinate systems was developed for the human knee. For the purpose of this research it will be adapted for the rabbit knee.

1.4 How a Six Degree of Freedom Goniometer Measures Joint Motion

The goniometer, or kinematic linkage, is attached directly to both the tibia and femur. As the bones move relative to each other, the output from the motion sensors within the goniometer is recorded by a computer. This output, however, does not reflect the exact location of the bones for two reasons. 1) Due to the difficulty of aligning the goniometer with the coordinate axis on each bone during mounting the final data have to be corrected for any misalignment. 2) The goniometer's location, remote from the joint, causes certain rotations and translations that it records to be exaggerated or diminished. This is because the motion of the joint constantly changes the orientation of the motion sensors relative to the joint coordinate system. To convert the output data into the form suggested by the ISB coordinate system, the displacements measured by the goniometer must be processed using a series of transformation equations as shown in Figure 1.5.

The first transformation is from the tibial coordinate system to the tibial attachment point of the goniometer. From there a transformation is performed through each link of the goniometer. Finally, the last transformation is made from the femoral attachment point to the femoral coordinate system. The transformation equations are in the form of rotation and translation matrices which define the location of one link relative to the previous link in the goniometer. By multiplying these transformation equations together, a global transformation equation is generated which reflects the location of any point in the tibial coordinate system relative to the femoral system. Using this system the location of the origins of the coordinate systems can be recorded. In addition, the relative location of any points or surfaces on the two bones can also be recorded. This allows the goniometer to determine the relative location of say the femoral condyles and the tibial plateaus, or ligament insertion points.
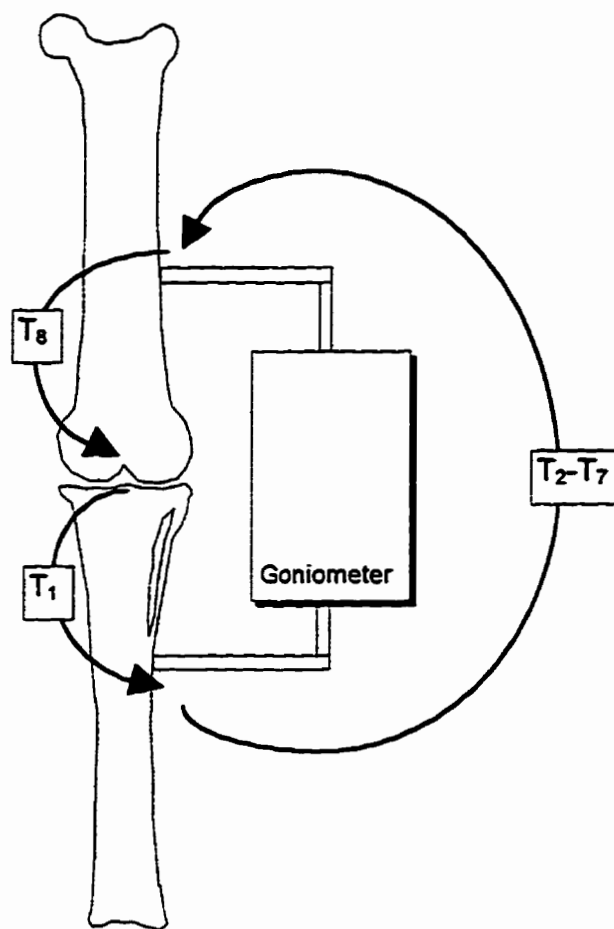
FIGURE 1.5: A system of transformations are used to relate the data recorded by the goniometer back to the joint. The first transformation is from the tibial coordinate system to the goniometer attachment point. Six more tranformations are then made, one for each link of the goniometer. The last transformation is made from the femoral attachment point to the femoral coordinate system.

1.5 Relevant Research in Bone Motion Analysis

The first researchers to create a kinematic linkage, capable of measuring joint motion in terms of all six degrees of freedom, were Kinzel *et al.* (1972). Until this study, joint motion analysis had always simplified the knee joint to reduce the number of degrees of freedom. One example of this is modeling the knee as a revolute joint. With this simplification there is only one degree of freedom, and motions are recorded in terms of flexion angle. This type of modeling is only useful for very basic investigations. Such a massive simplification eliminates the possibility of gaining any precise knowledge of the mechanics of the joint.

Kinzel *et al.*'s research is published in two parts. Part I presents the analytical basis for a six degree of freedom kinematic linkage, and Part II describes the design and construction of kinematic linkage. Part II also details an investigation using the kinematic linkage to determine the relative motion between the articular surfaces of the humerus and scapula in a dog. The theory behind their spatial linkage is to connect seven links together using six revolute joints. From Grubler's equation for mobility (Hartenburg and Denavit, 1964), a total of seven links and six mechanical joints gives a total of six degrees of freedom.. The linkage, shown in Figure 1.6, is primarily constructed out of aluminum and the six variable angles are measured by precision potentiometers. Kirschner-Ehmer splints are used to attach the device, shown in Figure 1.6, to the scapula and humerus.

To determine the motion of the bones the output data from the linkage had to be transformed into a useful form. The output data from each potentiometer were used to perform a series of matrix transformations from the coordinate system on the distal segment, through the linkage, to the coordinate system on the proximal segment. Kinzel *et al.*'s system of transformation equations reported the displacement of one segment, relative to the other, in the form of a rotation and a translation along a screw axis. This is shown in Figure 1.7. The screw axis is a single axis, along which the moving body can
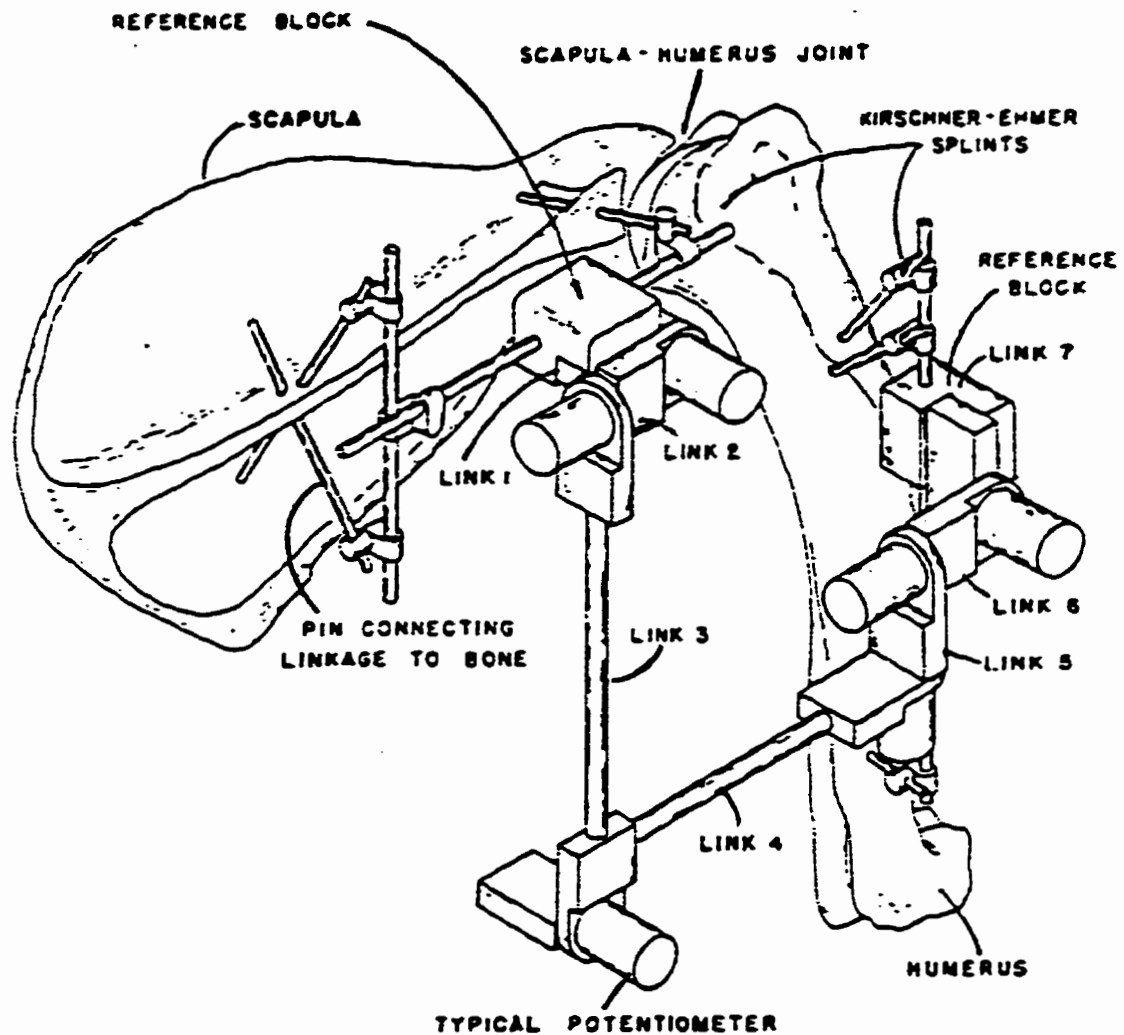
Figure 1.6: The kinematic linkage developed by Kinzel *et al*., for use on dogs, measures both rotations and translations using only rotary potentiometers (from Kinzel *et al*. 1972).
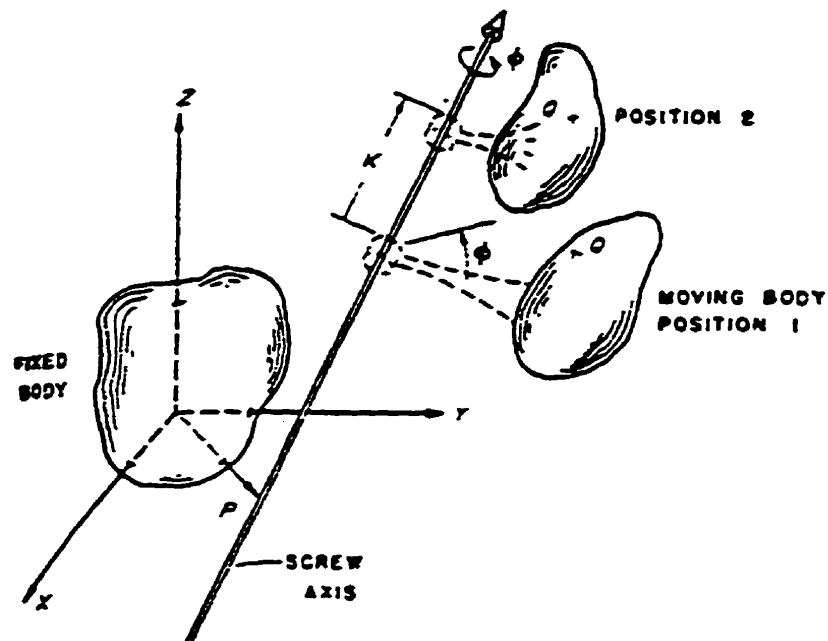
Figure 1.7: The system of transformation equations developed by Kinzel et al. state the motion of the moving body in terms of a rotation and a translation about a screw axis, which is defined relative to the fixed body. This system is mathematically precise, but does not translate well into a simple description of knee motion (from Kinzel et al. 1972).

be translated, and then rotated, relative to the fixed body, which will represent the total relative motion between the bodies. The screw axis method of reporting kinematic data is mathematically precise, but is not easily translated into the clinical system of describing joint motion. Kinzel *et al.* report that their linkage worked well but made no mention of how it was calibrated, and provided no estimation of accuracy.

A six degree of freedom kinematic linkage, designed for human cadaver knees, has been used by Hollis *et al.* (1991). The device was used to study unconstrained motion of the knee when subjected to externally applied varus-valgus and anterior-posterior loads. This linkage, shown in Figure 1.8, differs from the design of Kinzel *et al.* in that it uses both linear and rotary transducers. The rotations are measured by three rotary variable differential transformers, and the translations are measured by three linear variable differential transformers. As shown in Figure 1.8, this device is clamped directly onto the tibia and femur. To calibrate the linkage, 36 points were accurately marked on a 50 mm x 50 mm aluminum plate. The linkage was then used to measure the location of the points. The results from the linkage were then compared to the actual location of the points and the error was found to be 0.3 ± 0.2 mm.

The coordinate transformations discussed in conjunction with Hollis *et al.*'s kinematic linkage mention a series of six transformations, one for each link, required to transform a point in the tibial coordinate system into the femoral coordinate system. However, no mention is made about transformations from the bone coordinate system to the first link of the kinematic linkage. Perhaps, because they were dealing with a cadaver knee, cleaned of all surrounding tissue except the joint capsule, they were able to mount the linkage in a precise fashion. This could reduce the effect of the bone to linkage transformation to the point where it could possibly be ignored.

A recent study where joint motion was measured in vivo by a kinematic linkage was performed by Korvik *et al.* (1994). The objective of the study was to compare the three-dimensional kinematics of the intact and cranial cruciate ligament-deficient stifle of dogs. The linkage used for the study was based on the design of Kinzel *et al.* It was
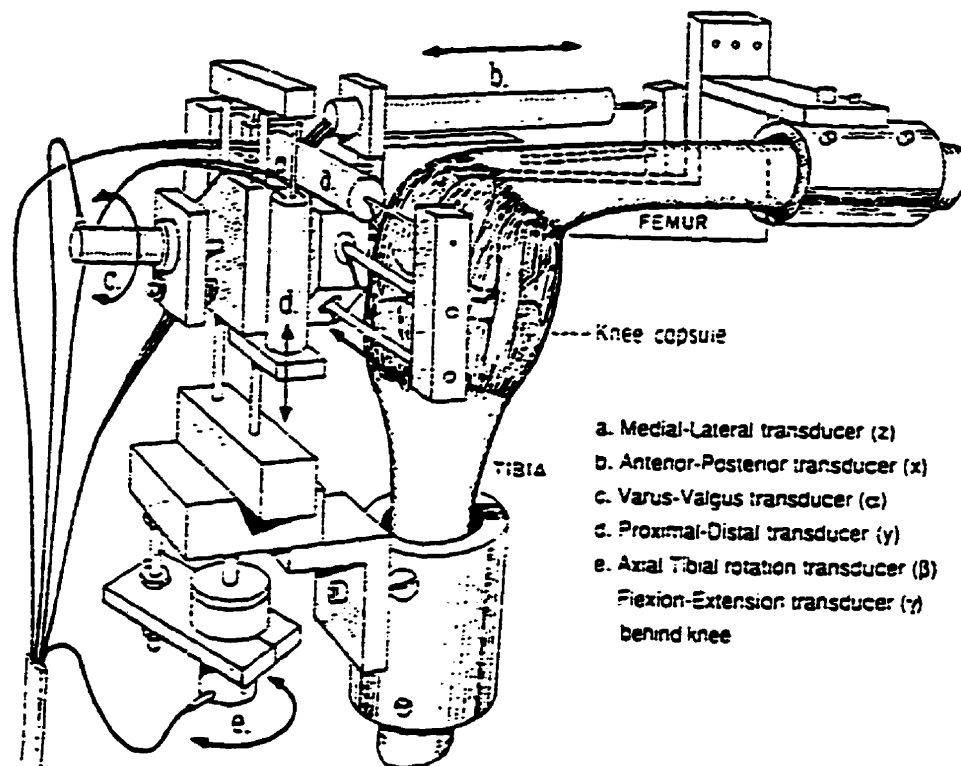
Figure 1.8: The kinematic linkage designed by Hollis *et al*. for use on human cadaver knees. This linkage used both linear and rotary variable differential transformers (from Hollis *et al*. 1991).

attached directly to the bones using the specially designed bone plate and mounting block system shown in Figure 1.9. The bone plates were mounted onto the bones, and then the dogs were given seven weeks to recover prior to testing. The linkage could then be attached to the bone plates by making four stab incisions. This system proved to be an effective method of accurately attaching the linkage in a repeatable fashion.

The average error and standard deviation for the experiments was 2.0 ± 1.5 degrees and 2.2 ± 1.8 mm. The method for calibrating the linkage is not mentioned. The system of transformations used in the testing is the same as that discussed in Section 1.4 and shown in Figure 1.5.

Evans et al. (1994) have created a six degree of freedom kinematic linkage to measure the motion between the healing segments of a broken bone. Their device is constructed of seven links constrained with either precision miniature ball bearings or miniature linear bearings. Hall effect devices are used to measure all six displacements; three linear and three rotary. The accuracy of the device, when mounted 50 mm from the fracture, is ± 0.045mm and ± 0.025 degrees. The system of transformations equations used in conjunction with this device is different than that discussed for the other devices described in this section. Instead of transforming a point from one bone coordinate system to the next using a series of matrices, the change in position is read directly from the output of the Hall effect devices, and then corrected with a simple set of equations. These equations account for the remote location of the device (up to 50mm from the fracture), and for the change in alignment of the Hall effect devices caused by the movement of the fracture. The very small motions measured across the fracture make this system of transformations practical.

These tests all show the potential value of six degree of freedom goniometers in the collection of three dimensional kinematic data in both human and animal models. In all cases the researchers were able to create an accurate and reliable device which generated useful data. The designs of the linkages fall into two basic categories: 1) seven links connected by six rotary joints and 2) seven links connected by three rotary
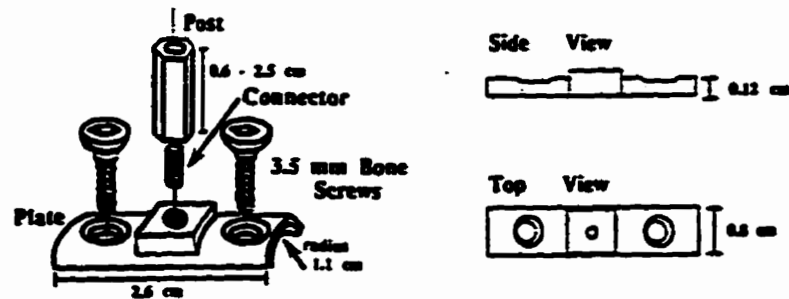
Figure 1.9a: The bone plates used by Korvick *et al*. were attached to the leg 7 weeks before testing and left in place for the 8 week duration of the testing, thus demonstrating good durability. The post was attached to the plate only for kinematic linkage attachment (from Korvick *et al*. 1994).
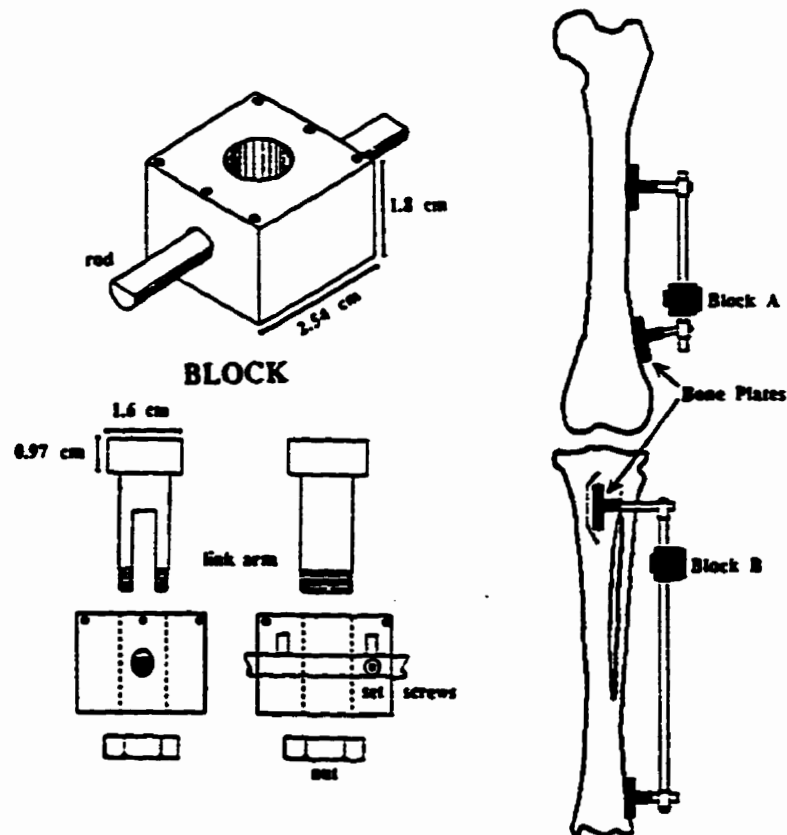
Figure 1.9b: Korvik *et al*.'s linkage was attached to the leg by first attaching a frame across the two plates mounted on each bone. The linkage was then connected to the frames using two sliding blocks (from Korvik *et al*. 1994).

and three linear joints. With all the devices, a system of transformation equations is required to translate the output from the displacement transducers into a more comprehensible form such as the coordinate system recommended by the ISB.

1.6 Justification of the use of a Goniometer to Measure Joint Motion

The goal of this project is to create a device which is capable of generating continuous kinematic data relating the location of the tibia to the femur. The requirement immediately eliminates many joint position monitoring systems such as X-rays, which would require the generation and analysis of hundreds of images in order to monitor motion. The only three systems located during the research for this project, which are capable of generating continuous kinematic data, are the six degree of freedom goniometer, the video dimension analyzer (VDA), and magnetic systems such as the Flock of Birds.

A VDA system determines bone position by digitizing a set of perpendicular video images of reflective markers attached to the femur and tibia. Motion of the bones is then determined by relating the location of the reflective marks to the bone coordinate systems using a system of transformation equations similar to that of the goniometer. There are two advantages of the goniometer over the VDA system. The first is that the output of the individual potentiometers of a goniometer can be monitored during testing to give an approximation of the joint motion. Figure 1.9 shows how a careful arrangement of the potentiometers can provide approximate measures of the standard clinical descriptions of joint motion. This allows a researcher to monitor, for example, flexion and tibial rotation during the course of an experiment. The second advantage of a goniometer, over the VDA system, is the relative simplicity. With a VDA system special cameras must be properly aligned relative to the leg in order to record the motion of the reflective balls attached to the femur and tibia accurately. This means that all test equipment must be designed so as not to block the camera's views of the reflective balls,

and precludes any testing which would involve the rabbit having freedom of motion. In comparison, a goniometer can easily be attached to a computer using a long cable.

The magnetic system, or Flock of Birds, involves a transmitter which establishes a magnetic field in which the receivers can sense their position to an accuracy of 0.8 mm and 0.15 degrees. Hence by attaching the transmitter to one leg and a receiver to each of the bones on the other the leg the relative position of the bones can be determined. This system has several problems for this application. The first problem is that the transmitter and receiver are strapped onto the leg of the animal. This creates the problem of skin and muscle motion compromising the accuracy of the results, compared to a system which uses bone pins. To attach the transmitter and receiver to the bones directly will require non-magnetic bone pins in order to not alter the magnetic field emitted by the transmitter. The second problem with the magnetic system is the plan to use the bone position measuring system inconjunction with a medial collateral ligament load cell developed at the University of Calgary. To use this load cell with the magnetic system would require that it be re-manufactured out of non-magnetic materials, and that the strain gauge leads were some how magnetically shielded. The final problem with the magnetic system is that it is quite large compared to a rabbit leg, which could create problems for some types of testing.

1.7 Significance of a Six Degree of Freedom Goniometer for the Rabbit's Knee

Rabbits are frequently used as a model for research as they are relatively inexpensive, readily available, and mature quickly. These attributes allow researchers to reduces the length and cost of experiments. In particular the rabbit knee has received a great deal of attention as it is similar to that of a human. However there is currently no device which is capable of precisely recording the *in vivo* relative motion of the tibia and femur in a rabbit's knee.

Based on the success of the research outlined in Section 1.5, creating a goniometer for the rabbit knee is a realistic goal which will increase our knowledge of knee mechanics. However, only four examples of six degree of freedom goniometers, similar to the type required, were located during research for this project. Given the tremendous potential value of goniometers, and limited numbers which exist, the task of design cannot be an easy one. A goniometer suitable for the rabbit knee will require a design which is both smaller, and lighter, than any of the examples discussed above. Once the goniometer has been created (Chapters Two and Three) it will then require a system of transformation equations (Chapter Four), calibration (Chapter Five), and testing on rabbits to evaluate its performance (Chapter Six). However, the potential value of having the ability to evaluate the kinematics of the rabbit knee *in vivo* justify the effort required to design the six degree of freedom goniometer.

CHAPTER TWO: The Design Process

2.1 Introduction

The development of the six degree of freedom goniometer occurred in two distinct steps. The first step was the design and manufacture of a preliminary model; which was then followed by the development of the final goniometer design. The original design was developed without the benefit of a systematic design process, and showed a lack of design experience. This design, however, provided an excellent learning opportunity for the development of the final design. The two most beneficial lessons learned from the original design were: 1) the importance of planning thoroughly how all the components will function together and 2) the need to plan the entire manufacturing process carefully in terms of how the components will be made, and then assembled. The complex three dimensional nature of this project greatly complicated both visualizing the design and communicating the design to the manufacturer.

The final goniometer design was developed by following a systematic design process. This combined with the lessons learned from the original design produced a much simpler and more functional design.

2.2 The First Design

The first goniometer design is pictured in Figure 2.1. This version of the goniometer was developed by first designing a frame. This frame was made up of seven links, connected by three rotary and three linear joints, and was capable of moving in terms of all six degrees of freedom. Potentiometers were then attached to the frame to measure its motions. The greatest problem with this design was its complexity. The number of moving parts increased both the size, and the internal friction, to an

unacceptable level. The forces required to move the goniometer through its full range of motion were sufficiently large that there was no chance of measuring the natural, unimpeded motion of the rabbit leg. The original design was, however, extremely valuable as a learning experience. This design showed that the ordering of the potentiometers, and their method of connection, are the key elements of a successful design.

2.3 The Final Design

The final design was developed by following a systematic process that, when combined with the knowledge gained from the original design, led to the success of this project. The design process followed is that developed by G. Pahl and W. Beitz in their book *Engineering Design, A Systematic Approach*. This process divides product development into four phases: 1) clarification of the task, 2) conceptual design, 3) embodiment design, and 4) detail design. By employing a methodical design process, the designer can be more confident in: identifying the best solution to the specified problem, identifying and preventing complications as they arise, decision making, predicting possible future difficulties, detecting and mitigating possible legal concerns, and most importantly, satisfying the customer's desires. There is no single design framework proposed, instead a versatile approach is taken which can then be adapted to specific design challenges.

2.4 Clarification of the Task

Clarification of the task is the first phase of the design process. At this point the specifications of the problem are determined, and then classified as either *demands* or *wishes*. Demands are defined as those requirements that must be satisfied under all circumstances for the design solution to be considered acceptable. Wishes are features
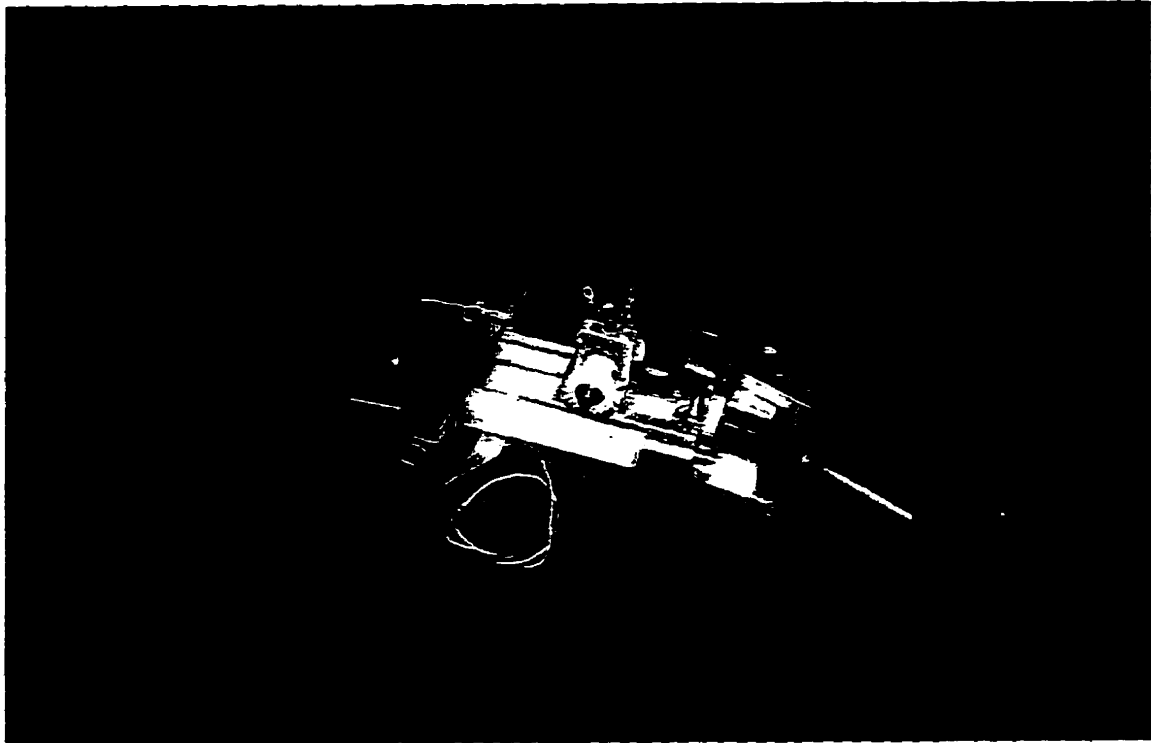
Figure 2.1: The first goniometer design. Note that this design was not completed due to the design problems which became evident during construction.

that will augment the design and should be taken into consideration whenever possible. However their inclusion in the design is not critical to the acceptability of the solution. This distinction is made to facilitate the selection of the most feasible design alternative.

To aid in the development of a complete set of design specifications Pahl and Beitz suggest the list of main headings shown in Figure 2.2. This complete list of headings covers many different design attributes. For each new product design a certain set of these headings will prove to be the most important when compiling the design specifications. When creating a specification list for a new design, each heading is subdivided into demands and wishes. Using this list of headings a complete set of specifications was developed for the goniometer, which is shown below in Table 2.1.

Table 2.1: Specifications for the Goniometer Design
_____

Geometry
Demands
- Capable of measuring motion in terms of all six-degrees of freedom. The expected magnitude of the motion , about the ISB coordinate system, is shown in Figure 2.3.
- Compatible with the joint size of a rabbit's knee, therefore less than 50mm in length.
- Overall size as small as possible.
Wishes
- Have a minimal physiological impact on the rabbit.
- Adaptable to other animals.

Kinematics
Demands
- Operate smoothly to allow natural motion of the knee joint.

Forces
Demands
- Minimize internal friction and overall weight, in order to reduce resistance to natural joint motion.

Main Headings	Examples
Geometry	Size, height, breadth, length, diameter, space requirement, number, arrangement, connection, extension.
Kinematics	Type of motion, direction of motion, velocity, acceleration.
Forces	Direction of force, magnitude of force, frequency, weight, load, deformation, stiffness, elasticity, intertia forces, resonance.
Energy	Output, efficiency, loss, friction, ventilation, state, pressure, temperature, heating, cooling, supply, storage, capacity, conversion.
Material	Flow and transport of materials. Physical and chemical properties of the initial and final product, auxiliary materials prescribed materials (food regulations etc).
Signals	Inputs and outputs, form, display, control equipment.
Safety	Direct protection systems, operational and environmental safety.
Ergonomics	Man-machine relationship, type of operation, operating height, clearness of layout, sitting comfort, lighting, shape compatibility.
Production	Factory limitations, maximum possible dimensions, preferred production methods, means of production, achievable quality and tolerances, wastage.
Quality Control	Possibilities of testing and measuring, application of special regulations and standards.
Assembly	Special regulations, installation, siting, foundations.
Transport	Limitations due to lifting gear, clearance, means of transport (height and weight), nature and conditions of despatch.
Operation	Quietness, wear, special uses, marketing area, destination (for example, sulfurous atmosphere, tropical conditions).
Maintenance	Servicing intervals (if any), inspection, exchange and repair, painting, cleaning.
Costs	Maximum permissible manufacturing costs, cost of tools, investment and depreciation.
Schedules	End date of development, project planning and control, delivery date.

Figure 2.2: Check list of main headings for drawing up specifications (from Pahl and Beitz, 1988).
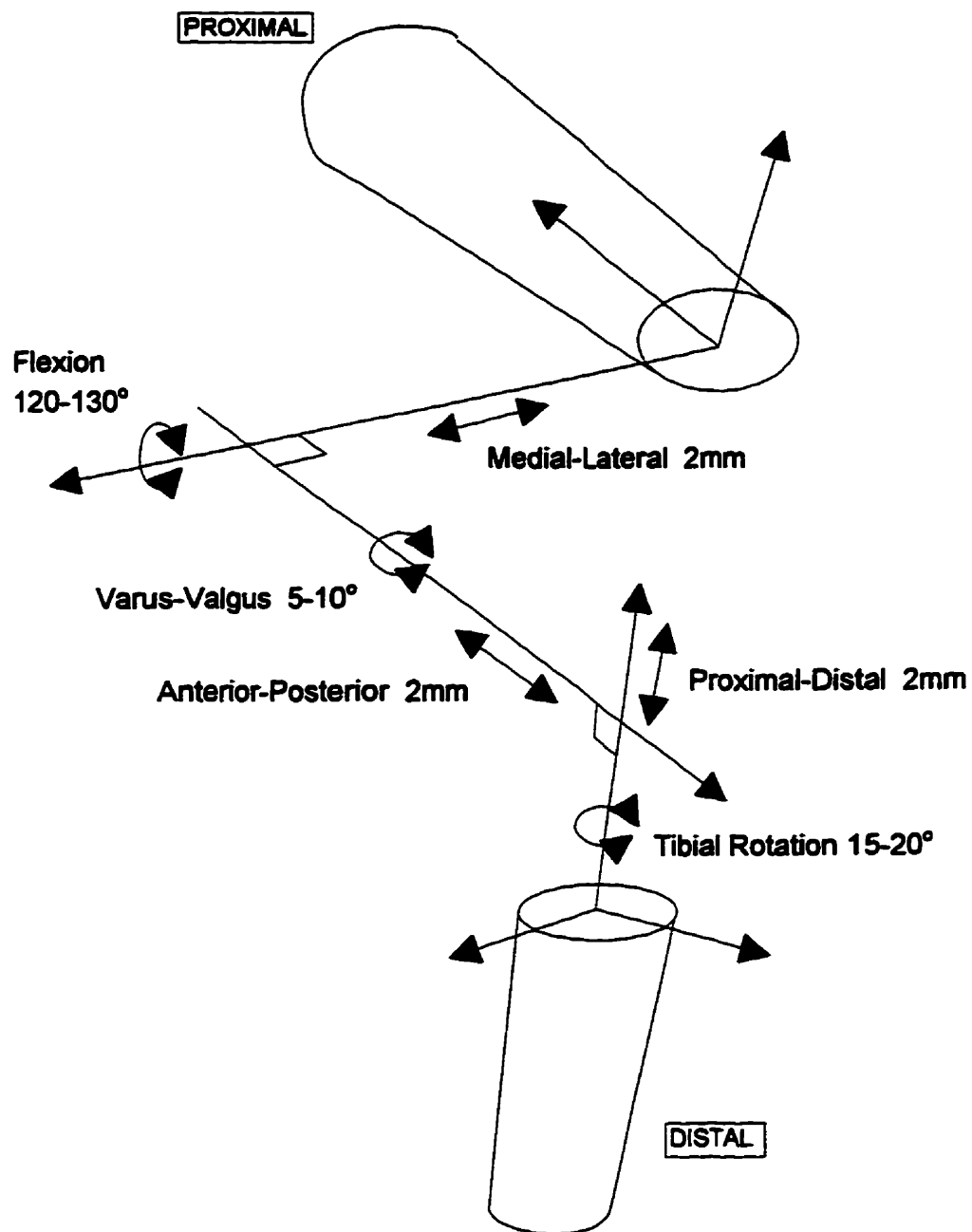
FIGURE 2.3: Estimated magnitude of rotations and translations about the ISB coordinate system within the rabbit knee.

Materials
Demands
- Rigid frame material to minimize errors due to deflections.
- Light weight.

Wishes
- Corrosion resistant.
- Capable of withstanding sterilization.
- Low cost.
- Easy to machine.

Operation
Demands
- Results accurate to ± 0.5mm or ± 2 degrees.
- Repeatable results, even with removal and reattachment of device.
- Instantaneous recordable output.

Wishes
- Simple operation.

Maintenance
Demands
- Durable enough to last the duration of an entire research project. Say 40 cycles of motion on 6 different animals for a total minimum durability of 240 cycles of motion.

Wishes
- Easy to maintain with simple readily available parts.

Others
Demands
- A mounting system which allows the goniometer to be removed and reattached to the rabbit in a secure, repeatable fashion.
- A data acquisition system which allows the output of the goniometer to be easily stored by a computer, and then recalled for analysis.

Determining the specifications for the goniometer is difficult due to the lack of similar devices and data which could be used to define the task. For example there is no set data stating that a goniometer for the rabbit knee must weigh less than certain amount in order to function properly. In addition one of the of the key criteria for a successful design is that the goniometer must allow the leg to move freely throughout its natural range of motion. However gauging the success of the goniometer in this area is

very difficult as there are very few data which could be used to define natural motion. Therefore the entire process of designing and testing the goniometer will have to be a learning experience. The first goniometer design is a good example of this as it proved to be too cumbersome to possibly allow the leg to move in a natural fashion.

The demands in Table 2.1 state that the goniometer must be able to measure displacements and rotations to an accuracy of ± 0.5mm and ± 2 degrees respectively. These demands are based on the expected magnitude of the motion, displacements of up to 2mm and rotations of 10-15 degrees, that the goniometer will be used to measure. Once the error in the output of the goniometer begins to exceed these values the data starts to lose any scientific significance.

These specifications establish a solid frame work of attributes which define a successful goniometer design. The next step in the design process will be to break the problem down into a series of smaller design problems, called Function Structures. Establishing these function structures is the basis of the Conceptual Design phase.

2.5 Conceptual Design

The purpose of the conceptual design stage is to define the problem at its most basic level. The overall functional requirement of the design problem is divided into its basic Function Structures. Each of these should be one easily understood part of the overall function of the design problem. The Function Structures can then be analyzed individually as smaller design problems. The solution to each of these function structure design problems can then be combined into a final solution. However, care must be taken when combining the function structures in order to avoid designs which are awkward due to an excessively modular nature. The designer should look for opportunities to combine function structures in the final design in order to achieve a elegant and global design. All the functional components of the design must be made to work in a smooth and complementary fashion.

Pahl and Beitz's recommended procedure for the conceptual design phase is shown in Figure 2.4. This procedure involves taking the overall function of the design problem, breaking it down into its basic function structures, finding a solution for each of the function structures, and then combining these individual solutions to fulfill the overall functional requirements.

2.5.1 Function Structures

For complex projects, the conceptual design stage is crucial in order to determine each function structure and, hence, break the problem down to a manageable size. The design of the goniometer; however, is very simple from a conceptual point of view. Figure 2.5 shows the goniometer design problem broken down into its functional structures. The motion of the tibia, relative to the femur, travels through the goniometer which must: 1) allow the motion to occur unimpeded, 2) measure the magnitude of the motion, and 3) record the motion. It is expected that some sort of power will have to be supplied to the goniometer in order to measure the displacements (energy in), and that this information will be returned in a recordable form (signal out).

2.5.2 Search for a Solution

At this point in the design process the Clarification of the Task step has created a framework of design specifications that define the design problem physically. In addition, the Function Structures have broken the problem down into discrete parts that define the design problem functionally. A search can now start to find design solutions for each of the function structures, which will be combined into a final design. This design must satisfy both the function structure, and the design specifications, to be considered a successful design.

The form of the final solution is controlled by the following requirements. If these are not met then the design is a failure.

- The overall length must be less than 50mm.
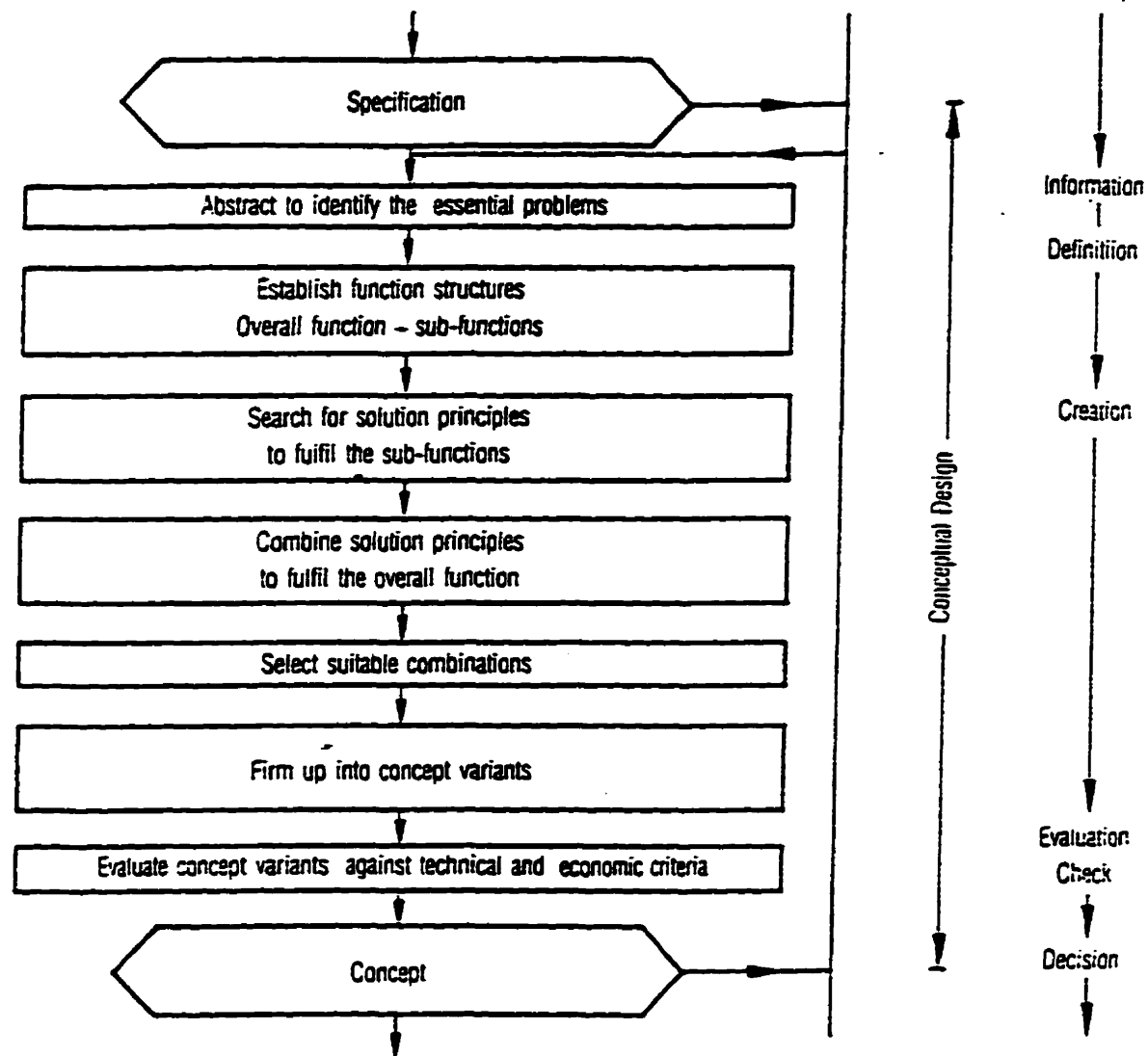
Figure 2.4: Steps of the conceptual design process. These steps were used as a guideline throughout the development of the goniometer (from Pahl and Beitz, 1988).

Energy

Motion of
Tibia
Relative
to Femur

Allow
Motion

Measure
Motion

Record
Motion

System Boundary

Signal
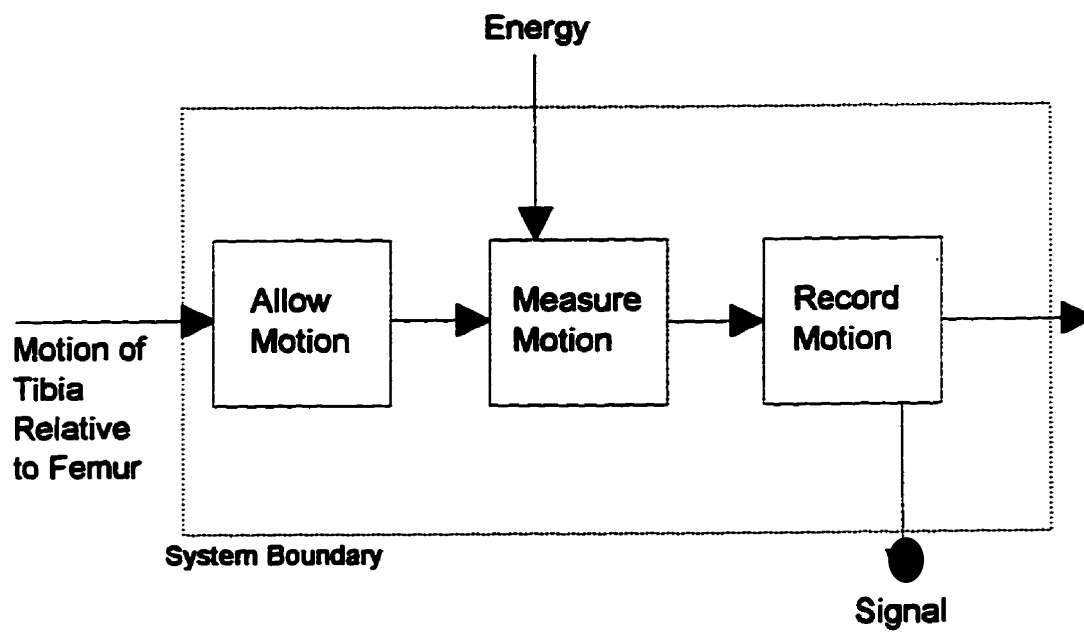
FIGURE 2.5: The goniometer design problem broken down into its
function structures.

- The goniometer must be capable of measuring the required range of motion as shown in Figure 2.3.

- The goniometer must be as light as possible.

- The internal friction must be minimized.

Chapter One outlines the related work that has occurred in the field of bone motion measurement. This work shows that for the accuracy required the most promising solution is some type of mechanical linkage (Kinzel *et al.*, 1972; Hollis *et al.*, 1991; Korvik *et al.*, 1994; Evans *et al.*, 1994). The linkage will contain seven links connected together with either six rotary joints, or three rotary and three linear joints. As explained in Chapter One, this combination of links and joints allows six degrees of freedom in accordance with Gruber's equation for mobility (Hartenburg and Denavit, 1964). The linkage will have to be directly attached to the bone, by some system of bone pins or plates, to prevent error due to skin slippage. The experience of other researchers also suggests that some type of electronic displacement measuring device, such as a potentiometer, is an effective means of measuring the motion of bones. The output from this type of electronic measurement device is also easily recorded by a computer.

2.5.2.1 *Function Structure: Measure Motion*

In Chapter One three different electronic displacement measuring devices are mentioned that have been successfully use with other kinematic linkage designs. These are potentiometers, Hall effect devices, and rotary/linear variable differential transducers (RVDT/LVDT). For this project, potentiometers have been chosen because they are: sufficiently accurate to meet the specified demands, and are the most affordable option. Though RVDT/LVDT's are the most accurate option, they were rejected because they are the most expensive. Once the goniometer design has proven its value for research then the extra cost of the RVDT/LVDT's could be justified. Hall effect devices were rejected because they were not recommended by the researchers who used these devices for their linkage, due to their limited linear range (Evans *et al.*, 1994). Other electronic

measuring devices such as strain gauges and encoders were also investigated but rejected for various reasons. Strain gauges due to the size and complexity of a unit capable of measuring 10mm of linear motion, and encoders due to cost and nonlinear step-wise nature of their output.

2.5.2.2 Function Structure: Allow Motion

The two basic linkage designs discussed in Chapter One were: seven links connected by six rotary joints, or seven links connected by three rotary and three linear joints. For this project the design employing three rotary and three linear joints has been selected. The primary reason for this decision is, with the six rotary joint design there is no direct correspondence between any of the potentiometer outputs and the coordinate system recommend by the ISB for reporting kinematic data. With the three rotary and three linear joint design there is a rough correspondence (depending on how accurately the goniometer is attached to the bones) between the potentiometer output and ISB coordinate system. This is particularly true of the rotations. The translations however, will be less accurate due to the goniometers location adjacent to the knee (for more information see Section 3.2.2). This allows researchers to monitor the output of the potentiometers during testing, and therefore have an approximation of the joint motion, without having to use the transformation equations first. A further advantage of using the three rotary and three linear design is that very small and light-weight linear potentiometers are available. This will help to reduce the size and weight of the goniometer over the design using six rotary joints.

At this point an important realization occurred. In the original design a frame capable of the required motion was designed first, and then the potentiometers were added to measure the motion of the frame. The problem with this design was that the potentiometer/frame combination was so complex that large frictional forces were inevitable. However the goniometer design can be greatly simplified if the potentiometers are used as part of the frame. Many precision potentiometers are

available which contain high quality bearings. By taking advantage of this, the only moving parts within the goniometer are the six potentiometers. Because the goniometer will be a very light weight, low friction design, the internal forces will be sufficiently low to prevent any damage to the delicate bearing within the potentiometers. Using this concept, all that is required to construct the goniometer is a few simple brackets to hold the potentiometers together. In this way a "chain" of potentiometers is created. Any random motion which is imparted on this "chain" will pass through the various links, being recorded by the appropriate potentiometers.

The concept of using the potentiometers as part of the frame is a good example of how function structures can sometimes be combined to create a more efficient design.

The final step in the embodiment of the goniometer is to analyze the ordering of the potentiometers within the goniometer. It seems logical that an efficient ordering of the potentiometers will reduce the overall size of the goniometer, and the complexity of the brackets required to hold the potentiometers together. Finally, the ordering of the rotary and linear potentiometers can affect the complexity of the transformation equations. If the rotary and linear potentiometers are randomly arranged within the goniometer, then the rotation of the rotary potentiometers will change the alignment of the linear potentiometers. However, if the three linear potentiometers are placed together at the end of the chain, their alignment will not change. In addition, if a rotary potentiometer is roughly aligned with the knee's axis of flexion, then the effect of this large rotation on the alignment of the other potentiometers can be minimized. Note as stated in Chapter One, the knee's axis of flexion moves as the knee bends, and hence precise alignment is impossible.

Figure 2.6 shows the goniometer design as it has been finalized to this point. Starting at the femur, the first potentiometer in the chain is a rotational potentiometer roughly aligned with the knee's axis of flexion. This is followed by the other two rotary potentiometers, and finally, the three linear potentiometers. The potentiometers will be connected together by simple brackets and the only moving parts will be the

Goniometer connected directly to femur and tibia by some type of bone pin system.

Rotary Potentiometer: Roughly aligned with knee's axis of flexion.

Rotary Potentiometers: Perpendicular to each other and the rotary potentiometer above.

Linear Potentiometers: All mutually perpendicular.
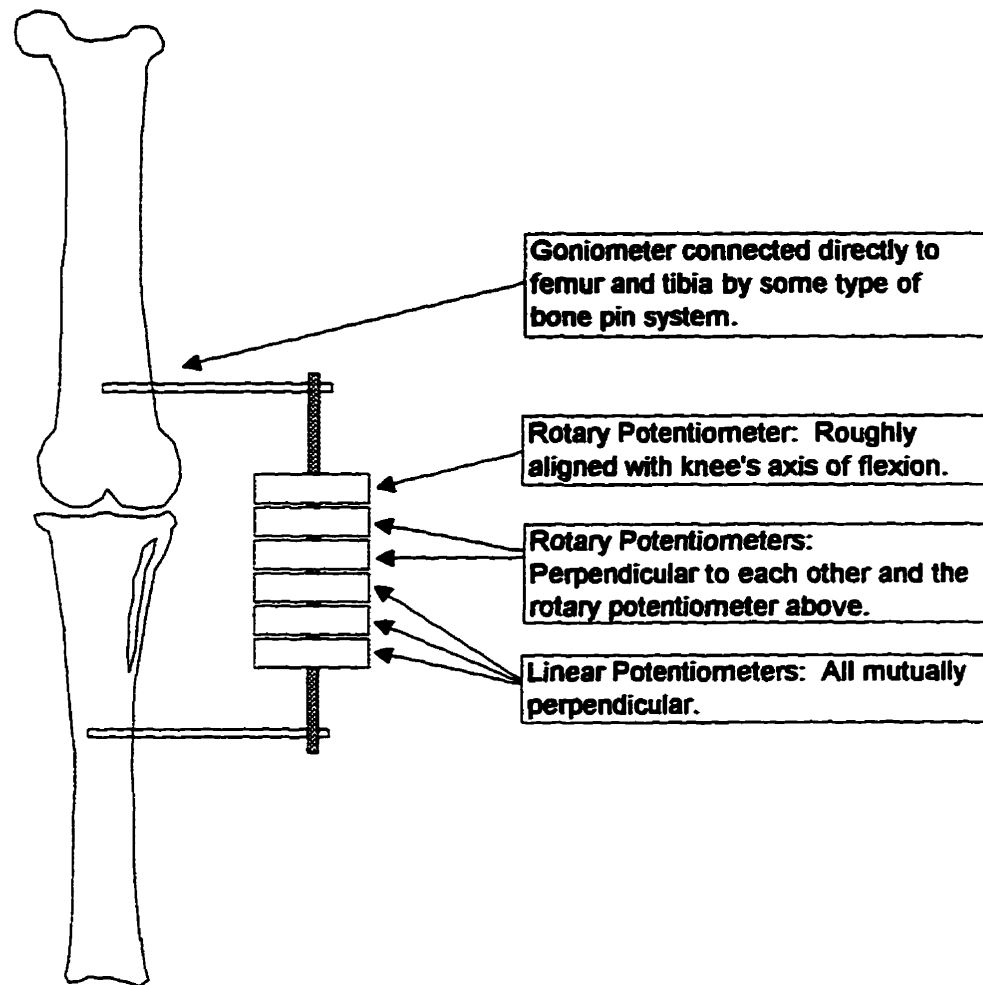
FIGURE 2.6: Goniometer Design Overview. The potentiometers will be connected together using a series of simple brackets. The final arrangement of the potentiometers will be that which minimizes the overall size of the goniometer.

potentiometers themselves. The optimum arrangement for the potentiometers, beyond what is shown in Figure 2.6, will be that which minimizes the overall size of the goniometer and requires the simplest connection brackets. This problem is dealt with in the embodiment phase of the goniometer.

2.5.2.3 *Function Structure: Record Motion*

The use of an electronic measuring device to record the goniometer's motion greatly facilitates data collection. The output from the potentiometers can easily be run through an analog/digital converter into a computer equipped with some form of data collection software. The data will then be stored in a file, readily available for analysis.

The next step in the design process is to move onto the final design stage. The challenge will be to use the frame work for the goniometer (shown in Figure 2.6) to create a final product which meets all of the functional and design requirements laid out within this Chapter.

CHAPTER THREE: Design Solution

3.1 Introduction

The conceptual design phase provided both an understanding of the complexity of the problem and a direction for finding a design solution. It has also established the foundation on which the physical embodiment of the design can begin.

The next phase in the design process is embodiment design. This step builds on the framework, created during the conceptual design phase, by combining design ideas until a working prototype is produced. Pahl and Beitz (1988) define embodiment design as "that part of the design process in which, starting from the concept of a technical product, the design is developed, in accordance with technical and economic criteria and in the light of further information, to the point where subsequent detail design can lead directly to production." The embodiment phase involves performing many different steps simultaneously in order to assure that the finished product will function as a unit. The constraints on one component will often affect the design of another component, thus flexibility and adaptability within a broad design approach are important. During this phase, the designer must also determine the method of production and provide solutions for any auxiliary design problems.

During the embodiment phase the design specifications are used as a guide. The demands form the framework within which the product will develop. The wishes are included whenever possible, as long as they enhance the overall design. The first step is to identify the specifications which will have the greatest impact on the design. These demands create an overall understanding of the layout and a starting point for the design. An effective layout will include checks for durability, production, assembly, operation, and cost. The design space will dictate attributes such as the size, shape, and weight of the product, which will determine the choice of mechanisms and materials. From the

layout, the shape of the components and the method of assembly begin to develop. Economics are of great importance and should be given the same status as the functional requirements.

In the design of the goniometer the physical layout is very important. The critical specifications for the goniometer are: a) the distance between the bone attachment points must be less than 50mm, and b) the weight and internal friction must be kept to a minimum. Ultimately these constraints will form the design space for the goniometer, control the selection of the components, and determine the method in which they are assembled.

During embodiment design, Pahl and Beitz feel that clarity, simplicity, and safety are fundamental. Clarity eliminates ambiguity in a design, and promotes reliable prediction of performance, as well as saving time and money. Simplicity ensures economic feasibility by utilizing a small number of simple parts that are easily assembled. Safety requires consideration of strength, reliability, accident prevention, and protection of the environment.

3.2 Embodiment of the Goniometer

3.2.1 Material Considerations

During the design process, the optimum goniometer design was determined to be a chain of potentiometers connected together by a series of brackets. To decide on the material for the brackets, the design specifications are consulted. The demands state that the goniometer must be as light as possible, yet sufficiently rigid to reduce error. The wishes are for a corrosion resistant goniometer capable of being sterilized.

The delicate nature of potentiometers make it difficult to create a corrosion resistant goniometer. Therefore a compromise is required. The mounting pins will be the only part of the goniometer in direct contact with the rabbit. They can be made of

surgical steel, which is corrosion resistant and easily sterilized, while the rest of the goniometer is protected from any corrosion damage by a plastic cover.

Long term studies will require that the goniometer and plastic cover are sterilized to protect the rabbit from infection. This can be done by gas sterilization without damaging the potentiometers.

With the goniometer protected from corrosion damage by the plastic cover, the material selection for the brackets is limited only by the need for a light-weight rigid material. Aluminum is chosen because it meets the material demands and is inexpensive and easy to work with.

3.2.2 Potentiometer Selection

The goniometer design calls for three rotary and three linear potentiometers to measure the rotations and translations. The design specifications call for potentiometers that are light-weight, have low internal friction, and a high level of accuracy. However high quality potentiometers meeting these requirements are difficult to locate. Features such as internal bearings are a necessity. A further constraint on potentiometer selection is that the data acquisition system, LabTech Notebook, used in conjunction with the goniometer is limited to a maximum input of 10 volts. Ideally the rotary potentiometers will be half (or quarter) turn units to maximize the voltage change caused by the smaller varus-valgus, and tibial axial rotations.

In order to select the linear potentiometers for use with the goniometer the magnitude of the linear motions must be known. Figure 2.3 (page 24) shows the expected magnitude of the linear motion, of the tibia and femur, about the ISB coordinate system. It is important to realize that the motions recorded by the potentiometers will vary in magnitude from the actual motion of the bones within the knee joint. This is due to the remote location of the goniometer. Figure 3.1 shows how pure tibial rotation causes both a rotation and a translation at the goniometer. This type of effect is also caused by flexion and varus-valgus rotations. The magnitude of these translations is a function of
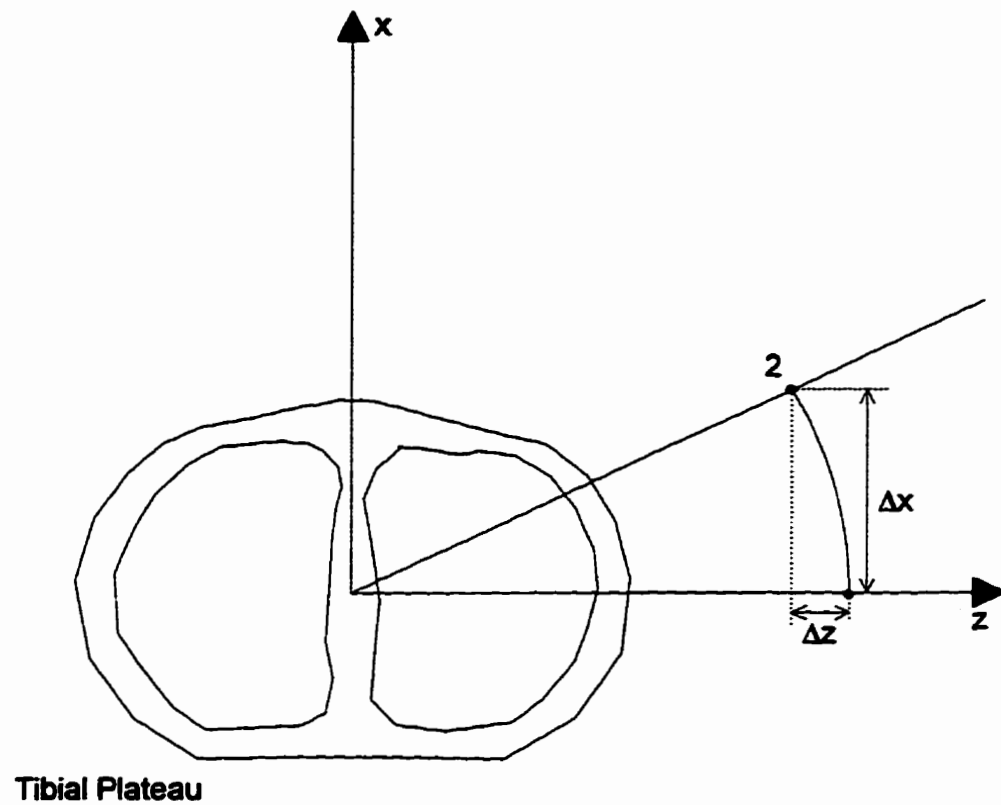
FIGURE 3.1: During pure tibial rotation the goniometer will move from point 1 to 2. The goniometer's remote location causes it not only to rotate, but also to translate by Δx and Δz.

distance from the joint to the goniometer, as well as the geometry of the goniometer itself. In order to select the potentiometers for the goniometer an estimation of the required range for each potentiometer is required. To aid in this process the preliminary goniometer design and its transformation equations were used.

The linear potentiometers chosen for the design were purchased from Techni Measure and are model 8FLP10A manufactured by Sakae. These conductive plastic linear potentiometers have an independent linearity tolerance of ±1.0%, a mass of 5g, internal friction less than 0.3 N, and an internal resistance of 1 kΩ. The range is 11mm, which is perfect for this project.

The rotational potentiometers are model LNB22, also manufactured by Sakae. They are a single turn, continuous rotation potentiometer with a maximum independent nonlinearity of ±0.5%, and an internal resistance of 10 kΩ. These are the smallest suitable potentiometer found and are very smooth operating. Their mass, however, is 22g which is much greater than the linear potentiometers.

The calibration of the potentiometers is described in Chapter 5.

3.2.3 Design Overview

The basic design concept for the goniometer, which was developed in Chapter Two, is to connect together a "chain" of three linear and three rotary potentiometers. This method allows the goniometer to record the three-dimensional motion of the rabbit knee joint in terms of the six degrees of freedom. The concept of a "chain" of potentiometers allows a random motion to travel through the goniometer being recorded by the appropriate potentiometers. The "chain" concept also allows the designer the freedom to arrange the potentiometers in the best possible order to simplify the design.

Chapter Two also recommends that the potentiometers themselves be used as part of the frame of the goniometer. This will reduce the complexity, the size and the weight, of the goniometer. Based on these concepts, the goniometer will be a chain of potentiometers held together by a series of brackets.

3.2.3.1 Potentiometer Arrangement.

The arrangement of the potentiometers is dictated by the kinematics of the knee joint. When the goniometer is attached to the leg it must not create any resistance to the knee's natural motion. To achieve this goal the ordering of the potentiometers is crucial. A poorly planned potentiometer order will cause the "chain" to work against itself and may even limit some ranges of motion. As an example of this the kinematic linkage developed by Hollis *et al.* (1991) is shown in Figure 3.2. This design is very elegant in that at 90 degrees of flexion the potentiometers are aligned so that each one measures one of the common clinical descriptions of knee motion, such as tibial rotation. However, if the linkage is visualized at full extension, then all of the linear potentiometers will be in a single plane. The potentiometer measuring anterior-posterior translation will be parallel to the proximal distal transducer, and all anterior-posterior motion will be prevented by the linkage. Hence this linkage is only capable of measuring all six degrees of freedom at certain joint angles. The second factor controlling the arrangement of the potentiometers is the design constraint stating that the overall length of the goniometer must not exceed 50mm. This is required so that it will be compatible with the joint space of a rabbit's knee. In determining the final arrangement of the potentiometers it is necessary to visualize how they can be arranged to best meet the following criteria: a) minimize the size of the goniometer, b) allow each potentiometer the freedom to move through its required range of motion, and c) allow the rabbit's leg to move freely through its entire range of motion with the goniometer attached to either leg, medially or laterally.

When determining the final arrangement of the potentiometers it was decided to not attempt to measure the clinical descriptions of joint motion directly. Instead the goal was to create a linkage, using three linear and three rotational potentiometers, that was capable of moving through, and hence measuring all six degrees of freedom, regardless of the orientation of the bones. This system complicates the transformation equation as
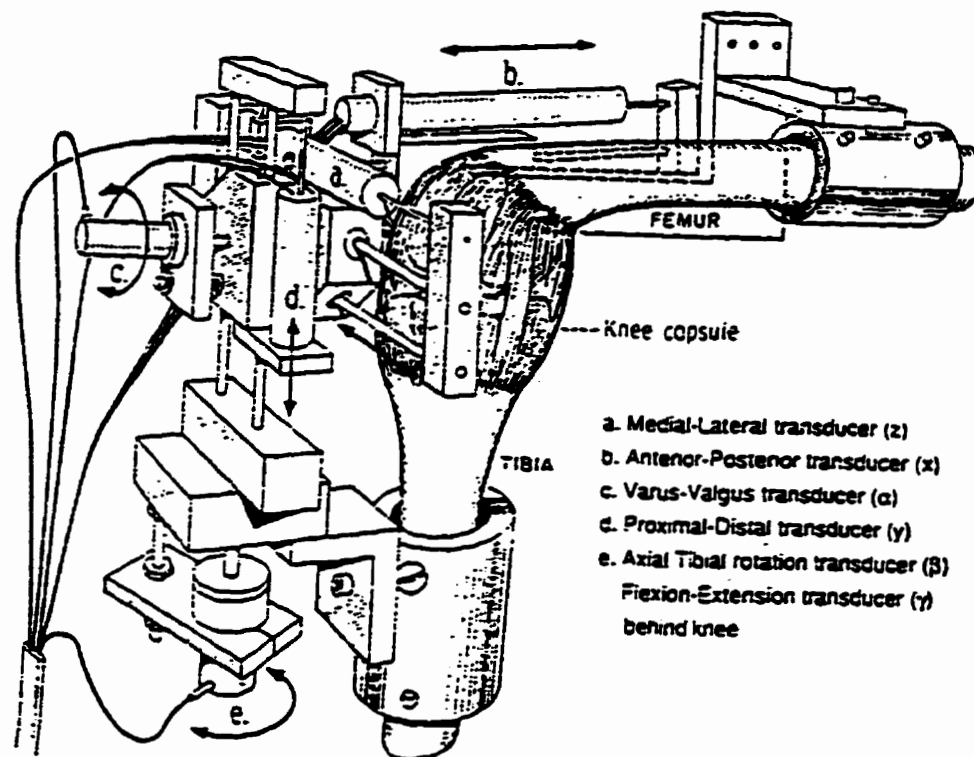
Figure 3.2: The kinematic linkage designed by Hollis *et al*. for use on human cadaver knees (from Hollis *et al*. 1991).

certain motions will be measured by more than one potentiometer, but this problem is easily handled using the system of matrix multiplication described in Chapter 4. The best arrangement for the potentiometers was to group the linear and rotary potentiometers together. This prevents the problems described regarding the linkage shown in Figure 3.2, where a rotation changes the orientation of the linear potentiometers and hence limits the range of motion.

The final arrangement of the potentiometers is shown in Figure 3.3. The chain starts at the femur with three mutually perpendicular rotary potentiometers. The first potentiometer in the chain is roughly aligned with the axis of flexion. This solves the problem of this large rotation changing the alignment of the other potentiometers. In addition this arrangement allows rotary potentiometer number two to roughly measure varus-valgus motion and rotary potentiometer number three to roughly measure tibial rotation. Next in the chain are the linear potentiometers. Because they are anchored to the tibia anterior-posterior translation is roughly measured by linear potentiometer number one, and proximal-distal translation is roughly measured by linear potentiometer number three. Depending on joint angle, medial-lateral translation will be measured by a combination of linear potentiometers two and three. In all cases the clinical descriptions of knee motion are described as being "roughly" measured by a certain potentiometer. This is because the goniometer will never be attached to a leg in perfect alignment with the ISB coordinate system. The exact motion of the bones, measured by the goniometer, will be determined by the transformation equations.

This potentiometer arrangement creates a good balance between allowing all six degrees of freedom of motion, at all joint angles, while still giving a rough estimation of all three clinical rotations, and two of the translations, used to describe knee joint motion. This will allow researchers to monitor everything but medial-lateral translation during the course of an experiment, by observing the output of the appropriate potentiometer. With the ordering of the potentiometers finalized, the design of the brackets to connect the potentiometers together, can be considered.
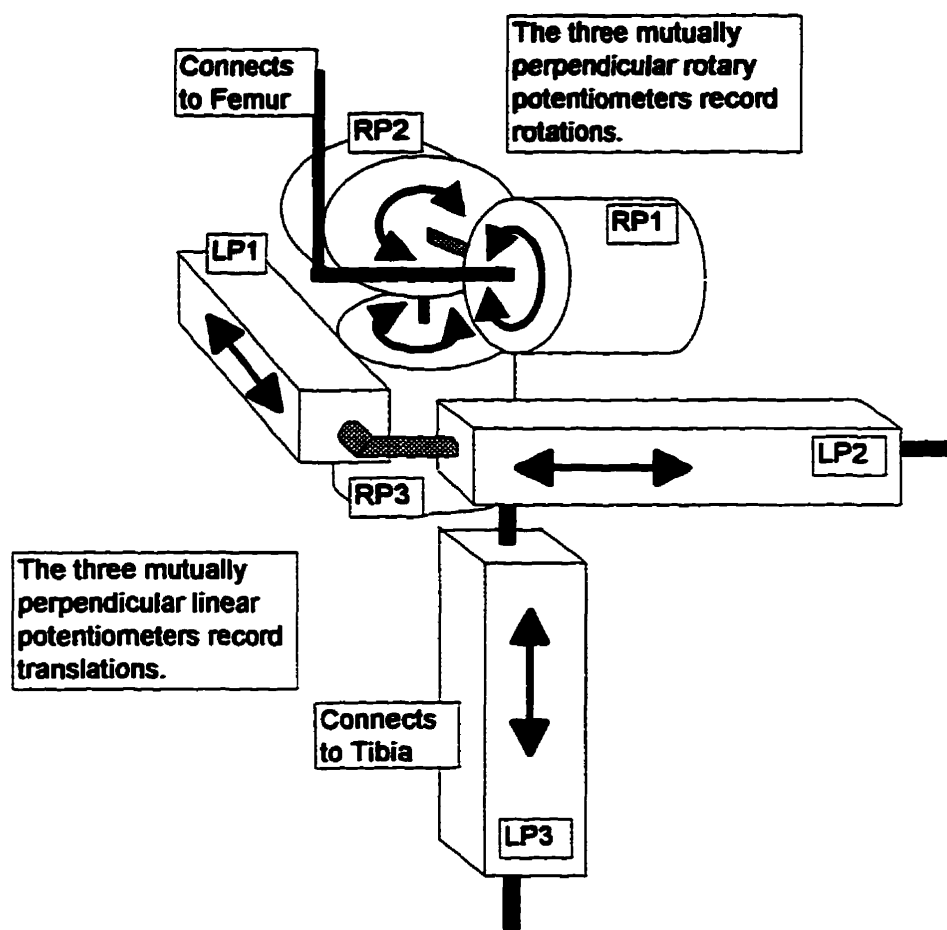
Figure 3.3: As a random motion passes through the goniometer it is recorded by the appropriate linear (LP) and rotary (RP) potentiometers. Either the shaft or housing of each potentiometer is connected to the proceeding potentiometer creating a chain. For details of potentiometer connection see Figure 3.5.

3.2.3.2 Bracket Design.

The design of the brackets is also controlled by the design constraints detailed in Chapter Two. The constraints which are the most relevant are, the goniometer should be: a) as light as possible, and b) sufficiently rigid to prevent errors due to internal deflections.

The internal forces in the goniometer are caused by its mass and the frictional resistance of its moving components, the potentiometers. The potentiometers operate very smoothly. The manufacturer's rating for the friction in the linear potentiometers is less than 0.3 N. In addition the potentiometers are also very light. The linear potentiometers each weigh 5g and the rotary potentiometers each weigh 22g. Therefore the forces caused by friction and mass are expected to be so low that even very small brackets will be able to transmit the loads easily, with a minimum of deflection. (This has been proven to be a reasonable assumption as the goniometer has been attached to numerous rabbit legs, which have undergone a total of several hundred cycles of flexion. The goniometer has provided accurate results and shows no sign of any plastic deformation or fatigue in the brackets.)

The brackets were manufactured out of aluminum, which is a light-weight rigid material. This allows the brackets to be very small and light, while still being sufficiently rigid to prevent deflections. With the bracket size minimized, the majority of the goniometer's mass is due to the potentiometers. Therefore, with light-weight potentiometers, the design constraints of low mass and high rigidity have been met.

In addition to the brackets that connect the potentiometers together, the linear potentiometers require a stabilizing rod system to prevent the shafts from rotating within the potentiometers. This system is shown in Figure 3.4. A Nylatron block is attached to the side of the potentiometer, and contains a hole in which the stabilizing rod slides. Nylatron is chosen for this piece because of it's self lubricating quality, and resistance to creep. The stabilizing rod is cut from 1/16" drill rod, which is used because of its rigidity and smooth finish. An aluminum block connects the stabilizing rod to the

47
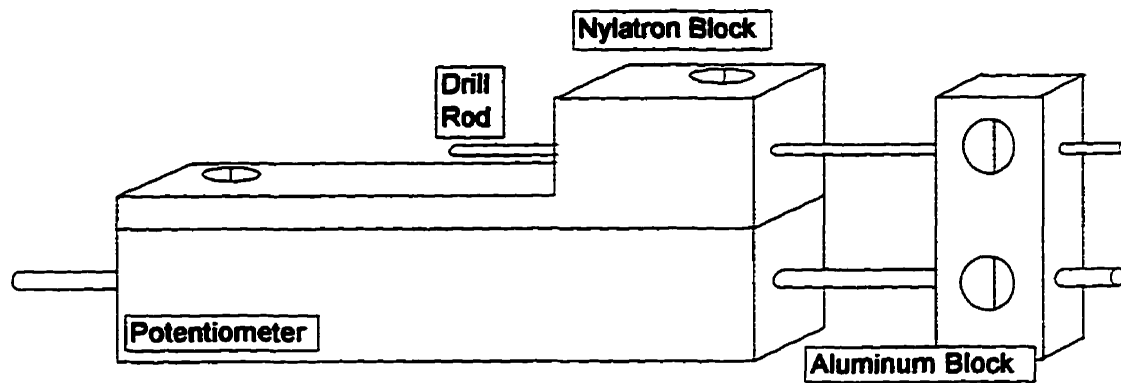
FIGURE 3.4: Stabilizer rod system. The aluminum block anchors the potentiometer shaft to the drill rod, which, slides freely within the Nylatron block. This prevents the potentiometer shaft from rotating within the potentiometer.

potentiometer shaft using two set screws. Each of the three linear potentiometers is fitted with the stabilizing rod set-up.

In total six different brackets are required to connect the potentiometers together. The brackets are lettered a-f and their exact dimensions are shown in Figure 3.5. Figures 3.6a and b detail how the potentiometers are connected together using the brackets and stabilizing rods. Note that Figure 3.6a does not show linear potentiometers 2 and 3, and that Figure 3.6b does not show rotary potentiometers 1 and 2.

Now that the goniometer design has been finalized, a system is required for attaching it to the tibia and femur. At either end of the chain, a 50mm long, 4mm diameter aluminum rod is attached. Each rod has two sliding aluminum connection blocks, which are used to attach the rods to the bone pins, as shown in Figure 3.7.

3.2.3.3 Bone Pins.

The bone pins are the only part of the goniometer that will be in direct contact with the rabbit. This direct contact mandates that the pins must be manufactured out of surgical stainless steel to minimize rejection and corrosion within the rabbit, both of which could negatively affect test results. The other demand on the bone pins is that they are capable of rigidly connecting the goniometer to the tibia and femur.

The bone pins used with the goniometer are 1/16" threaded K-wire. Two pieces are threaded into 3/64" pre drilled holes, which pass entirely through the bone, perpendicular to the long axis. Two pieces of wire are needed for each bone to ensure that the goniometer is rigidly attached. A single piece of K-wire is unsuitable because it could easily rotate within the bone, during testing, and cause errors.

3.2.4 Final Design

The final design of the goniometer is shown in Figure 3.8. The minimum distance between the bone pin connection blocks is 40mm, so the goniometer passes the criteria of being less than 50mm long. The total weight of the goniometer is 116g. The
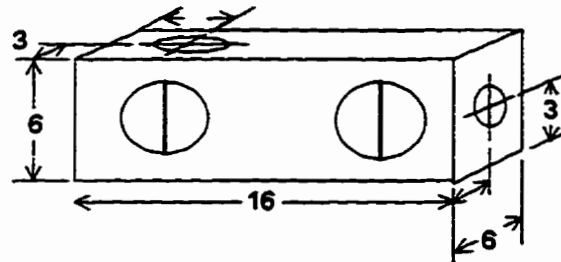
FIGURE 3.5a: Bracket a (Dimensions in mm).
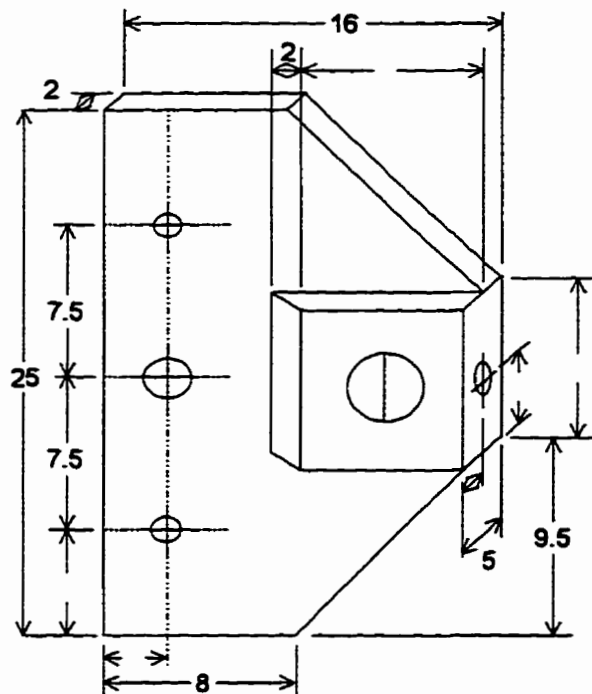
FIGURE 3.5b: Bracket b (Dimensions in mm).
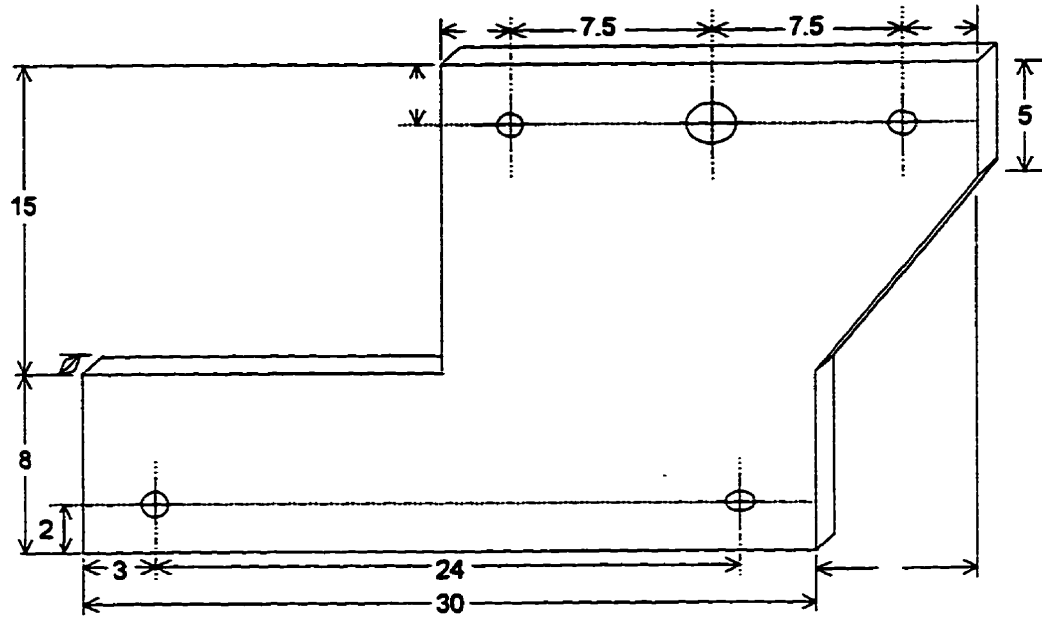
FIGURE 3.5c: Bracket c (Dimensions in mm).
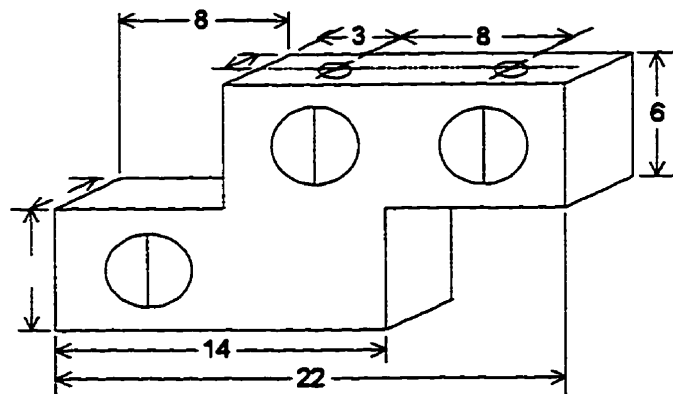
FIGURE 3.5d: Bracket d (Dimensions in mm).
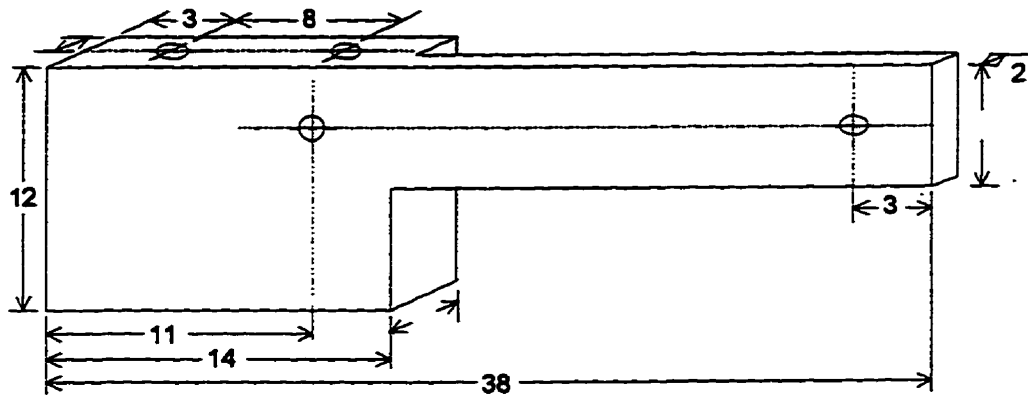
FIGURE 3.5e: Bracket e (Dimensions in mm).
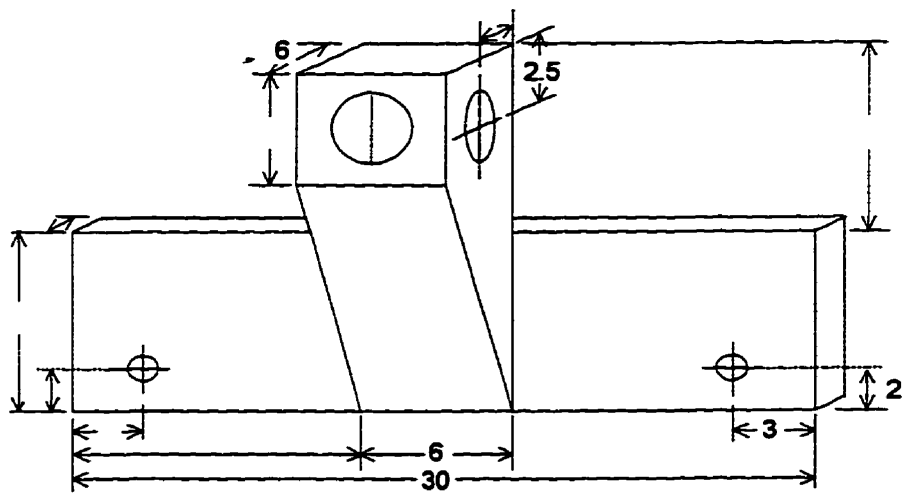
FIGURE 3.5f: Bracket f (Dimensions in mm).
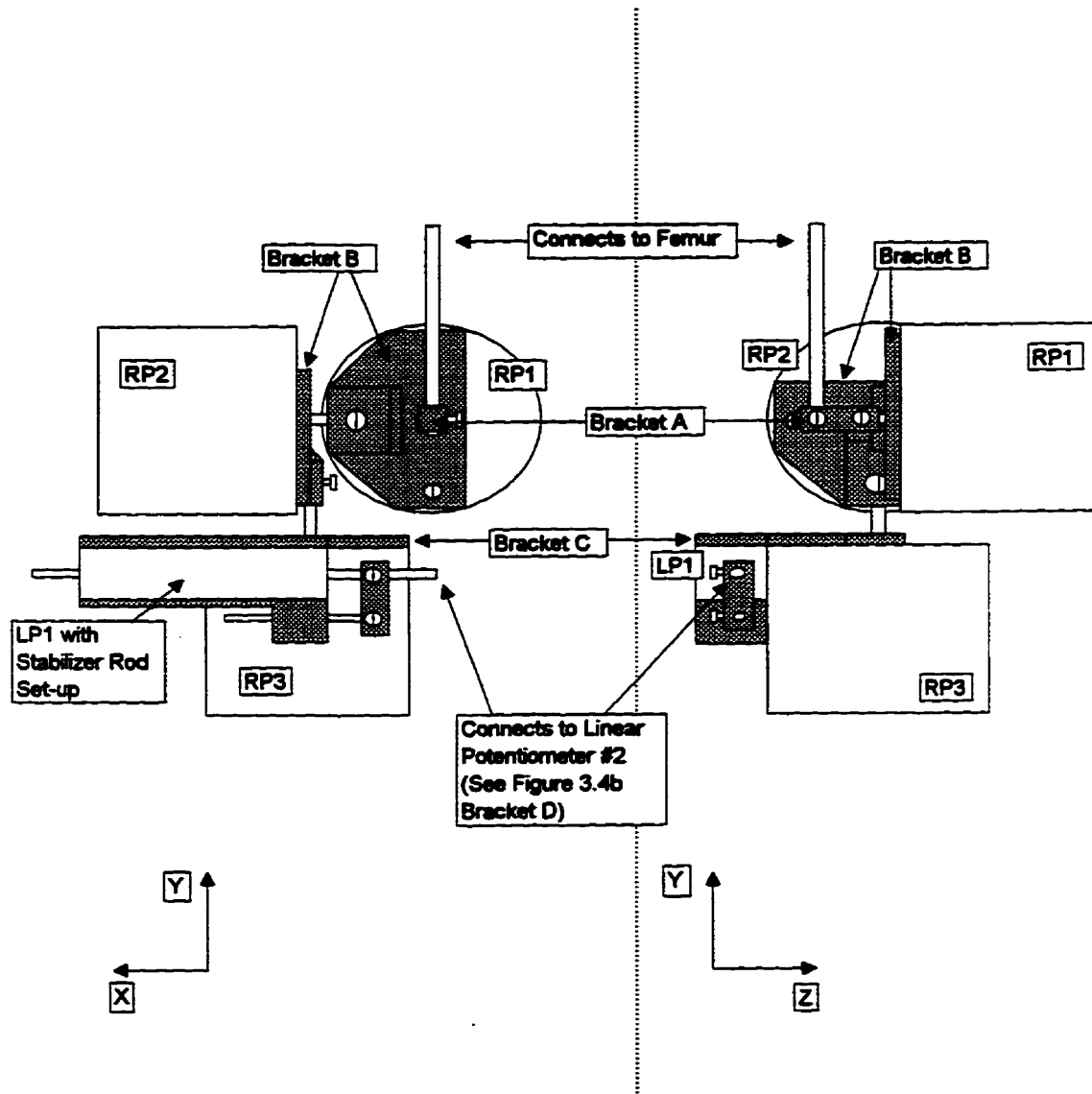
FIGURE 3.6a: Connection of Rotary Potentiometers. Note that for clarity
linear potentiometers 3 and 4 are not shown. See Figure 3.6b for details of
linear potentiometer connection.
LP = Linear potentiometer
RP = Rotary potentiometer
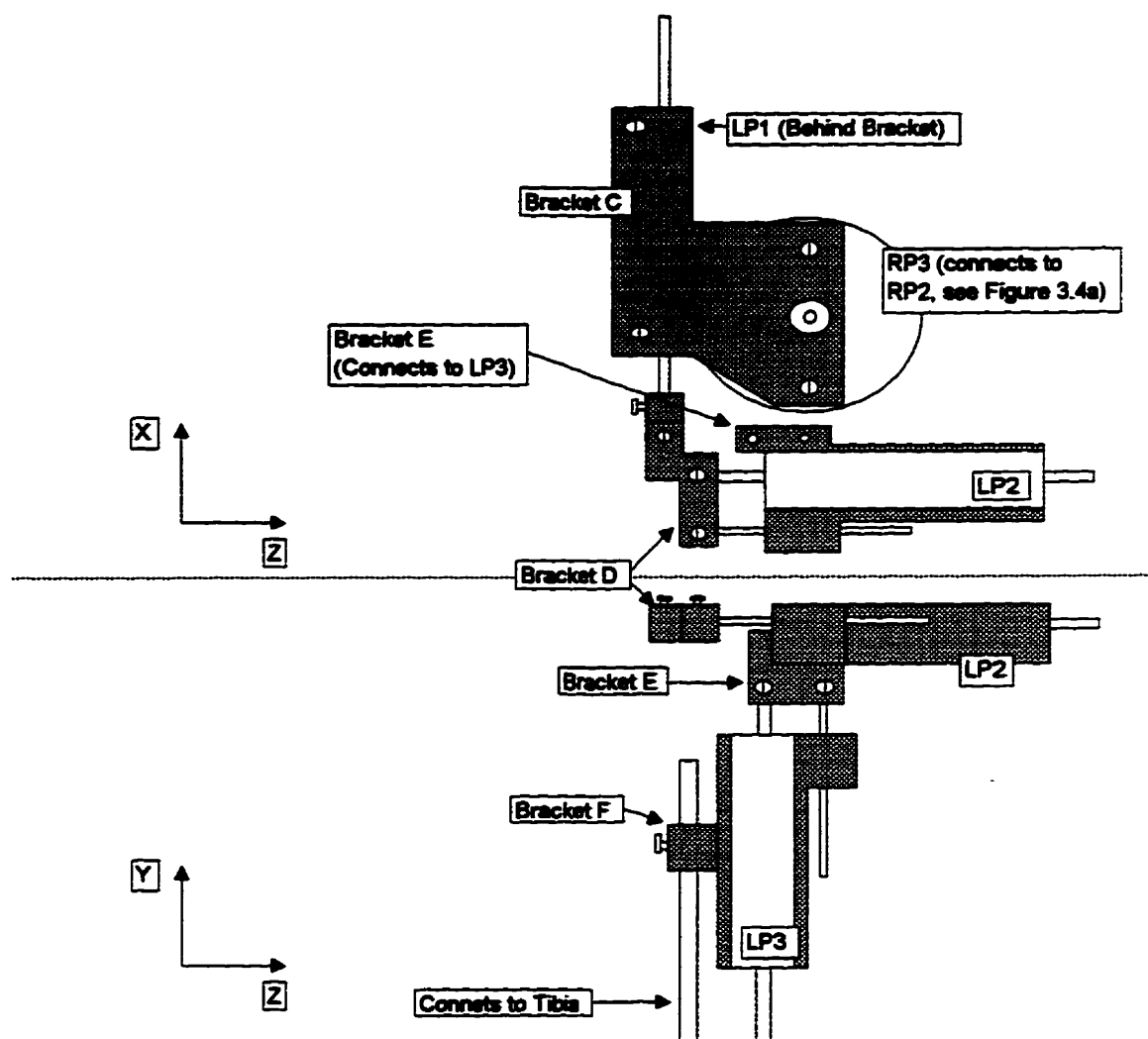
FIGURE 3.6b: Connection of Linear Potentiometers. Note that for clarity rotary potentiometers 1 and 2 are not shown. See Figure 3.6a for details of rotary potentiometer connection.

LP = Linear potentiometer

RP = Rotary potentiometer

Femur

Rod connects to
goniometer via
bracket A.
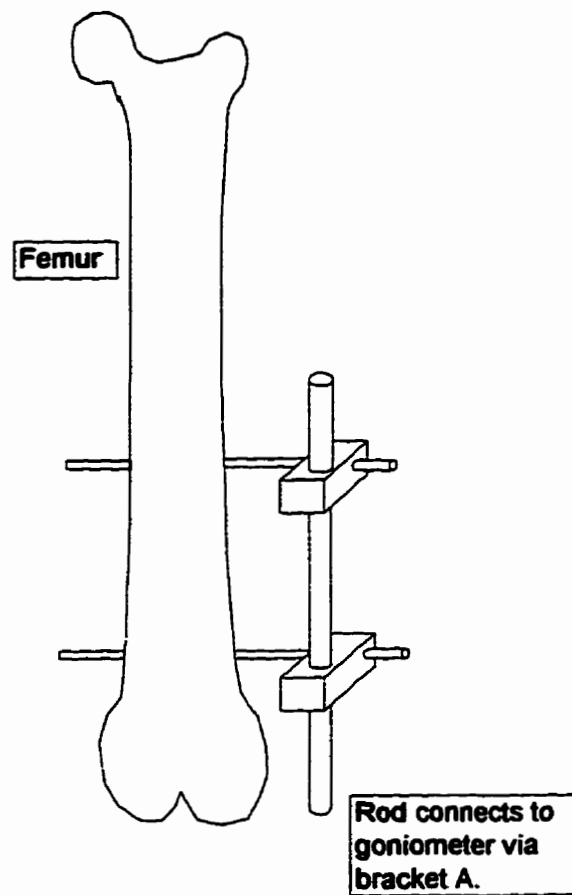
FIGURE 3.7: The goniometer connects to the femur and tibia via the
bone pin and connection block system shown above. The connection
blocks anchor the bone pins to the rods using set screws.
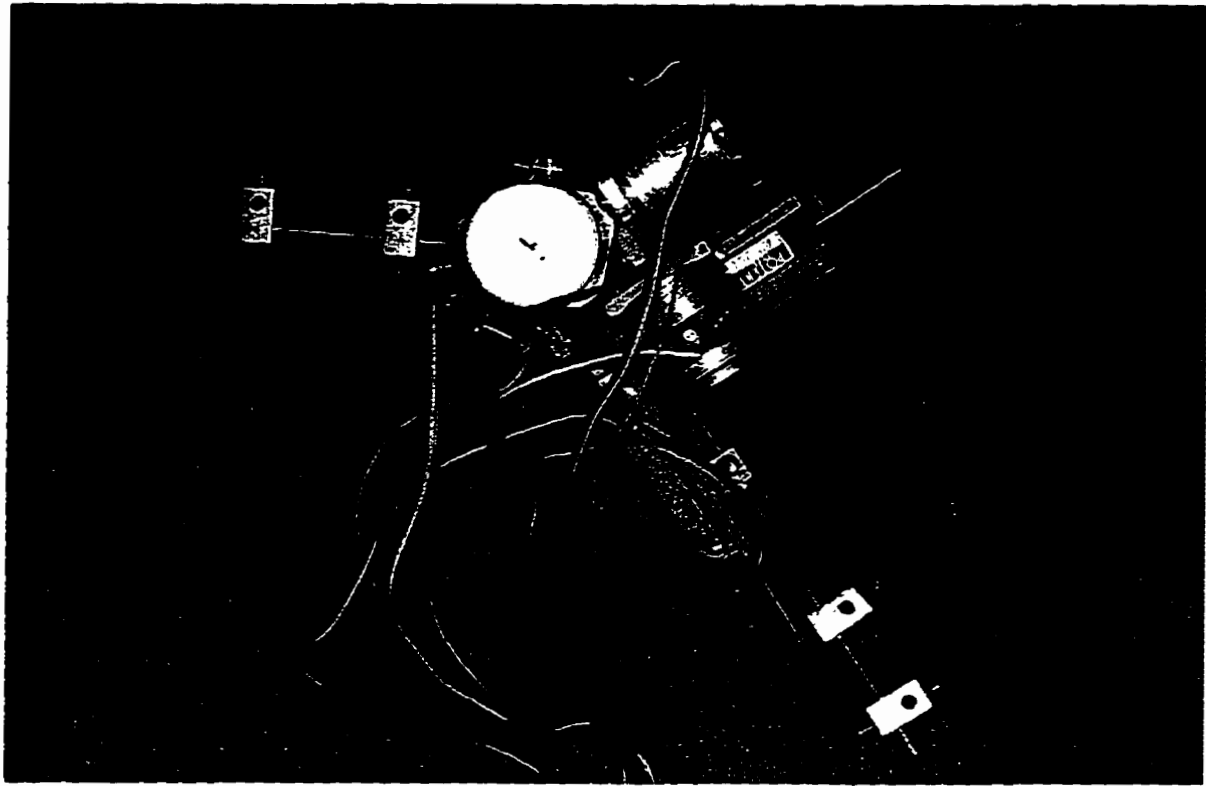
Figure 3.8: The final goniometer design.

potentiometers weigh 81g and are the lightest models available that are suitable for this application. The frame of the goniometer weighs only 35g, hence the total weight has been kept to a minimum. The goniometer is able to record the motion of the knee accurately, with a minimal impact on its natural motion, because of the: a) smooth operation of the potentiometers, b) rigidity of the frame, and c) light-weight design.

3.3 Safety Considerations

Safety is a factor in almost every engineering design and includes problems of strength, reliability, and accident prevention. Pahl and Beitz consider safety to be one of the basic rules of embodiment. The designer can increase the safety of a design by three different techniques. The direct method, which is the most effective, involves including safety from the start in order to preclude danger. The indirect method, which should be avoided, involves the use of protective systems. Finally, safety warning systems should only be used as a last resort. The demand for safety can complicate a design as well as increase the cost, but the long term advantages of a safe design will usually outweigh the disadvantages.

Safety, in the design of technology, can be divided into four categories. They are *component safety* (properly designed parts), *functional safety* (safe operation of the product), *operator safety* (safety of the product user), and *environmental safety* (safety of humans not using the product). During the design of any product the safety of each component should be analyzed throughout each step of the design process.

The design of the goniometer requires safety to be analyzed from both a medical and engineering perspective. The medical perspective requires that the device should not cause any unnecessary injury to the rabbits, and not compromise the safety of the operator. The engineering perspective requires that the device be evaluated in terms of strength, toughness, reliability, and component protection.

During the embodiment of the goniometer, safety is always a consideration. In terms of the rabbit's safety, the biggest concern is contamination of the leg, which could lead to infection in a longitudinal test on a live animal. This problem is solved by using stainless steel for the mounting pins. These pins are the only components in direct contact with the rabbit. Operator safety is not considered a problem as the goniometer has no sharp edges and operates with a very low current. Safety from the engineering perspective is accounted for by a sturdy design and a proper selection of materials. It should be noted that the goniometer is durable and able to withstand the loading expected during testing, but not rough treatment. Therefore careful handling is required.

3.4 Auxiliary Functions

To make the goniometer a useable product, several auxiliary functions must be provided. The first is a system for collecting the output data. In addition, a method must also be devised by which the goniometer can be mounted in a reliable and repeatable fashion.

3.4.1 Data collection

Data collection is currently being performed using a BRAND D/A converter connected to a PC running LabTech Note Book version 7.0.0. To facilitate the goniometer's connection to the computer and power supply, a connection box has been constructed. It connects all of the potentiometers to a single power supply and allows for the individual monitoring of any of the six potentiometers, using a digital multi-meter. The goniometer, connection box, power supply, and computer link-up system is shown in Figure 3.9. In addition to recording the output of the potentiometers, LabTech Note Book is also used to record the time and monitor the power supply (to check that the output is constant during testing.)
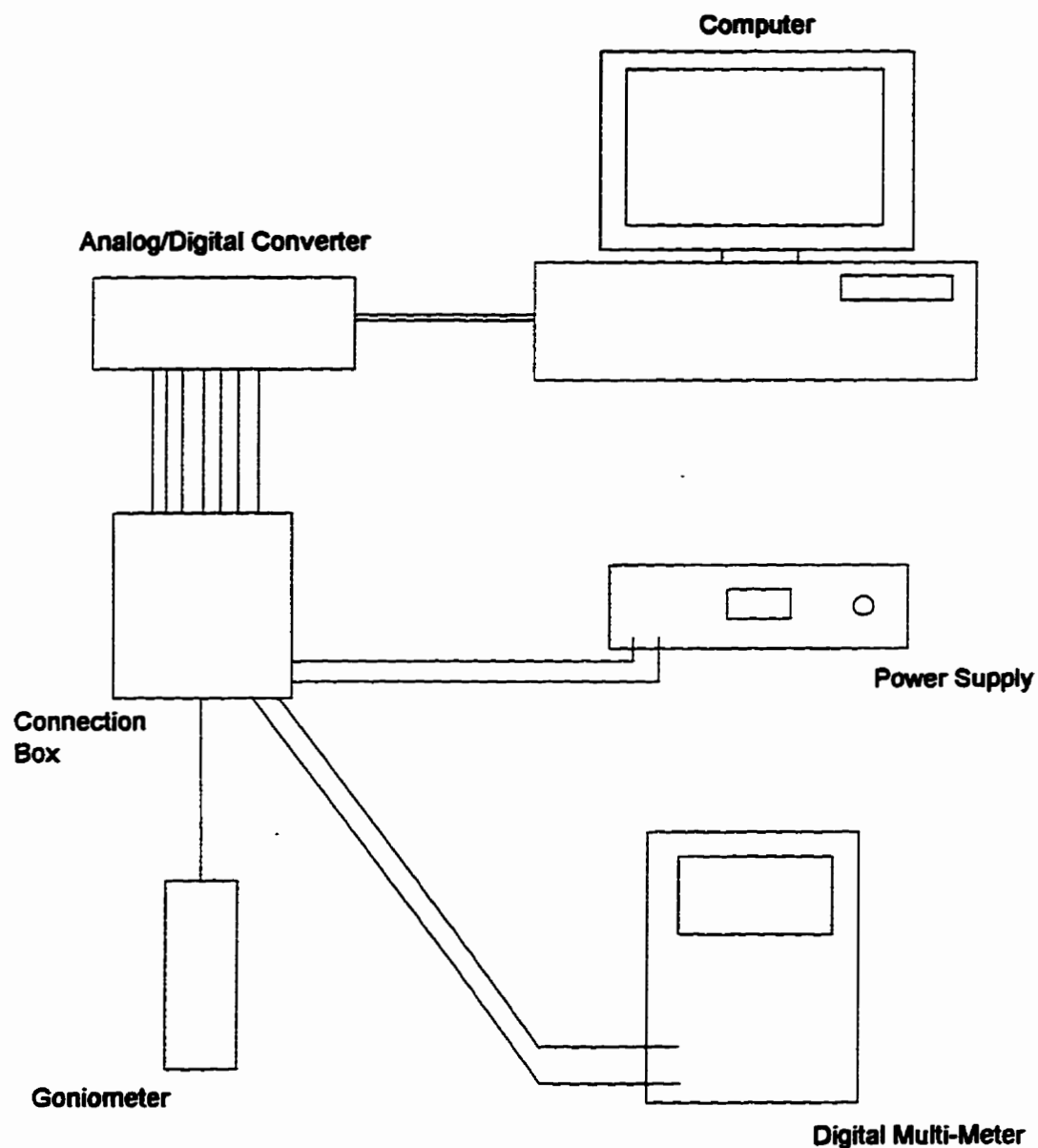
FIGURE 3.9: Goniometer/Data Acquisition Set-up. The connection box connects the goniometer to the analog/digital converter and power supply. The connection box also allows the digital multi-meter to monitor either the power supply or any of the potentiometers individually.

3.4.2 Mounting of the goniometer

As mentioned earlier, in section 3.2.1, the goniometer will be attached to the rabbit using two pieces of K-wire inserted into both the tibia and the femur. This was another one of the difficult challenges in the goniometer design process. For the mounting system to be acceptable it must provide two functions. The first is to ensure the proper insertion of the K-wire into each bone. This requires that both pieces of K-wire, in each bone, are properly located, parallel, and pass squarely through the bone. This task is complicated by the complex shape of the bones, and the large muscle mass surrounding a rabbit's leg. The second function of the mounting system is to provide a method for reattaching the goniometer in a repeatable fashion. Longitudinal studies will require that the goniometer be removed from the leg for long duration's of time and then reattached with the same initial alignment. However, because of the goniometer's ability to measure six degrees of freedom, it is capable of assuming many different alignments. The challenge, therefore, is to develop a system which ensures that the goniometer has the same initial alignment, each time it is attached to a rabbit.

The mounting jig shown in Figure 3.10 was designed to achieving both of the key functions of the mounting system. The mounting jig's first role is to act as a drill guide. V-notched guide tubes, shown at the tibial end of the mounting jig in Figure 3.10, and detailed in Figure 3.11, act as the drill guide. These tubes are clamped into the mounting jig, and the V-notch at the bottom is used to centre the tube over the bone. By inserting a drill into the tube, a pilot hole for the K-wire, which passes squarely through the bone, can easily be drilled. Without moving the mounting jig, the K-wire is inserted into the pilot holes with the assistance of the guide tubes. This process has proven to be a reliable and simple method of securely inserting the K-wire into the bones.

The large muscles surrounding the femur make aligning the guide tubes on this bone more difficult than on the tibia. The easiest system is to insert the K-wire into the femur first. Once the K-wire has been inserted into the femur, the guide tubes are removed from the mounting jig. The K-wire is then securely clamped into the jig as
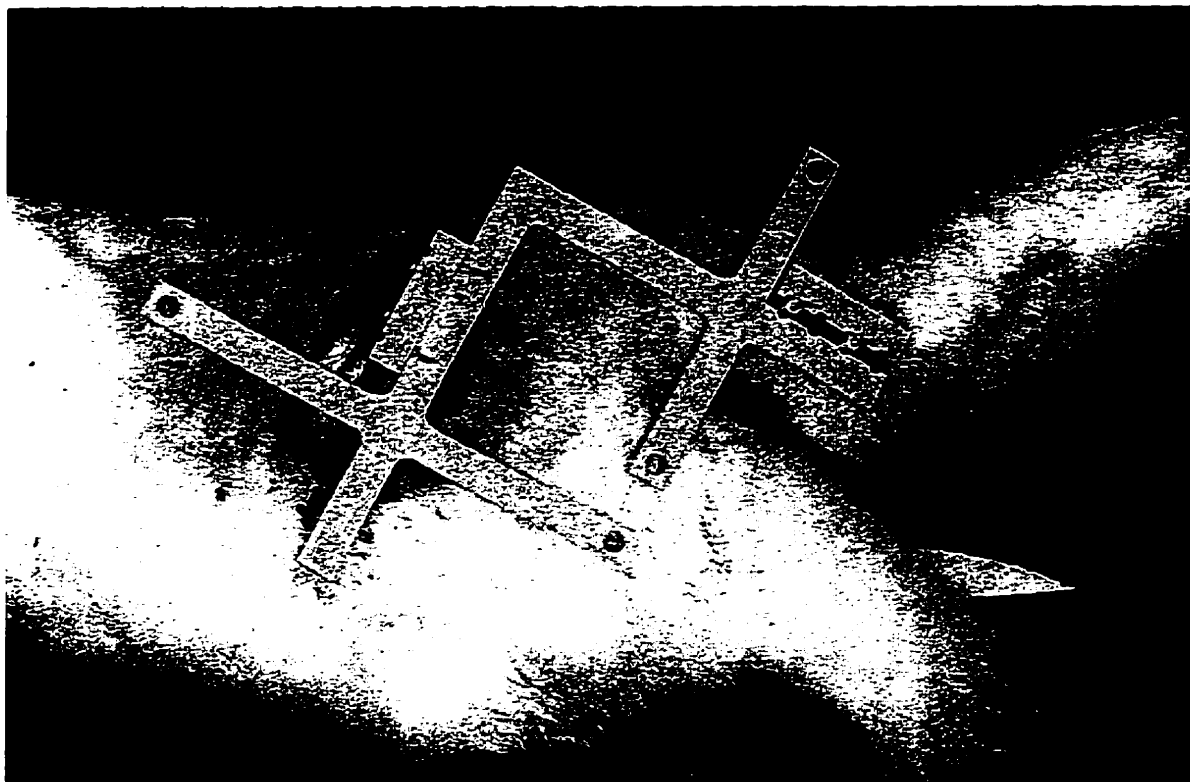
Figure 3.10: The mounting jig is shown during the insertion of the bone pins. At the tibia, the bone pins have just been inserted, with the assistance of the guide tubes, which are clamped into the mounting jig. At the femur, the guide tubes have been removed, and the bone pins are shown clamped into the mounting jig.
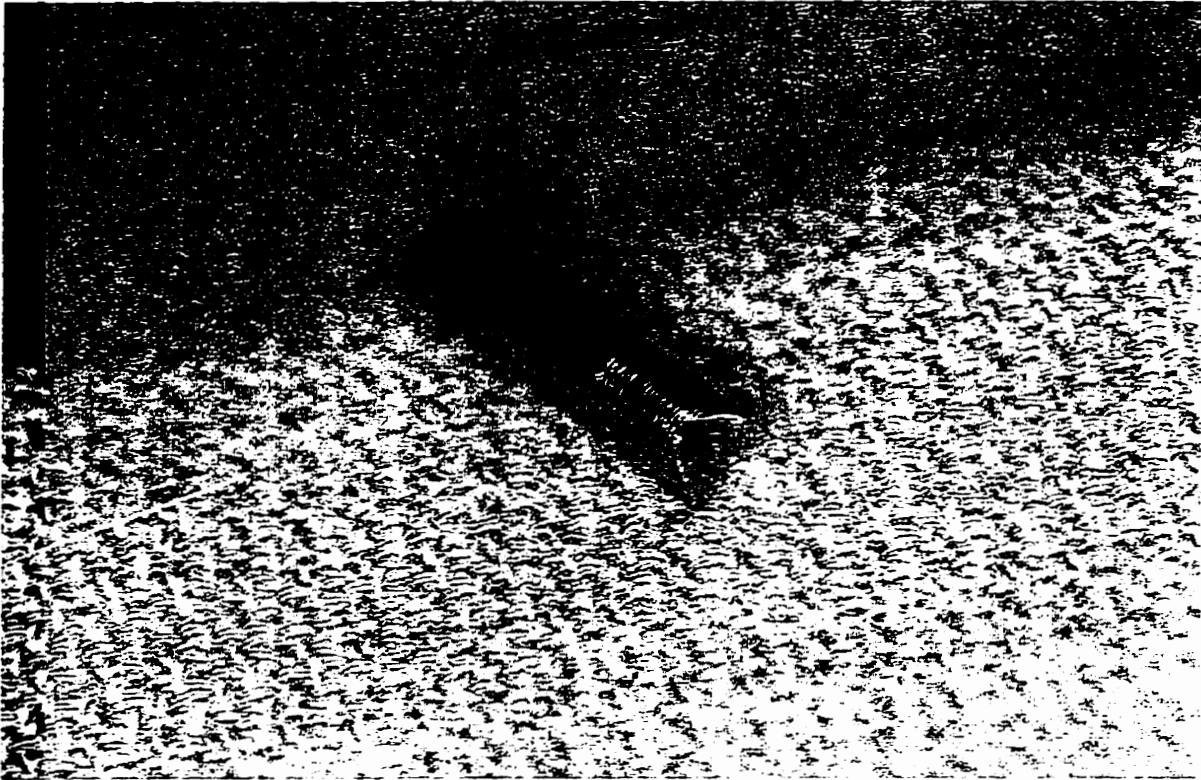
Figure 3.11: Detail of one of the guide tubes, showing the V-notch, which assists in aligning the mounting jig over the bone.

shown at the femoral end of the mounting jig in Figure 3.10. This holds the jig securely to assist in inserting the K-wire into the tibia. After the K-wire has been inserted into the tibia these wires are also clamped by the mounting jig.

With the K-wire securely held by the mounting jig, the goniometer is easily slid on, and secured, as shown in Figure 3.12. The mounting jig is removed, leaving the goniometer securely attached to the K-wire, as shown in Figure 3.13. When the goniometer was first attached to the knee its orientation had to be adjusted relative to the joint. This is done by moving the rod, attached to the goniometer, back and forth through the connection blocks shown in Figure 3.7. The process used was to line up the outside corner of the mounting jig with the patella, as shown in Figure 3.10. The K-wire was then inserted into the bone, and clamped into the jig. Next the goniometer was slid onto the K-wire and the connection blocks were adjusted, to roughly align the shaft of rotary potentiometer number one, with the axis of flexion. Finally, the mounting jig was removed, and the leg was manually moved through its full range of motion to ensure that the goniometer did not cause any hindrance. After this initial adjustment further mounting of the goniometer requires only that the corner of the mounting jig be lined-up with the patella. This ensures the correct orientation of the goniometer relative to the joint.

The jig shown in Figure 3.10 was used to attach the goniometer in conjunction with a load cell, designed to measure the force in the medial collateral ligament. This load cell extended ~70mm distally from the knee. This forced the K-wire in the tibia to be inserted further from the knee than would be optimal. Ideally the pins should be located as close to the joint as possible, and at least 2 cm apart, to minimize any errors due to deflections. However, the goniometer is designed to accommodate the bone pins being located anywhere along the long axis of the bone.

The ability to clamp the K-wire into the mounting jig solves the problem of reattaching the goniometer in a repeatable fashion. Clamping the K-wire into the jig assures consistency in the initial alignment of the goniometer. Chapter Five investigates

Figure 3.12: The goniometer is shown, connected to the bone pins, which are securely clamped into the mounting jib. This point in the mounting procedure can be used as a datum for long term testing. Note the plastic film between the goniometer and the leg to protect the electronic components.
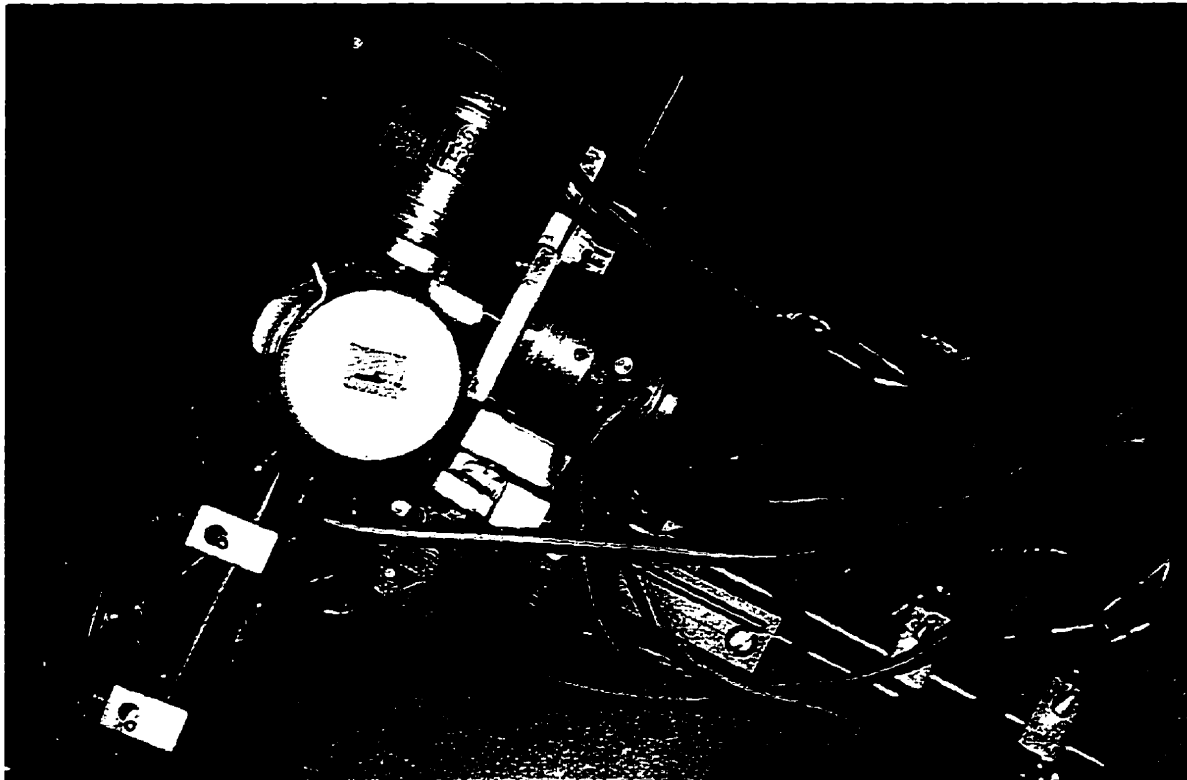
Figure 3.13: The goniometer is shown attached to the bone pins after the mounting jig has been removed.

the effectiveness of the mounting jig in assuring the consistent initial alignment of the goniometer. Long-term studies will require some type of a removable bone pin, as leaving the K-wire in the bone, beyond the duration of a single session of data collection, is obviously undesirable.

3.5 Non-Technical Considerations

In the design of products there are many factors which must be considered besides the basic functional ability of a product. For a product to be fully accepted it must possess more than the simple ability to perform the required task. Other important factors which must be included are usability, appearance, and comfort. Although these factors are outside of the technical range of engineering design they must be given serious consideration.

Rating the goniometer in terms of its usability, appearance, and comfort, the only area where it could be criticized is its usability. Almost every aspect of the goniometer's operation is very straightforward, except for the insertion of the K-wire into the bones. For this operation, practice is required to insure that the K-wires are securely inserted. The factor that complicates the insertion of the K-wire is the nature of the rabbits' anatomy. To insert the wire, it is necessary to work around, and through, both skin and muscle. The complex shape, and small size, of the bones further complicates the process. The very functional design of the mounting jig is a great asset in attaching the goniometer. Two practice rounds, using a rabbit leg, have proven sufficient to gain the necessary skill to attach the goniometer consistently to live rabbits.

CHAPTER FOUR: Transformation Equations

4.1 Introduction

For the output data of the goniometer to be of maximum value, they need to be presented in a simple, easily understood form. In Chapter One the ISB Standardization and Terminology Committee's recommendations for standardization in the reporting of kinematic data were presented. The recommendations were intended as a guide for the uniform presentation of kinematic data, with the intent of making publications easier to read and allowing for more straightforward comparisons of data sets. In addition, the recommendations present kinematic data in a form which is both mathematically precise, and easily understood by engineers and physicians.

4.2 Joint Coordinate System

The convention recommended by the ISB committee is shown in Figure 4.1. This system has been adopted for reporting the output data from the goniometer. The purpose of this coordinate system is to allow the relative position of two bodies to be specified. A Cartesian coordinate system is first attached to each body. O_p and O_d represent the origin of the coordinate system attached to the proximal and distal segments respectively. The convention states that the positive x-axis is anterior, the positive y-axis is proximal and the positive z-axis is defined by the right hand rule. F, the floating axis, is the common perpendicular to the z-axis of the proximal segment (z_p) and the y-axis of the distal segment (y_d).

$$F = \frac{j_d \times k_p}{|j_d \times k_p|}$$

Where j_d and k_p are vectors along y_d and z_p respectively.
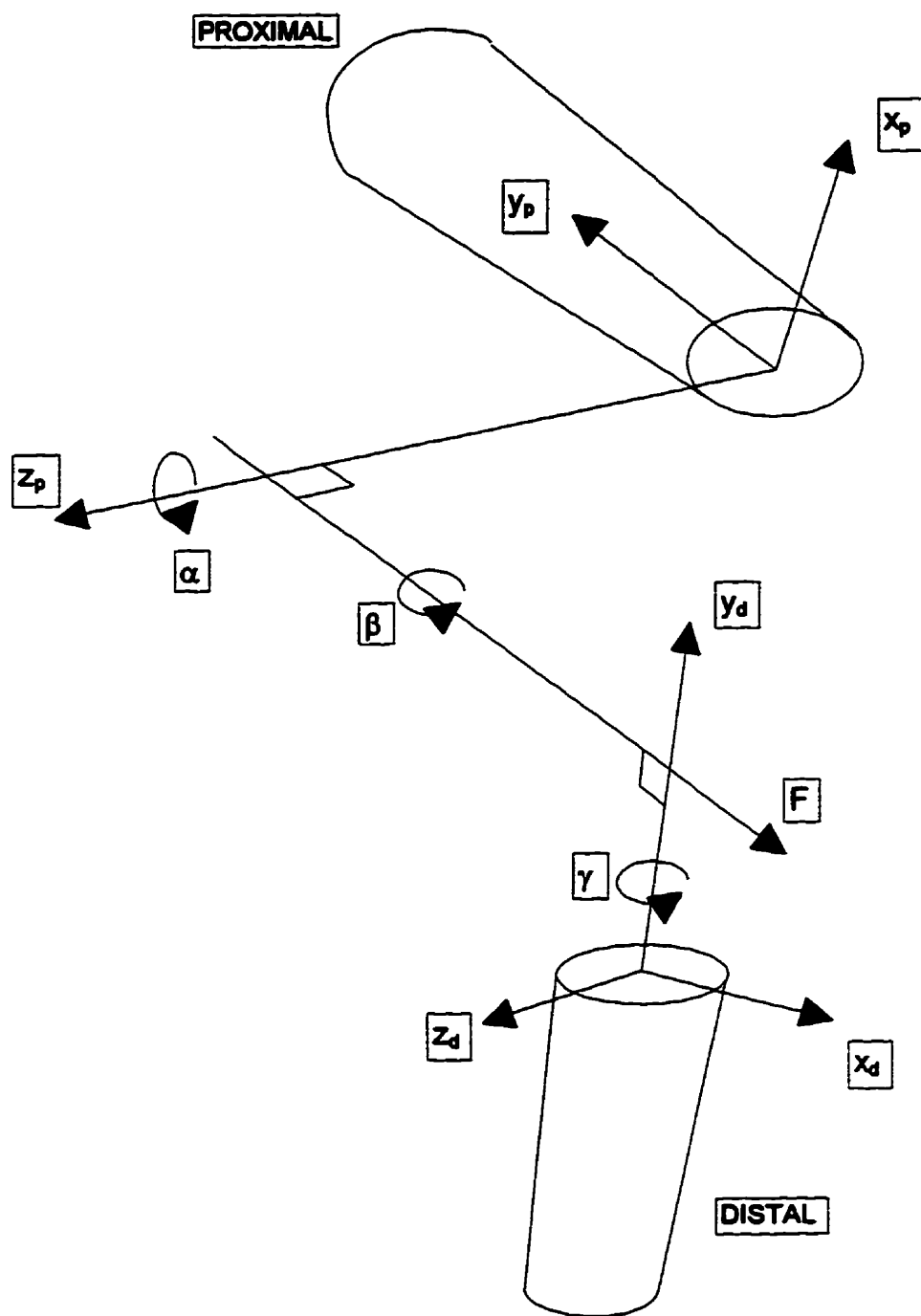
FIGURE 4.1: ISB coordinate system for reporting kinematic data.

The relative rotation of the bodies is taken as the spin of each body about z_p, y_d, and the floating axis. The positive direction is determined by the right hand rule. These rotations are shown in Figure 4.1 as α, β, and γ. The magnitudes of α and γ are the angles between the floating axis and a reference axis in each body. α is the angle between the floating axis and x_p. γ is the angle between the floating axis and x_d. β is a measure of the rotation about the floating axis and is the angle between x_p and z_d.

Joint translations are defined as the relative position of the origins, of the bone coordinate systems. Translations can be thought of in terms of a translation vector whose components are measured along the same axis as the rotations. Hence, the three translations are measured along the z_p, y_d, and floating axis.

The advantage of this coordinate system is that it gives a mathematically precise method of describing joint motion which is compatible with the traditional clinical descriptions of joint motion. In the knee, the rotation α measures flexion-extension, β measures varus-valgus rotation, and γ measures axial tibial rotation. The translations along the z_p, y_d, and floating axis measure medial-lateral, proximal-distal, and anterior-posterior translations respectively.

4.3 Location of the Bone Coordinate Systems

The joint coordinate system requires that a Cartesian coordinate system be located on both the proximal and distal segments. For the rabbit knee, this requires that a set of coordinate axes be established on both the tibia and femur. The coordinate systems are established using bony landmarks as reference points. The method used to locate the coordinate axis on each bone is adapted from a system developed by Grood and Suntay (1983), for the human knee.

Starting with the tibia, the y-axis is located so that it passes midway between the two intercondylar eminences proximally, and through the centre of the ankle distally. The z-axis is defined as a line connecting the approximate centre of each tibial plateau.

The error in locating the plateau centres has no effect on quantifying rotational displacements as all rotations reported are relative. Finally the x-axis completes the Cartesian coordinate system, and is defined as the cross product of the y- and z-axes.

In the femur the y-axis passes through the centre of the femoral head proximally, and at the knee, it passes through the most distal point on the posterior surface of the femur, midway between the medial and lateral condyles. The z-axis runs through the most distal point on the posterior surface of each femoral condyle. The x-axis once again completes the Cartesian coordinate system, and is defined as the cross product of the y- and z-axes.

In order to locate the origin of the femoral coordinate system closer to the approximate axis of flexion the origin is translated along the x-axis. The distance that the origin is translated equals 75% of the distance from the most distal point on the posterior surface of the femoral condyles to the proximal end of the patellar femoral groove. The new z-axis is parallel to the original z-axis and passes through the new origin. The y-axis still passes through the femoral head proximally but now passes through the new origin distally. And finally, the x-axis is recalculated as the cross product of the new y- and z-axes.

4.4 Transformation Equation Theory

To calculate the three translations and three rotations, the location of the tibial coordinate system must be known relative to the femoral system. This information is calculated by using the output data from the goniometer, to perform a series of transformations from the tibia to the femur. The final goniometer design is based on the work of others but contains many new design ideas. For this reason none of the previously developed systems of transformation equations could be directly applied to this goniometer design. Originally it was attempted to calculate the transformations directly, based on the geometry of the goniometer, using a system similar to that

developed by Evans *et al.* (1994). This method became extremely cumbersome as the effect of each additional link was combined with the previous one. Appendix A contains this early set of transformation equations which were useful in the calibration of the goniometer (described in Chapter Five.) In the end a method of coordinate transformations, using matrices, was developed for performing the transformations. This method is based on the systems developed by Grood and Suntay (1983), and by Kinzel *et al.* (1972).

To complete the transformation process a set of coordinate axes is located on each of the bones, and on each link of the goniometer. The overall transformation matrix is calculated by first transforming from the tibia to the first link of the goniometer, and then from link to link through the goniometer until the femur is reached. This system is shown in Figure 4.2.

The matrices used for the transformations are:

$$\begin{vmatrix} 1 & 0 & 0 & 0 \\ 0 & \cos\theta & -\sin\theta & 0 \\ 0 & \sin\theta & \cos\theta & 0 \\ 0 & 0 & 0 & 1 \end{vmatrix}$$

for rotations about the x-axis,

$$\begin{vmatrix} \cos\theta & 0 & \sin\theta & 0 \\ 0 & 1 & 0 & 0 \\ -\sin\theta & 0 & \cos\theta & 0 \\ 0 & 0 & 0 & 1 \end{vmatrix}$$

for rotations about the y-axis,

$$\begin{vmatrix} \cos\theta & -\sin\theta & 0 & 0 \\ \sin\theta & \cos\theta & 0 & 0 \\ 0 & 0 & 1 & 0 \\ 0 & 0 & 0 & 1 \end{vmatrix}$$
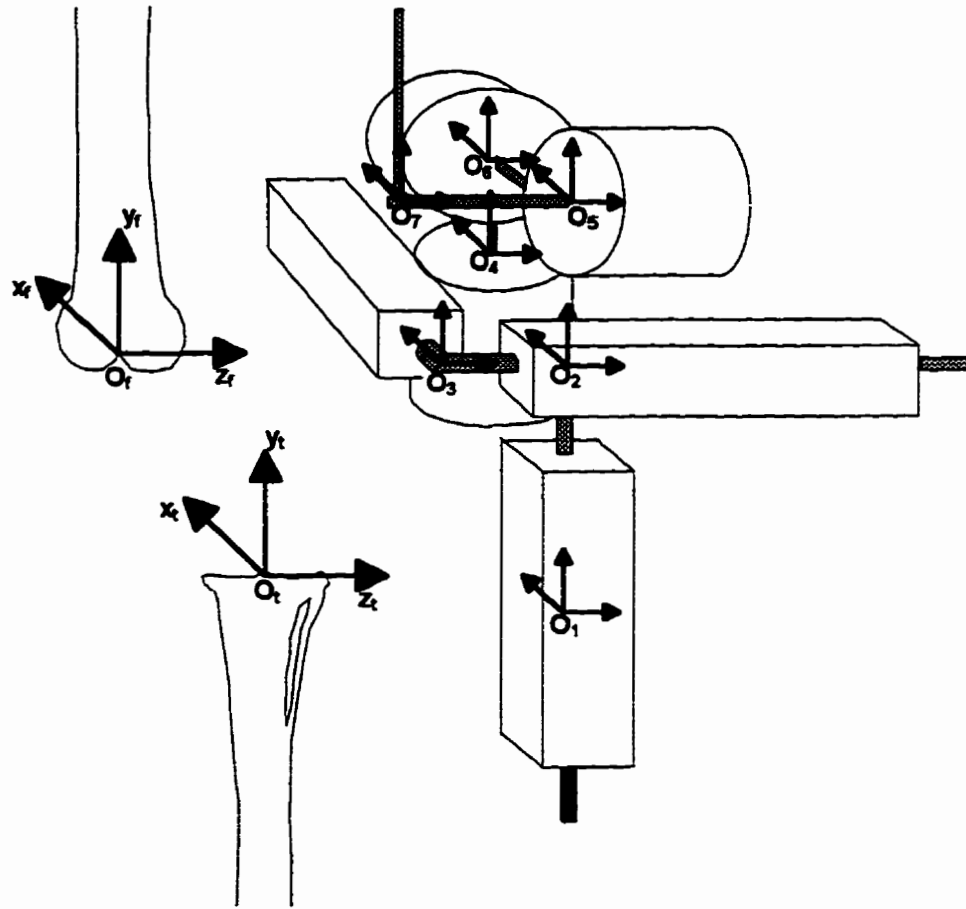
$$[\,\text{Trans}\,] = [O_7 \blacktriangleright O_f]\,[O_6 \blacktriangleright O_7]\,[O_5 \blacktriangleright O_6]\,[O_4 \blacktriangleright O_5]\,[O_3 \blacktriangleright O_4]\,[O_2 \blacktriangleright O_3]\,[O_1 \blacktriangleright O_2]\,[O_t \blacktriangleright O_1]$$

FIGURE 4.2: A set of coordinate axis is attached to each link of the goniometer and to both the femur and tibia. The overall transformation matrix between the femur and tibia is then calculated by multiplying the individual transformation matrices between each of the coordinate systems.

for rotations about the z-axis, and

$$
\begin{vmatrix}
1 & 0 & 0 & X_t \\
0 & 1 & 0 & Y_t \\
0 & 0 & 1 & Z_t \\
0 & 0 & 0 & 1
\end{vmatrix}
$$

for translations along any axis, where X_t, Y_t, and Z_t represent the translation along the respective axis. The transformations from link to link within the goniometer will include a fixed translation, based on the geometry of the goniometer, and either a variable rotation or translation which is based on the output of the potentiometers. If the three rotation and one translation matrix shown above are multiplied together the result is the transformation matrix recommended by the ISB Standardization and Terminology Committee.

The coordinate system on the first and last link of the goniometer is located on the bone pins. Transformation matrices are required which reflect the location of the bone pins relative to the bone coordinate systems.. These transformations will almost always involve three translations and three rotations, as there is no simple way to locate the bone pins precisely during surgery.

After establishing all of the transformation matrices from one coordinate system to the next, the overall transformation matrix can be calculated. Starting at the tibia, the individual transformation matrices are multiplied together producing the overall transformation matrix. This matrix is then multiplied by a 4x4 matrix, containing the coordinates of four points, on the tibia, in terms of the tibial coordinate system. To simplify the calculations, the points used are the origin of the coordinate system and the three unit vectors representing the x-, y-, and z-axes. Hence the matrix multiplied by the overall transformation matrix is:

$$
\begin{vmatrix}
0 & 1 & 0 & 0 \\
0 & 0 & 1 & 0 \\
0 & 0 & 0 & 1 \\
1 & 1 & 1 & 1
\end{vmatrix}
$$

where the ones in the bottom row are simply place holders. The matrix resulting from the final multiplication is used to calculate the three rotations in terms of the joint coordinate system discussed in part 4.1, using the following formulas.

$$\sin \alpha = F \cdot j_p$$

$$\cos \beta = -k_p \cdot j_d \qquad \beta - \pi/2$$

$$\sin \gamma = F \cdot k_d$$

where,

$$F = \frac{j_d \times k_p}{|j_d \times k_p|}$$

j_p and j_d are unit the vectors representing y-axis, and k_p and k_d are unit vectors represent the z-axis, of the proximal and distal coordinate systems respectively.

The translations are read directly out of the final matrix, as the origin of the tibial coordinate system is given in terms of the femoral system.

The preceding process gives the location of the tibia relative to the femur at a given moment in time. To produce data representing the motion of the tibia relative to the femur the entire matrix multiplication process must be carried out for each recorded goniometer output.

4.5 Determining the Bone to Bone Pin Transformation Equations

To apply the above theory, to generate kinematic data, the locations of the bone pins relative to the bone coordinate system are required. This information can then be used to derive the transformation equations from the bone to bone pin coordinate systems.

4.5.1 Locating the Bone and Bone Pin Coordinate Systems

After a test is completed the distance along the bone pin from each of the goniometer connection blocks to the bone is measured. With the pins left in the bone, the whole leg is removed from the rabbit. The bones are first cleaned with a scalpel, and

then soaked in bleach to remove any remaining tissue as shown in Figure 4.3. The next step in the process is to mark the boney landmarks which will be used to locate the coordinate system on each bone.

A Mitutoyo Coordinate Measuring Machine is used to determine the relative location of the boney landmarks and both ends of the bone pins. This machine is capable of measuring the three dimensional location of a point to ±0.001 mm. The relative location of the boney landmarks and the bone pins can be used to locate the bone and bone pin coordinate systems, and the transformation matrix between them.

Figure 4.4 shows a femur with the boney landmarks and bone pins numbered in no particular order. The first step in locating the femoral coordinate system is to locate the origin. This will be midway between points 12 and 13 (P_{12} and P_{13}). The origin, P_{15}, is found using the midpoint formula:

$$P_{15} = (\frac{x_1 + x_2}{2} , \frac{y_1 + y_2}{2} , \frac{z_1 + z_2}{2}) \tag{1}$$

The y-axis runs from P_{15} to P_{14}. The vector Y_f, connecting these points, and hence parallel to the y-axis, is calculated using the formula:

$$Y_f = < x_2 - x_1 , y_2 - y_1 , z_2 - z_1 > \tag{2}$$

The subscript f will be used to denote the femoral coordinate system. The x-axis will be perpendicular to the plane formed by Y_f and a vector traveling from P_{15} to P_{12}. This vector will be called $P_{15,12}$ and is calculated using formula (2). The x-axis will be represented by X_f which is the cross product of these vectors.

$$X_f = Y_f \times P_{15,12}$$

Figure 4.5 shows the coordinate system attached to the femur.

As mentioned in section 4.2, the origin is now shifted along the x-axis in order to orient the z-axis closer to the axis of flexion. To translate the origin along the x-axis the ratio R of the magnitude of the shift M_s, and the length of the vector X_f (L_{xf}) is calculated.

$$R = \frac{M_s}{L_{xf}} \tag{3}$$
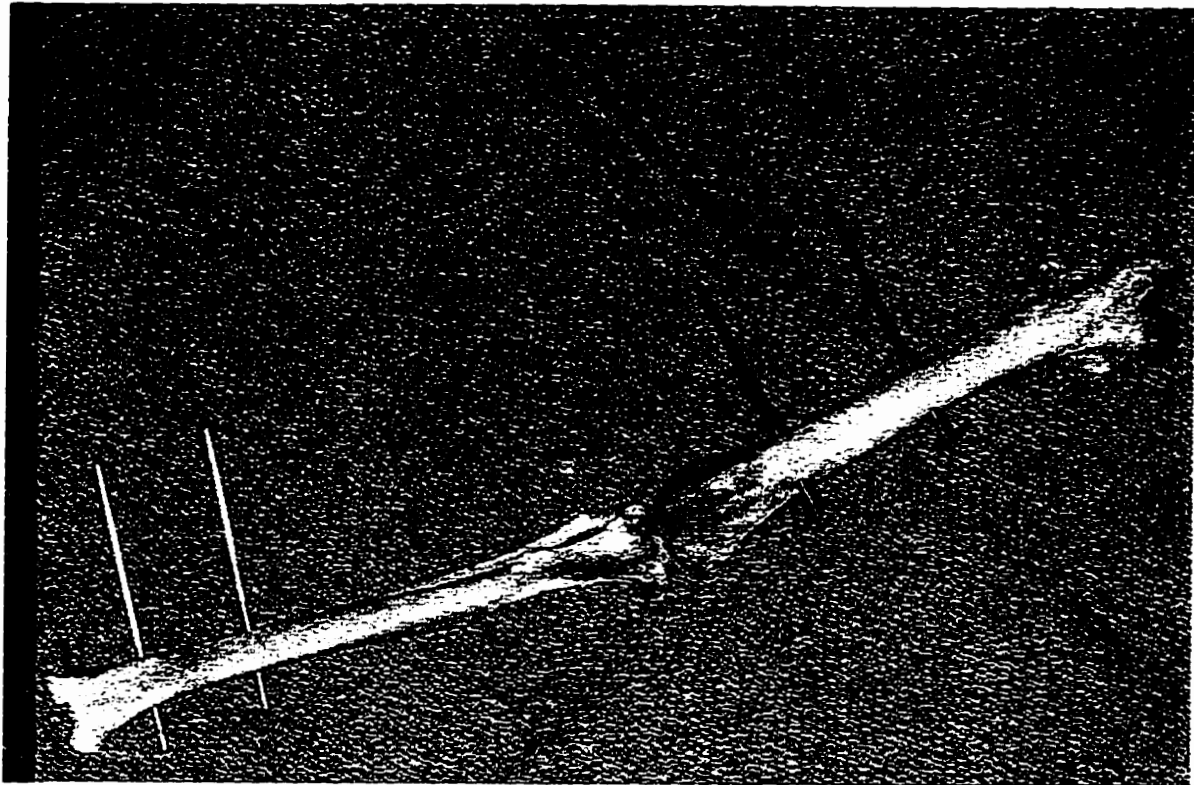
Figure 4.3: The femur and tibia are shown, cleaned of flesh, ready for the measurement of the relative location of the bone pins, and the boney landmarks.
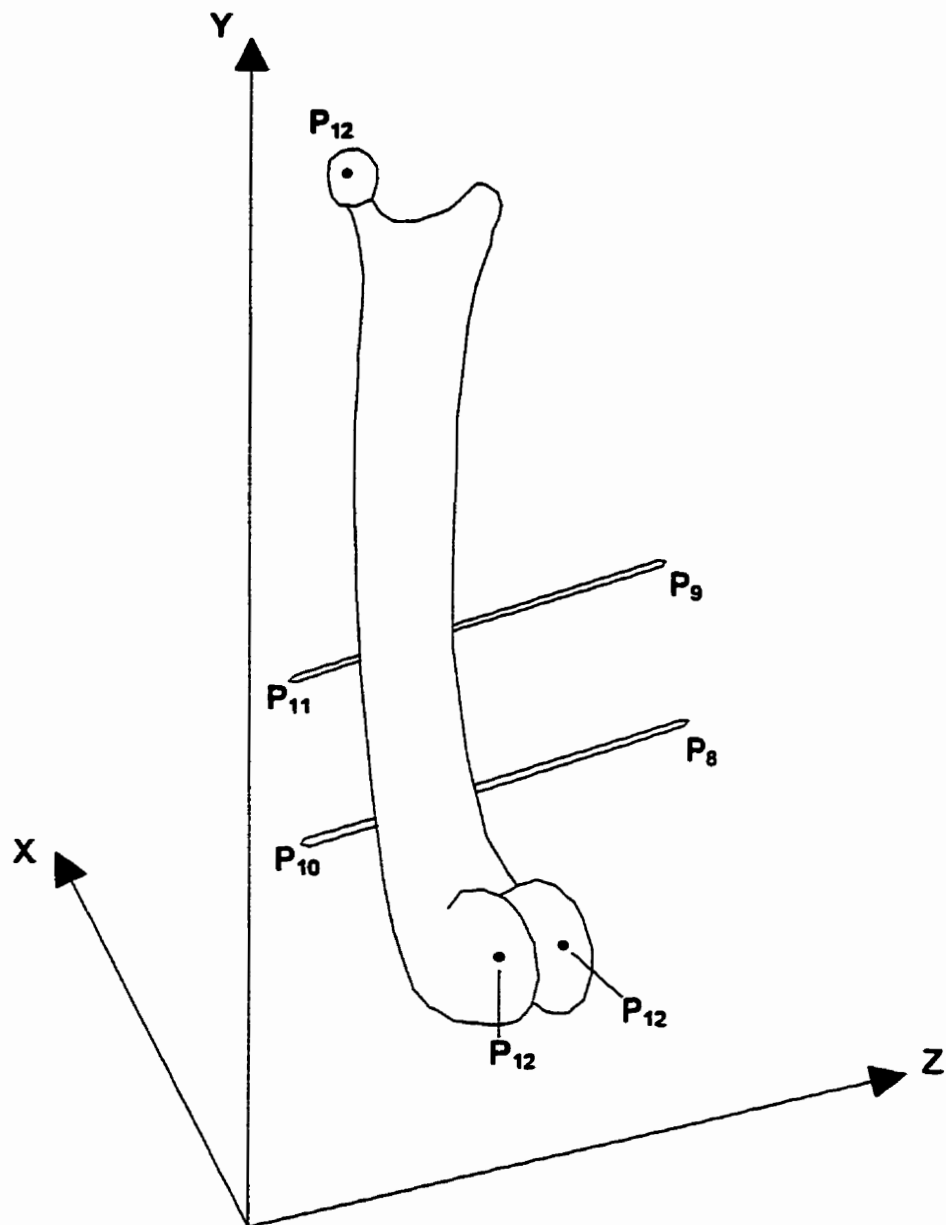
FIGURE 4.4: Illustration of femur showing boney landmarks and bone pins randomly numbered. Also shown is the global coordinate system used with the coordinate measuring machine when determining the relative location of the points.
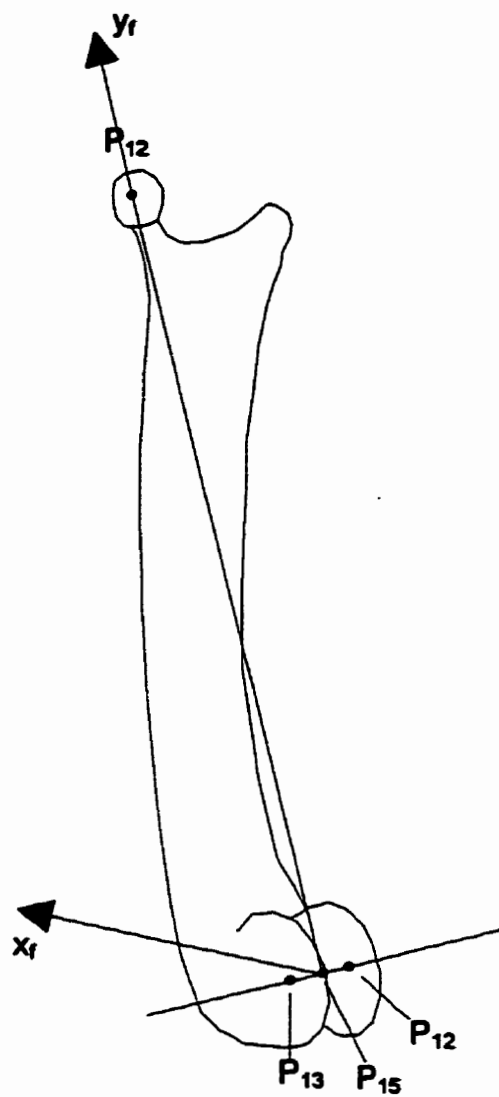
FIGURE 4.5: Illustration of femur showing Initial location of x- and y-axes.

M_t equals 75% of the distance from the most distal point on the posterior surface of the femoral condyles to the proximal end of the groove in which the patellar tendon travels. The origin P_{15} will have to be shifted along X_f R times the length of X_f. The new point will be called P_{16} and is calculated as follows:

$$P_{16} = (\, x_{P15} + (R * x_{Xf})\,,\, y_{P15} + (R * y_{Xf})\,,\, z_{P15} + (R * z_{Xf})\,) \tag{4}$$

Figure 4.6 shows the femoral coordinate system with the origin shifted. With the origin moved, Y_f is recalculated, this time as a vector running from P_{16} to P_{14}. X_f is also recalculated as the cross product of the new vector Y_f and the previous vector $P_{15,12}$. For use in further calculations Y_f and X_f are recalculated as unit vectors.

At this point the origin of the femoral coordinate system has been located, and unit vectors representing the x- and y-axes have been calculated, relative to the global coordinate system. The same process can be used for the tibial coordinate system, with the exception that the origin does not have to be shifted.

The next step in the process is to locate the origin of the bone pin coordinate system, and calculate the unit vectors representing the x- and y-axes. The origin of the bone pins coordinate systems is located on the central axis of the bone pin, proximal to the knee, on the inside edge of the goniometer mounting block. The y-axis runs parallel to the shaft connecting to the goniometer. In the case of the tibia, the positive y-axis runs towards the goniometer, and for the femur, the positive y-axis runs away from the goniometer. For both bones, the z-axis is parallel to the bone pin proximal to the knee, and is positive in the lateral direction, for the right leg. The x-axis completes the Cartesian coordinate system.

From the measurements taken after testing it is possible to calculate the distance from points P_{10} and P_{11} to the inside edge of the attachments blocks for the goniometer. These points are labeled P_{17} and P_{18} in Figure 4.7. Note: this requires that the distance from the bone to the inside edge of the mounting blocks be measured before the goniometer is removed from the bone pins.
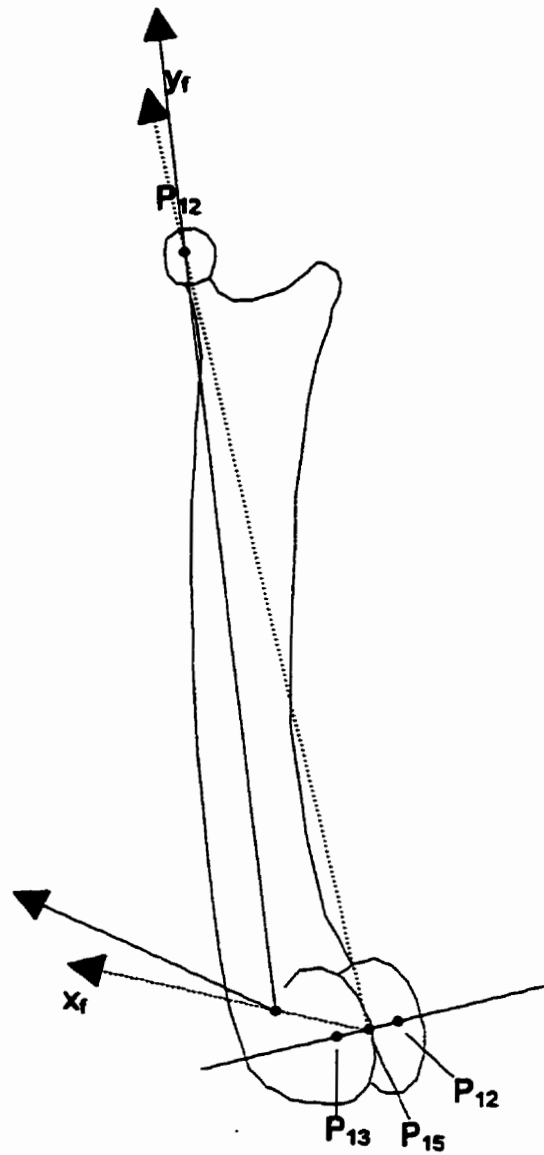
FIGURE 4.6: Illustration of femur showing corrected location of x- and y-axes. The z-axis completes the right-handed coordinate system.
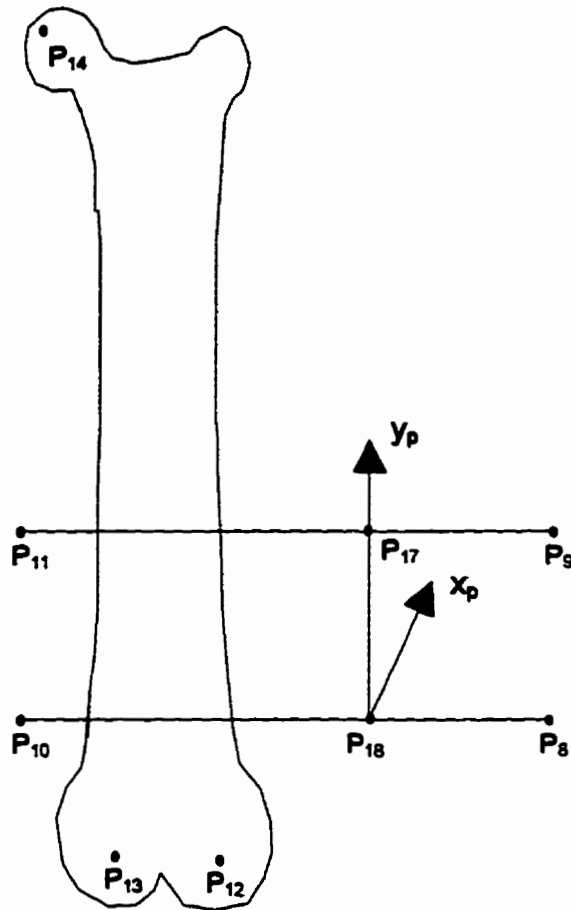
FIGURE 4.7: Illustration of femur and bone pins showing the location of the bone pin coordinate system. The z-axis completes a right hand coordinate system.

The vector $P_{11,9}$ is calculated using formula (2). To calculate the coordinates of P_{17} the ratio W of the distance from P_{11} to P_{17} and the distance from P_{11} to P_9 is used.

$$W = \frac{D\ (P_{11}, P_{17})}{D\ (P_{11}, P_9)}$$

Hence the vector $P_{11,17}$ is:

$$P_{11,17} = W * P_{11,9}$$

and

$$P_{17} = (\ x_{P11} + x_{P11,17}, y_{P11} + y_{P11,17}, z_{P11} + z_{P11,17}\ )$$

The location of P_{18} is calculated the same way.

The vector from P18 to P17 will be called Y_p, where the subscript p denotes the bone pin coordinate system. This vector is calculated using formula (2), and will represent the y-axis of the bone pin coordinate system. X_p is the cross product of $P_{18,17}$ and $P_{18,8}$. This vector will represent the x-axis of the bone point coordinate system. Figure 4.6 shows the bone pin coordinate system attached to the bone pins in the femur. As with the femoral system X_p and Y_p should be converted into unit vectors for use in further calculations.

Now that the bone and bone pin coordinate systems have been located, relative to the global coordinate system, the transformation matrix between the two systems can be calculated.

4.5.2 Determining the Bone to Bone Pin Transformation Matrix

The translation from the femoral coordinate system to the bone pin coordinate system is equal to the distance between the origins. The origin of the femoral system is located at P_{16} and that of the bone pin system is located at P_{18}. Hence the translation between the origins is equal to the distance from P_{16} to P_{18}. And the translation matrix is:

$$|T| = \begin{vmatrix} 1 & 0 & 0 & X_{P16\text{-}P18} \\ 0 & 1 & 0 & Y_{P16\text{-}P18} \\ 0 & 0 & 1 & Z_{P16\text{-}P18} \\ 1 & 1 & 1 & 1 \end{vmatrix}$$

To determine the rotation matrix that reflects the location of the two sets of coordinate axes relative to each other is a more complex process. In section 4.5.1, unit vectors were calculated which represent the x- and y-axes of each coordinate system. These unit vectors are established relative to the global coordinate system used when locating the points with the theodolite. To determine the rotational orientation of the bone pin system, relative to the femoral system, both sets of coordinate axes are translated to the origin of the global system as shown in Figure 4.8. With the origin of all three coordinate systems aligned, the femoral system is rotated until its axes are aligned with those of the global system. The bone pin coordinate system is then rotated by the same amount. This gives the unit vectors representing the axes of the bone pin coordinate system, in terms of the femoral system. The details of this process are outlined below.

The first step is to align the femoral coordinate axes with the global coordinate axes. This is done by rotating the vectors representing the x- and y-axes of the femoral system, about the global axes, until the x- and y-axes of both systems are aligned. If the x- and y-axes are aligned then the z-axis must also be aligned. The order in which the femoral coordinate axes are rotated about the x-, y-, and z-axes of the global system is not important. However, when calculating the rotation matrix, the x, y, and z rotation matrices must be multiplied together in the same order as the rotations were performed.

The y-axis of the femoral coordinate system can be aligned with the global y-axis by rotating it about the x- and z-axes of the global system. Figure 4.9a shows Y_f in the x y plane of the global system. To align Y_f with the y-axis it must be rotated by θ about the z-axis. The rotation is performed using the rotation matrix given in section 4.4. A rotation about the z-axis is calculated as follows:
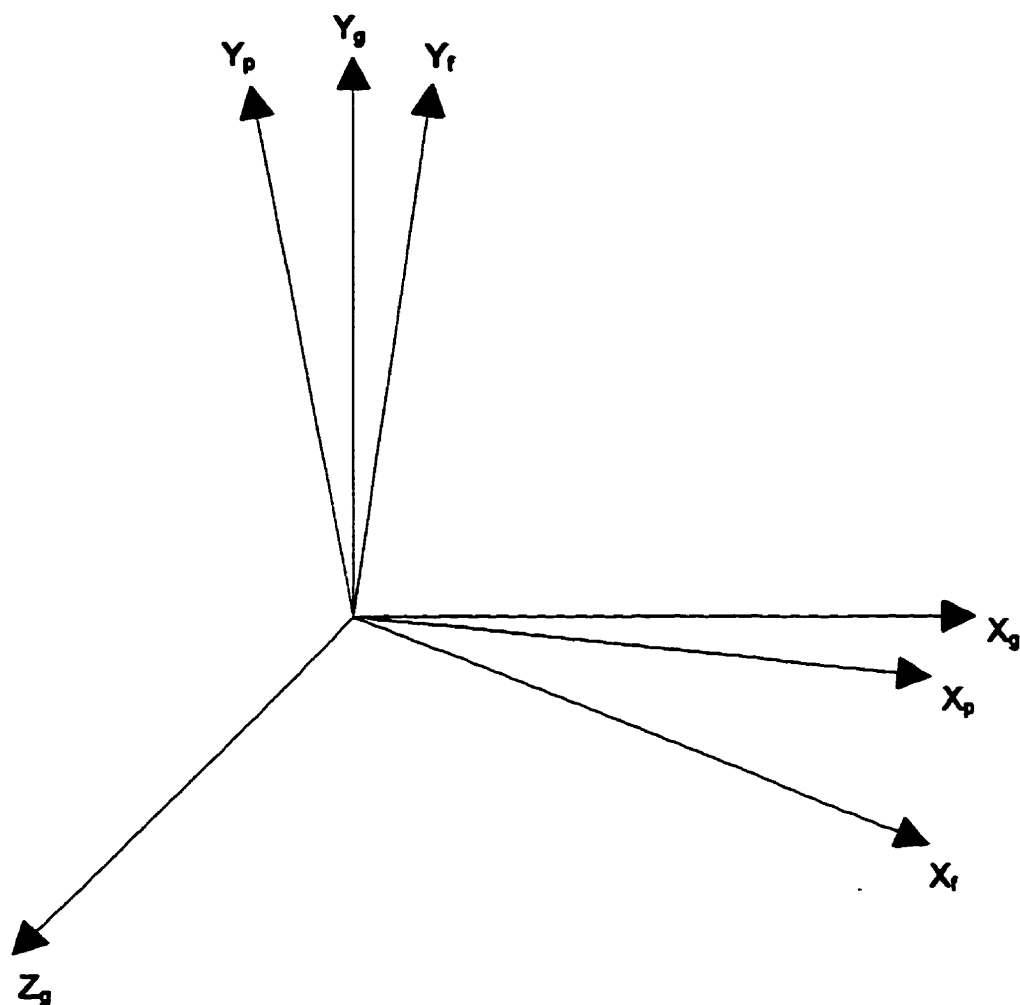
FIGURE 4.8: The femoral and bone pin coordinate systems shown translated to the origin of the global coordinate system in order to calculate the rotational transformation matrix between the two coordinate systems.
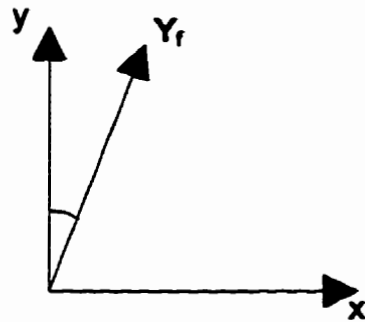
FIGURE 4.9a: Yf must be rotated by θ to align it with the global y-axis in the x y plane.
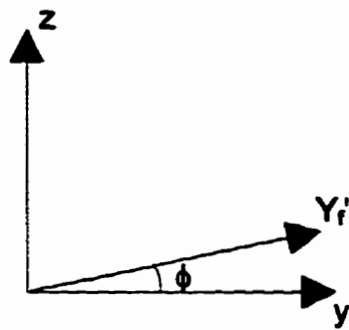
FIGURE 4.9b: Yf' must be rotated by φ to align it with the global y-axis in the y z plane.
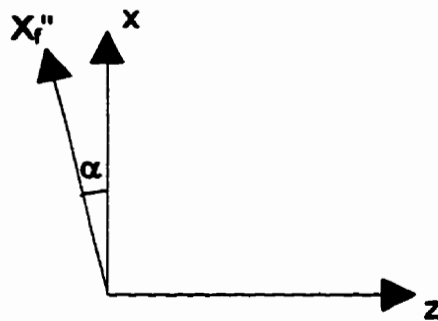
FIGURE 4.9c: Xf" must be rotated by α to align it with the global x-axis in the x z plane.

$$
|Z| \;=\;
\begin{vmatrix}
\cos\theta & -\sin\theta & 0 & 0 \\
\sin\theta & \cos\theta & 0 & 0 \\
0 & 0 & 1 & 0 \\
0 & 0 & 0 & 1
\end{vmatrix}
\begin{vmatrix}
x_{Y_p} \\
y_{Y_p} \\
z_{Y_p} \\
1
\end{vmatrix}
\;=\;
\begin{vmatrix}
x_{Y_p}{}' \\
y_{Y_p}{}' \\
z_{Y_p}{}' \\
1
\end{vmatrix}
$$

The result of this multiplication is Y_f' which must be aligned with the y-axis in the y z plane. Figure 4.9b shows that Y_f' must be rotated about the x-axis by ϕ. Again this is done using the rotation matrices.

$$
|X| \;=\;
\begin{vmatrix}
1 & 0 & 0 & 0 \\
0 & \cos\phi & -\sin\phi & 0 \\
0 & \sin\phi & \cos\phi & 0 \\
0 & 0 & 0 & 1
\end{vmatrix}
\begin{vmatrix}
x_{Y_p}{}' \\
y_{Y_p}{}' \\
z_{Y_p}{}' \\
1
\end{vmatrix}
\;=\;
\begin{vmatrix}
0 \\
1 \\
0 \\
1
\end{vmatrix}
$$

If the rotations are done correctly, the result will be that shown, which indicates that Y_f is now aligned with the global y-axis. X_f is also multiplied by the same two rotation matrices, in the same order, giving X_f''. The next step is to align X_f'' with the global x-axis. Figure 4.9c shows that X_f'' must be rotated α degrees about the y-axis.

$$
|Y| \;=\;
\begin{vmatrix}
\cos\alpha & 0 & \sin\alpha & 0 \\
0 & 1 & 0 & 0 \\
-\sin\alpha & 0 & \cos\alpha & 0 \\
0 & 0 & 0 & 1
\end{vmatrix}
\begin{vmatrix}
x_{X_p}{}'' \\
y_{X_p}{}'' \\
z_{X_p}{}'' \\
1
\end{vmatrix}
\;=\;
\begin{vmatrix}
1 \\
0 \\
0 \\
1
\end{vmatrix}
$$

Once again, if the rotations are done correctly, the result will be that shown, which indicates that the x-axis are aligned.

Multiplying the X, Y, and Z rotation matrices together gives an overall rotation matrix M. Note the order is important.

$$
|M| \;=\; |Y| \; |X| \; |Z|
$$

X_p and Y_p are now multiplied by this matrix, which rotates them by the same amount that X_f and Y_f were rotated. At this point the femoral, and bone pin coordinate systems, are in their original rotational orientation. Because the femoral system, is aligned with the global system, the unit vectors X_p and Y_p, of the bone pin coordinate system, are expressed with respect to femoral system. To calculate Z_p the cross product of X_p and Y_p is taken. X_p, Y_p, and Z_p can be written as a 4x4 matrix. The first column will represent the relative location of the origin of the bone pin and femoral coordinate

system, but for now zeros will be placed there. Ones are put in the bottom row as place holders. If the unit vectors X_p, Y_p, and Z_p are written in terms of the bone pin coordinate system then the matrix will be all ones and zeros. If the vectors are written in terms of the femoral system, they will be the vectors calculated above. This relationship can be written as follows:

$$\begin{vmatrix} 0 & x_{X_p} & x_{Y_p} & x_{Z_p} \\ 0 & y_{X_p} & y_{Y_p} & y_{Z_p} \\ 0 & z_{X_p} & z_{Y_p} & z_{Z_p} \\ 1 & 1 & 1 & 1 \end{vmatrix} = |R| \begin{vmatrix} 0 & 1 & 0 & 0 \\ 0 & 0 & 1 & 0 \\ 0 & 0 & 0 & 1 \\ 1 & 1 & 1 & 1 \end{vmatrix}$$

where, R is the rotational transformation matrix between the femoral and bone pin coordinate systems. Therefore,

$$|R| = \begin{vmatrix} x_{X_p} & x_{Y_p} & x_{Z_p} & 0 \\ y_{X_p} & y_{Y_p} & y_{Z_p} & 0 \\ z_{X_p} & z_{Y_p} & z_{Z_p} & 0 \\ 1 & 1 & 1 & 1 \end{vmatrix}$$

The complete transformation matrix TR, is the product of the translation and rotation matrices.

$$|TR| = |T| \, |R|$$

The process for calculating the transformation matrix from the tibial coordinate system, to the tibial bone pin system, is very similar to that outlined above. The major difference is that the unit vectors for the tibial coordinate system, are calculated in terms of the bone pin coordinate system, which is the opposite of the process for the femur. The reason is; for the tibia, the transformation is from bone to bone pin, instead of from bone pin to bone. The three unit vectors, representing the x, y, and z-axis of the tibial system, in terms of the bone pin system, are assembled into a 4x4 matrix, along with the relative location of the tibial origin. This matrix, and the transformation matrix calculated for the femur, are entered directly into the computer program outlined below.

4.6 Processing the Kinematic Data

The vast amount of matrix multiplication required to generate a reasonable amount of kinematic data is best handled by a computer. A program called RHINO has been developed in conjunction with the goniometer for processing the output data. This program, written in C, reads in the goniometer output file and generates a new file containing the relative location of the tibia and femur in terms of the coordinate system described in section 4.2.

As input, the program requires: 1) the 4x4 matrix containing the unit vectors representing the tibial coordinate system in terms of the tibial bone pin coordinate system, described in section 4.5.2. 2) the transformation matrix for transforming from the femoral bone pin coordinate system to the femoral system, also described in section 4.5.2. 3) the goniometer output data from a test recorded in a file. The data in the file must be in columns in the following order: the output from rotary potentiometers number 1, 2, and 3 followed by the output from linear potentiometers number 1, 2, and 3 (for potentiometer numbering see Figure 3.2).

Figure 4.10 shows a simple flow chart of how the program functions. The program reads the first line of data from the input file, then uses this to calculate the transformation matrices between each link of the goniometer. Starting at the tibia, the transformation matrices are all multiplied together. The matrix resulting from the multiplication is then used to calculate the rotation and translation of the tibia relative to the femur. The program then repeats this process until the end of the input file is reached. The result is an output file containing the relative location of the tibia and femur, versus the time interval of the data sampling, during testing. Appendix B contains the source code for RHINO.

The present version of the program only calculates the rotations as this is all that was required for the testing described in Chapter 6. However, the program can be modified fairly easily to calculate the translations.
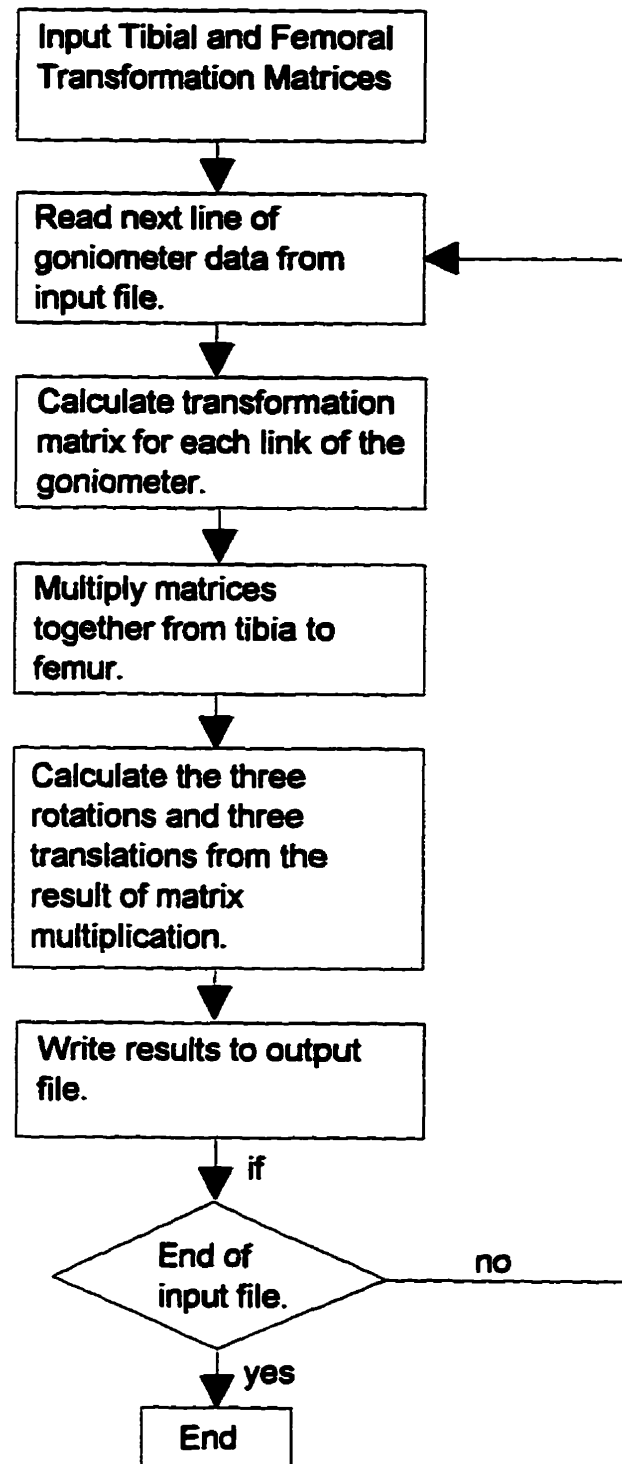
FIGURE 4.10: Flow chart for the computer program RHINO, which, calculates the relative motion of the tibia and femur using the goniometer output data.

After the test data have been collected, the procedure for processing the kinematic data, to determine the three rotations α, β, and γ, is as follows:

1. Calculate the 4x4 matrix containing the unit vectors representing the tibial coordinate system in terms of the tibial bone pin coordinate system, and the transformation matrix for transforming from the femoral bone pin coordinate system to the femoral system. These are described in section 4.5.2

2. Enter these two matrices directly into the program RHINO using an editor, and recompile the program (it is clearly marked in the source code where to enter the matrices).

3. Copy the raw output data into a new file and delete all information except the output from the three rotary potentiometers. The output should be in three columns representing the output from rotary potentiometers number 1, 2, and 3.

4. The output data from the potentiometers must be converted from volts to degrees. To convert the output of rotary potentiometer number one into degrees, the initial mounting data are used. When the goniometer is attached to the bone pins, yet still secured by the mounting jig, the voltage output is recorded. This value represents 90 degrees of flexion and is used along with the potentiometer calibration factor (Chapter Five) to convert the voltage output into degrees. For rotary potentiometers number two and three the voltage output is converted into a positive or negative rotation about a set of axes mounted onto the potentiometer. The zero point for both of these axes is the output of the potentiometer when the shafts of all three rotary potentiometers are mutually perpendicular. To ensure that this value does not change, the shafts of rotary potentiometers two and three have been filed flat on one side. For rotary potentiometer number two the value is 7.855 V and for rotary potentiometer number three the value is 4.900 V. The output in degrees is calculated by subtracting the zero value from the potentiometer output and multiplying the remainder by the potentiometer calibration factor.

5. The new output data file can then be processed by RHINO. The output file from RHINO will contain three columns of data representing the values of α, β, and γ.

CHAPTER FIVE: Discussion of Results

5.1 Introduction

With a working prototype of the goniometer completed, the next step in design process is to calibrate the individual potentiometers, and then test the accuracy of the goniometer as a whole. The purpose of calibrating the potentiometers is to: 1) check the linearity of their output, and 2) determine the calibration factors which will be used to convert the voltage output into units of displacement. Testing the goniometer as a whole will involve determining how accurately the goniometer can repeatedly locate a random point in space. In addition, the goniometer design will be evaluated to determine the accuracy with which it can be removed and then reattached to a rabbit. The ability to reattach the goniometer consistently will be crucial for long term studies.

5.2 Calibration of the Potentiometers

Calibration of the potentiometers involves recording the output of the potentiometers for a series of known displacements, in both directions, and then checking the linearity of the output. The slope of the voltage-displacement curve is the calibration factor for the potentiometer, and the error in the linearity, is the error in the output of the potentiometer.

5.2.1 Calibration of the Linear Potentiometers

The linear potentiometers were calibrated using a Mitutoyo displacement transducer which is accurate to 0.001 mm. Each potentiometer was mounted in the transducer and moved both ways through its entire range of motion in increments of 0.1 mm. Using an input voltage of 10v the output for each potentiometer was recorded.

The voltage versus displacement curves for all the potentiometers were very linear and showed no hysteresis. The plot for potentiometer number one is shown in Figure 5.1a. Table 5.1 shows the calibration factor and R^2 value for each of the linear potentiometers.

Table 5.1: Slope and Linearity of the Linear Potentiometers Calibration Curves.

Potentiometer	Calibration Factor	Linearity (R^2 value)
One	1.0949 mm/v	1.0000
Two	1.1166 mm/v	1.0000
Three	1.0861 mm/v	1.0000

5.2.2 Calibration of the Rotary Potentiometers

The rotary potentiometers were calibrated using an 8 inch diameter 360 degree protractor, incremented to 0.5 degrees. Each potentiometer was mounted in the centre of the protractor and a pointer was attached to the shaft as shown in Figure 5.2. The rotary potentiometers used for the goniometer are all 360 degree units but the expected rotations that they will be measuring are all much less than 360 degrees (120 degrees for potentiometer 1 and less than 30 degrees for potentiometers 2 & 3). Hence only a small portion of the entire range of each potentiometer will be used by the goniometer. To find the most linear portion of each rotary potentiometer's range a rough, initial calibration of the entire range was performed. The most linear portion of each potentiometer was then calibrated more precisely. Using an input of 10v, the output for each potentiometer was recorded as it was rotated both ways through its expected range in 0.5 degree increments. The voltage versus displacement plot for rotary potentiometer number one is shown in Figure 5.1b. All the rotary potentiometers were very linear and showed no hysteresis. The results of calibration are shown in Table 5.2.

Figure 5.1a: Calibration Curve for Linear Potentiometer
Number One

Figure 5.1b: Calibration Curve for Rotary Potentiometer
Number One
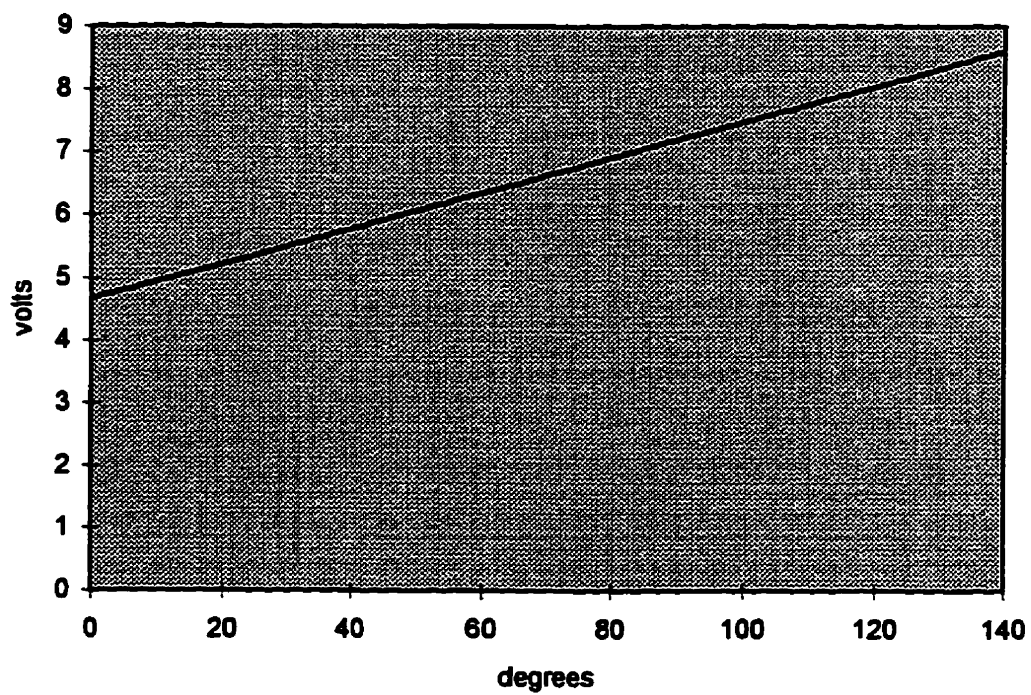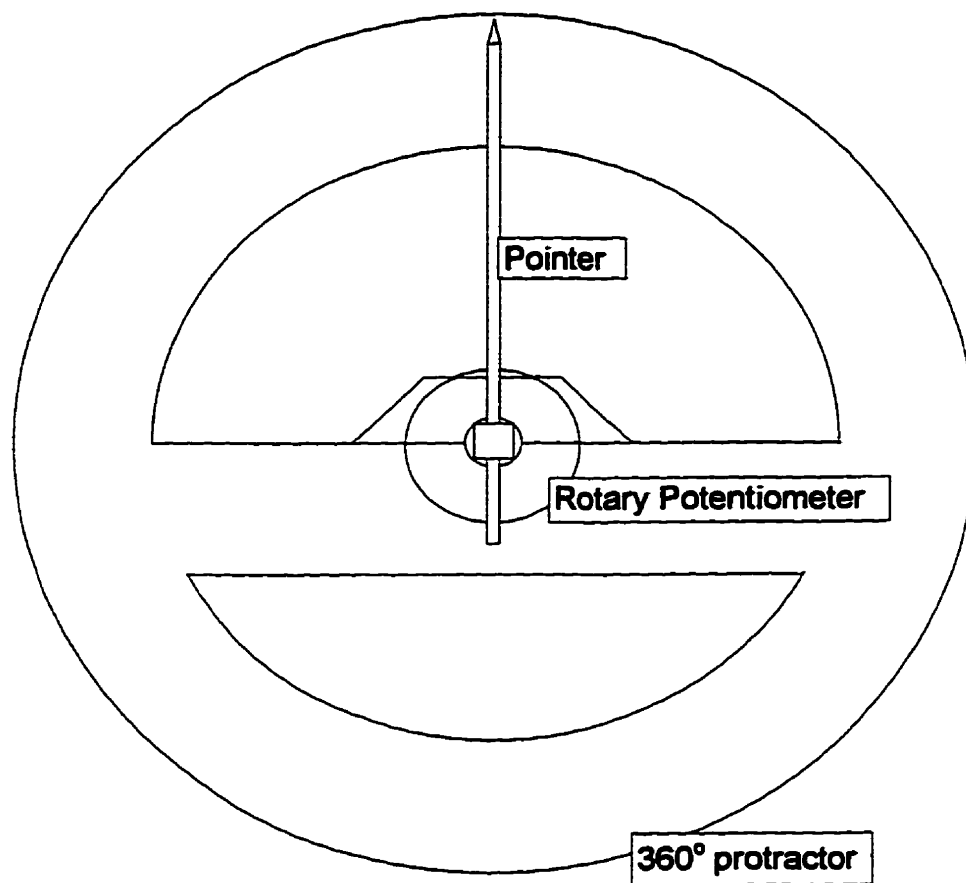
FIGURE 5.2: Rotary potentiometer calibration system, showing the potentiometer mounted in the center of the protractor, with a pointer attached to the shaft.
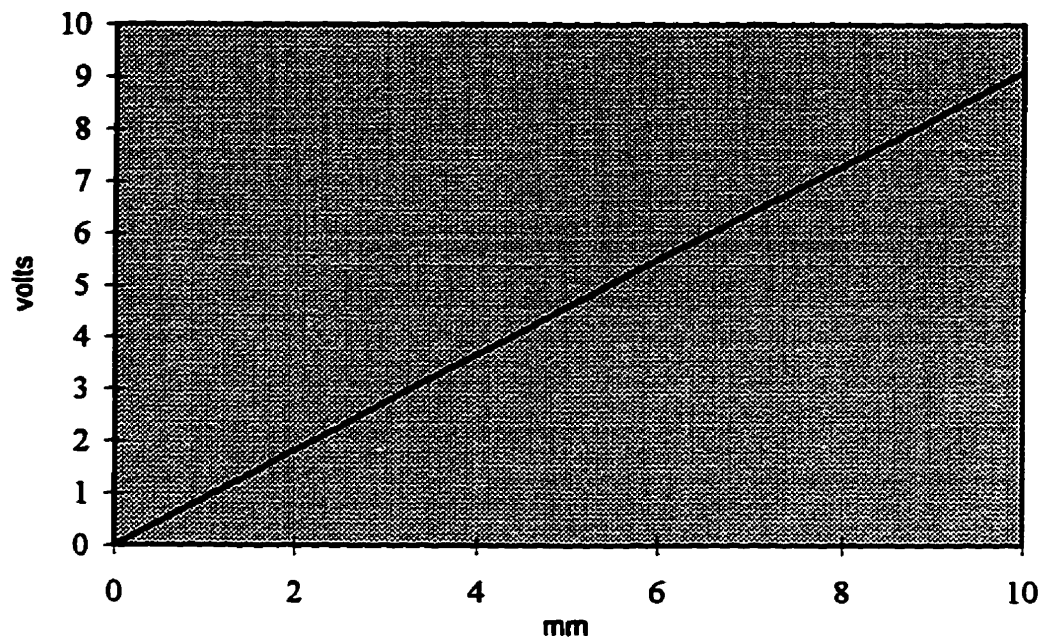
Table 5.2: Slope and Linearity of the Rotary Potentiometer's Calibration Curves.

Potentiometer	Calibration Factor	Linearity (R^2 value)
One	35.463 °/v	1.0000
Two	34.658 °/v	1.0000
Three	35.558 °/v	1.0000

5.3 Testing the Error in the Goniometers Output

Quantifying the error in the output of the goniometer is a complex task. Sources of error directly associated with the goniometer include: the linearity of the potentiometers' output, defections of the goniometer's frame, and deflects of the bone and bone pins. Indirect sources of error include the accuracy of the data acquisition system, the linearity of the power supply, and its ability to hold a fixed voltage accurately. For this research project, the error in the goniometer's output has only been investigated to the extent necessary to confirm that the output is reasonably reliable, compared to other similar devices, and the list of demands for the goniometer stated in Chapter Two. An in-depth calibration of goniometer would require the use of a system similar to those developed by Sommer *et al.* (1980), and Suntay *et al.* (1983). These systems are necessarily complicated and involve the use of both mathematical and mechanical models for quantifying the error. It is encouraging to note that Suntay *et al.* have discovered that "theoretical error analysis consistently overestimates the actual measurement error", hence the total error is less than the sum of the individual errors. Another interesting concept which could be used to calibrate the goniometer would involve the use of a robot. The goniometer could be attached to a rabbit leg in the standard fashion. The femur, for example, could be firmly anchored, while the robot was used to move the tibia through a known range of motion. The known path of the tibia could be compared to the output from the goniometer, thus generating an estimation of the error in a situation more closely resembling an actual test.

The accuracy of the goniometers output was initially tested by anchoring one end of the goniometer to a heavy flat base. The other end of the goniometer was then moved to various random locations, within the goniometer's expected range of motion. At each new location the goniometer was held in place using a clamping system. The output from each of the six potentiometers was recorded, and the location of the moving end of the goniometer was carefully measured. To measure the location of the moving end a square was used to mark the location of the end, in the horizontal plane, onto a piece of paper attached to the base. A set of Mitutoyo digital calipers, accurate to 0.01 mm, were then used to measure the three dimensional position of the pointer, using the centre of the base as the origin.

After a total of ten measurements were taken, the change in position of the pointer predicted by the potentiometers was compared to that shown by the measurements. In order to calculate the change in position predicted by the potentiometers the equations given in Appendix A were used. The difference between the two sets of measurements was 0.59 ± 0.46 mm (mean $\pm$ SD).

This system of calibration does not give an absolute error for each of the three rotations and three translations. It does, however, predict the overall accuracy of the goniometer because the output from both the linear and rotary potentiometers is used to predict the change in position.

The problem with this calibration system is that there is no way to differentiate between error due to the goniometer and error in measuring the three dimensional location of the moving end of the goniometer. To solve this problem the goniometer was recalibrated using a calibration system developed by Hollis et al. (1991). This system involves using the goniometer to measure the distance between points on a steel plate. In a similar fashion to the calibration system described above, one end of the goniometer is attached to a heavy base. A pointer is attached to the other end of the goniometer which is moved from point to point on the steel plate. At each new location the output of the goniometer is recorded. Finally the distance between the points

predicted by the goniometer is the actual distance. The distance between the points on the steel plate can be accurately measured, therefore, the error between the measured location and the predicted location will be due almost entirely to the goniometer.

To perform this calibration a 50 mm x 50 mm sheet of tin was mounted onto a block of wood. A sharp pin was then used to make 12 small dents in the tin, in a circular pattern. The same pin was then attached to the moving end of the goniometer and used as a pointer for locating the small dents on the sheet of tin. The fixed end of the goniometer was held in place by attaching it to a heavy base. To simulate a test situation the fixed end was considered the tibia, and the wooden block was suspended within the range of motion of the femur. Figure 5.3 shows a preliminary calibration using this system. During the actual calibration everything was as shown in the figure, except for a piece of tin attached to the wooden block, as described above. As before the distance between the points predicted by the goniometer was compared to actual distance measured by the Mitutoyo digital calipers (accurate to 0.01 mm). Once again the equations in Appendix A were used to calculate the location of the moving end of the goniometer. The error found between the two sets of measurements was 0.28 ± 0.21 mm (mean $\pm$ SD). This value compares well to the estimated error of 0.3 ± 0.2 mm (mean $\pm$ SD) calculated for the linkage developed by Hollis et al. (1991).

5.4 Testing the Error in the Repeated Mounting of the Goniometer

One of the requirements for the goniometer was that researchers should be able to remove it from a rabbit, and then reattach it in a consistent fashion. The mounting jig, described in Section 3.4.2, makes this possible. To test the effectiveness of the mounting jig to align the goniometer consistently, a repeated attachment test was performed.

Two whole rabbit legs, with bone pins already in place, were used to evaluate the ability to reattach the goniometer consistently. Six tests were performed on each leg. For each test, the bone pins were anchored using the mounting jig. The goniometer was attached, and the initial reading from each of the potentiometers was recorded. Next the

Figure 5.3: Calibration of the goniometer. The goniometer was used to measure the distances between the points marked on the board, these distances were then compared to the distances measured using digital calipers. The picture shows the calibration performed using a wooden board. For the final calibration a sheet of tin was attached to the board, as described in the text, to improve the accuracy.
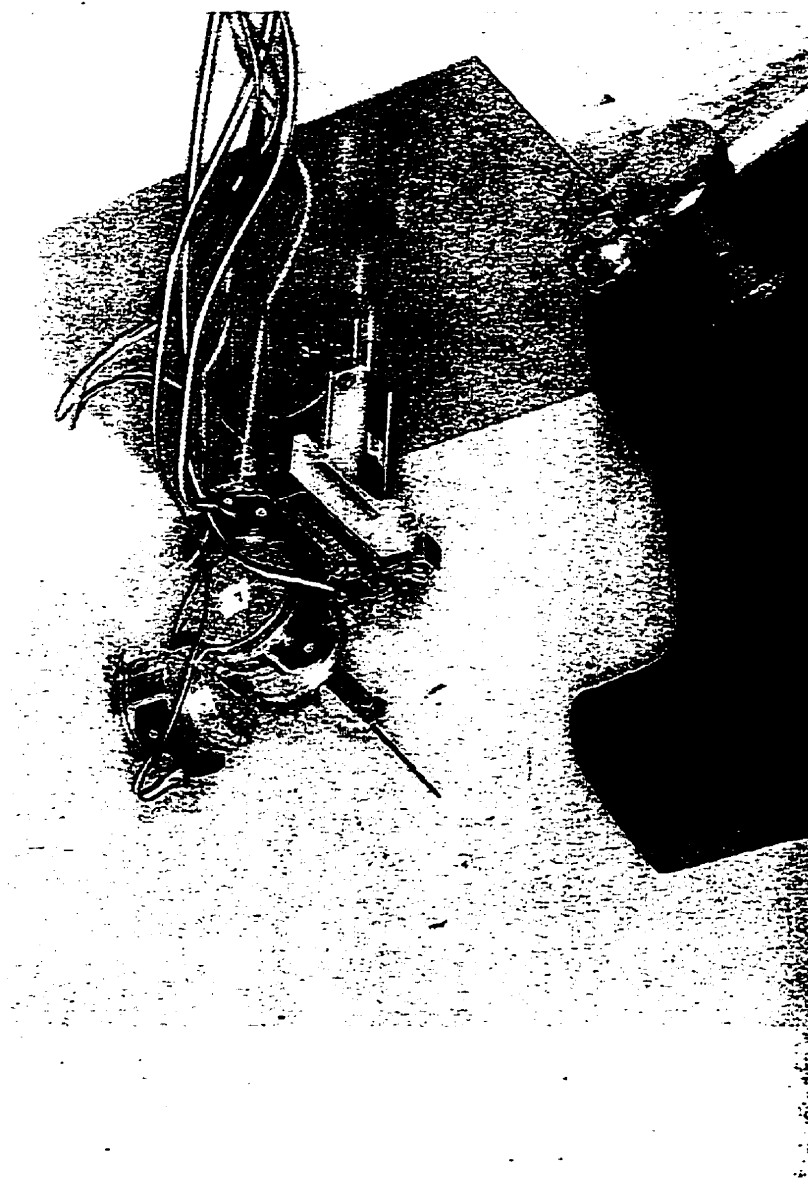
mounting jig was removed, leaving the goniometer in place. The leg was then manually moved through 10 full flexion cycles. Finally the goniometer was removed and the procedure was repeated. Table 5.3 shows the error in the initial reading for each of the legs individually, and for both legs together.

Table 5.3: Error in the Initial Reading when Reattaching the Goniometer (standard deviation).

Test	Rotary Potentiometers (degrees)			Linear potentiometers (mm)		
	One	Two	Three	One	Two	Three
Leg 1	0.165	0.216	0.228	0.002	0.019	0.257
Leg 2	0.184	0.478	0.268	0.004	0.097	0.033

As shown in Table 5.3 the mounting jig is very effective in aligning the goniometer in a consistent fashion. It is interesting to note that the value for linear potentiometer number three on Leg 1 is much higher than the others. This could be caused by the complex geometry of the goniometer. A very small change in the other five potentiometers, from one test to the next, could be reflected as a large change in the remaining potentiometer. Even with this one larger error value, the magnitude of the error in the initial attachment values is less than the estimated error in the goniometer's output.

CHAPTER SIX: Application of the Goniometer to Measure the Force on the Medial Collateral Ligament Versus Tibial Rotation

6.1 Introduction

The goniometer was designed to allow joint research to be conducted *in vivo*. This is significant because most research into the structural properties of ligaments has left only the joint capsule, or even just the ligament in question, intact. *In vivo* testing should provide the most accurate representation of how the ligaments perform as the knee is moved through its entire range of motion. The goal of this research was to prove the value of the goniometer so that *in vivo* testing of the structural properties of the ligaments of the knee can begin.

For this pilot study the goniometer was used in conjunction with a load cell, to determine the force on the Medial Collateral Ligament (MCL) versus tibial rotation, at 60, 90, and 120 degrees of flexion. The tests were performed on the right legs of New Zealand white rabbits, separated at the pelvis, with all muscles and ligaments intact. The long range goal of this project is to establish a force versus rotation curve for the MCL at one joint angle. This information will allow a known load to be applied to the MCL, by using the goniometer to monitor both the joint angle and tibial rotation. Research can then begin into the effect of varying amounts of loading on the healing of the MCL. Eventually a set of guide lines could be established stating the magnitude of loading suggested, for optimal healing, versus say the cross-sectional area of the ligament. This type of information could be very useful in the rehabilitation of knee injuries, and could serve as a basis for similar investigations into the other ligaments of the knee.

6.2 Materials and Methods

The right legs of five one year old New Zealand white rabbits were used in this experiment. Force on the MCL was measured using a load cell, and joint motion was measured using the six degree of freedom goniometer.

The load cell, consisting of three mutually perpendicular strain gauged plates, attaches to the MCL at the tibial insertion. This is accomplished by removing a small bone chip, surrounding the tibial insertion of the MCL, from the tibia. The distal end of the load cell is attached to the tibia, and the proximal end is connected to the bone chip. To insure that the alignment of the MCL is not altered by the attachment of the load cell, the mounting holes are drilled before the bone chip is fully removed. Figure 6.1 shows the load cell attached to the right leg of a rabbit. Note: the connection between the MCL and the medial meniscus was cut during the attachment of the load cell. This was done to be consistent with the MCL tensile testing procedure used at the University of Calgary.

Pre testing surgery involved harvesting the right leg of the rabbit, and then attaching the load cell to the MCL, and the goniometer to the lateral side of the leg. The load cell is attached to the leg first, as this requires precise surgery which would be complicated by the goniometer. The load cell was then removed from the leg, to prevent it from being damaged, while the bone pins were inserted for the goniometer. The distal end of the load cell was then attached to the tibia while the proximal end was left free. The load cell was then zeroed. Next the proximal end of the load cell was attached to the bone chip containing the tibial insertion of the MCL. With the joint at approximately 90 degrees of flexion the pre-load on the MCL was measured to check that it was close to the expected value of ~3N. Figure 6.2 shows a rabbit leg with both the load cell and goniometer in place.

The basic testing procedure involved rotating the foot externally at joint angles of 60, 90, and 120 degrees. A total of twelve rotations were performed at each joint angle.

The testing started by performing six external rotations at each joint angle separately, starting with the smallest angle of flexion and moving on to the largest. This was followed by six more external rotations at each joint angle, for which the joint angle was determined randomly. Before each test the foot was allowed to return to its natural resting position in order to start each rotation from a consistent and natural position.

The joint angle for each test was determined using the goniometer. A digital multi-meter was used to monitor the output of rotary potentiometer number one, which was roughly aligned with the knee's axis of flexion. The initial reading, with the mounting jig still in place was taken as 90 degrees of flexion. The calibration factor for the potentiometer was then used to determine the output voltage for 60 and 120 degrees of flexion. The results from the final data transformations show that this system determined the flexion angle to within ± 3 degrees.

The output data from both the load cell and the goniometer were recorded by LabTech Note Book, at a sampling rate of 20 Hz. The power supply for the goniometer was set at 10 v, and monitored by LabTech Note Book to ensure a constant output.

After testing, all of the flesh was removed from the femur and tibia, while the bone pins were left in place. The bones were then soaked in bleach to remove any remaining tissue. Once the bones were completely cleaned, and dried, the boney landmarks were marked onto the bones. The three dimensional locations of the boney landmarks, relative to the ends of the bone pins, were then measured, in order to locate the goniometer relative to the femoral and tibial coordinate systems. This information was then used along with the goniometer output data to calculate the flexion angle, varus-valgus rotation and tibial rotation for each of the tests. This process is detailed in Chapter 4.

To determine the zero point to be used for the tibial rotation data, the initial value for each of the 12 individual tests at each joint angle was averaged. The tibial rotation and force data for each test were then combined to produce a force versus rotation curve for each test. Next the six similar tests at each joint angle (random and

Figure 6.1: The load cell is shown attached to a rabbit leg.
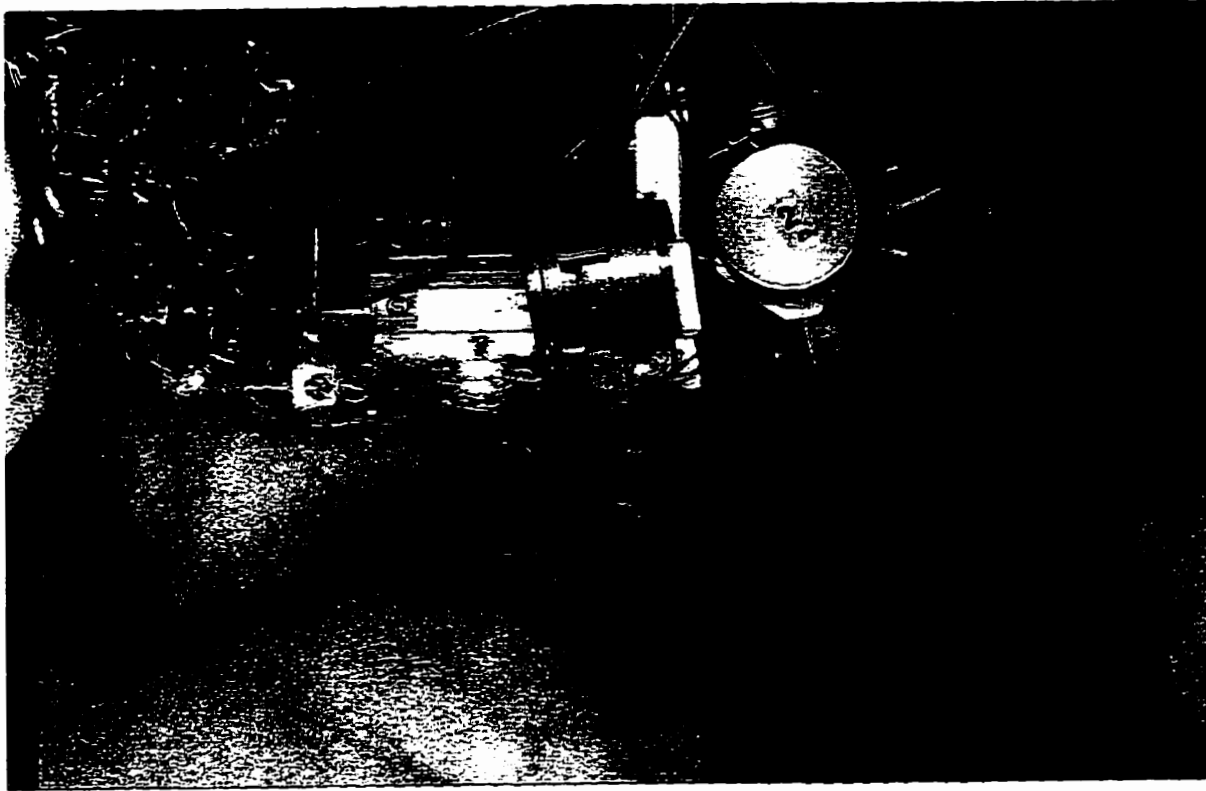
Figure 6.2: Both the load cell and the goniometer are shown attached to a rabbit leg, ready for testing.

non-random) were combined to create a force versus rotation file of all the similar data at each joint angle. This file was then run through the program BMDP which performed a polynomial regression on the data to determine a representative force versus rotation curve for each group of tests. Hence this process created ten force versus rotation curves at each joint angle, one random and one non-random for each of the five rabbits.

For two of the rabbit legs internal rotations were also performed using the same procedure of six non-random tests at each joint angle followed by random testing at all three joint angles. The data from these tests was processed in the same way as the data from the external rotation testing.

6.3 Results

For each individual rabbit the force versus rotation curve was very consistent at each joint angle. Figure 6.3 shows the raw force versus rotation data for rabbit one at 90 degrees of flexion. From the figure it is clear that the data are consistent from test to test. This is reinforced by the R^2 value of 0.914 generated by the polynomial regression. The average R^2 value for all 30 tests is 0.856. The average R^2 values, however, are not consistent for all joint angles. At 60 degrees the average R^2 value is 0.877, at 90 degrees the average R^2 is 0.892, and at 120 degrees the average R^2 value 0.801.

For each individual rabbit the force versus rotation curves generated from the non-random and random test data are very consistent. Figure 6.4 shows the random and non-random force versus rotation curves for rabbit one at 90 degrees of flexion.

Figures 6.5-6.9 show the random and non-random force versus rotation data, at all joint angles, for each individual rabbit. These curves show a consistent trend indicating that the MCL is recruited the earliest at 120 degrees of flexion and the latest at 60 degrees of flexion. In addition the slope of the force versus rotation curve is generally greater with increasing joint angle.

Figure 6.3: Raw Data for External Tibial Rotation at 90 Degrees of Flexion, for Rabbit #1
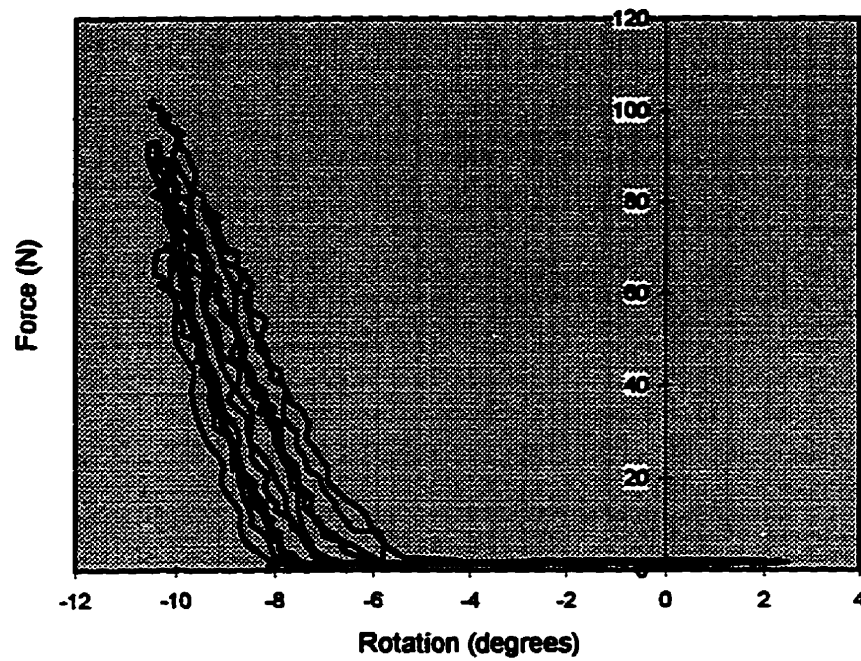
Figure 6.4: Best Fit Curves for Non-Random (a) and Random (b) External Tibial Rotation Data, at 90 Degrees of Flexion, for Rabbit #1.

Figure 6.5: Non-Random (a) and Random (b) Force
Versus External Tibial Rotation Curves for Rabbit #1

Rotation (degrees)

Figure 6.6: Non-Random (a) and Random (b) Force
Versus External Tibial Rotation Curves for Rabbit #2

Rotation (degrees)

108
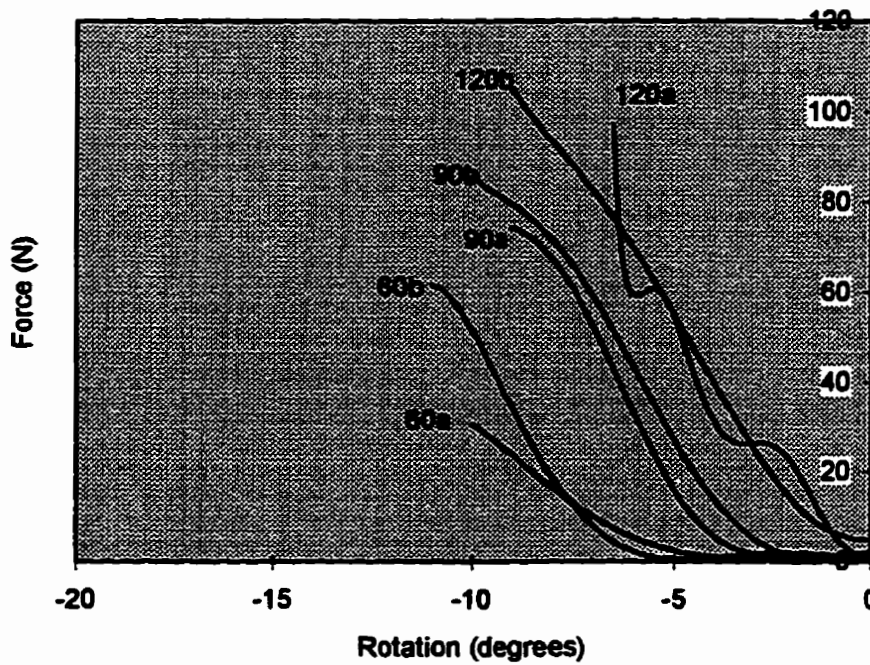
Figure 6.7: Non-Random (a) and Random (b) Force
Versus External Tibial Rotation Curves for Rabbit #3
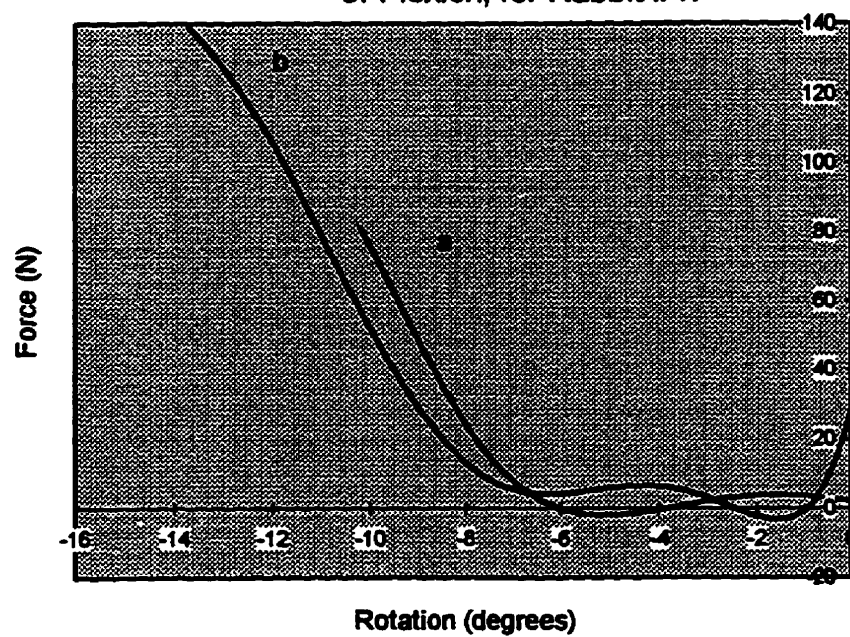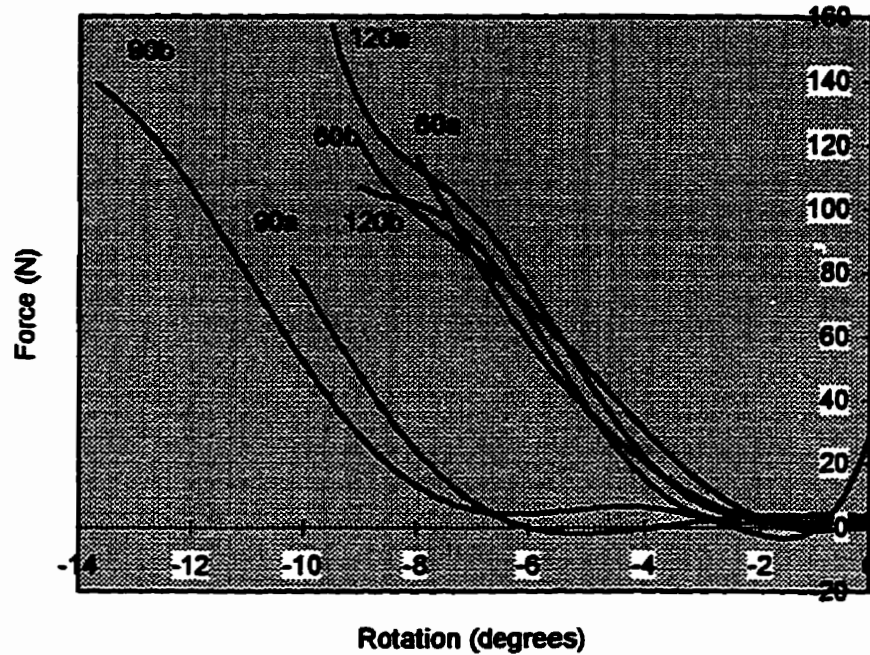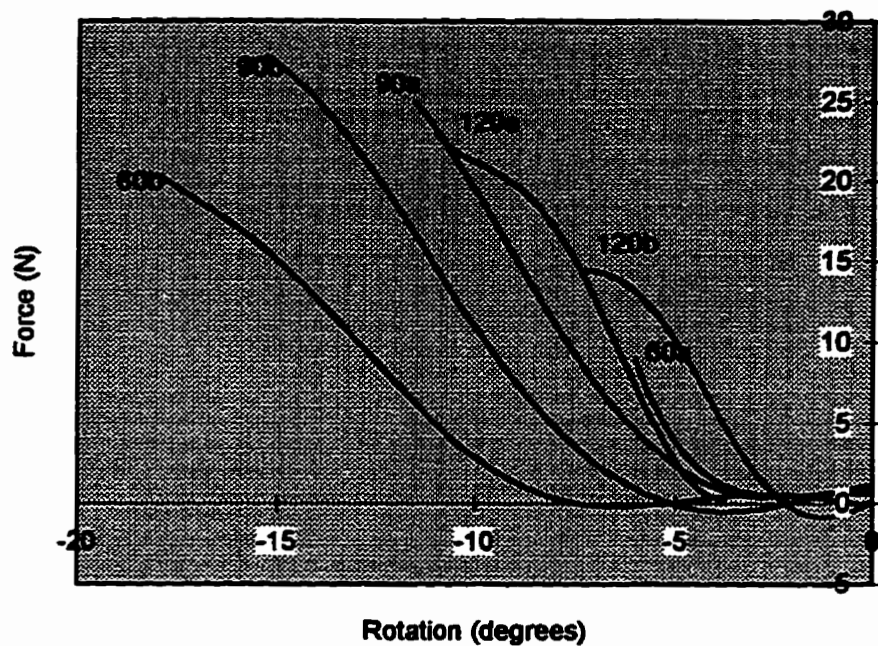

Figure 6.8: Non-Random (a) and Random (b) Force
Versus External Tibial Rotation Curves for Rabbit #4
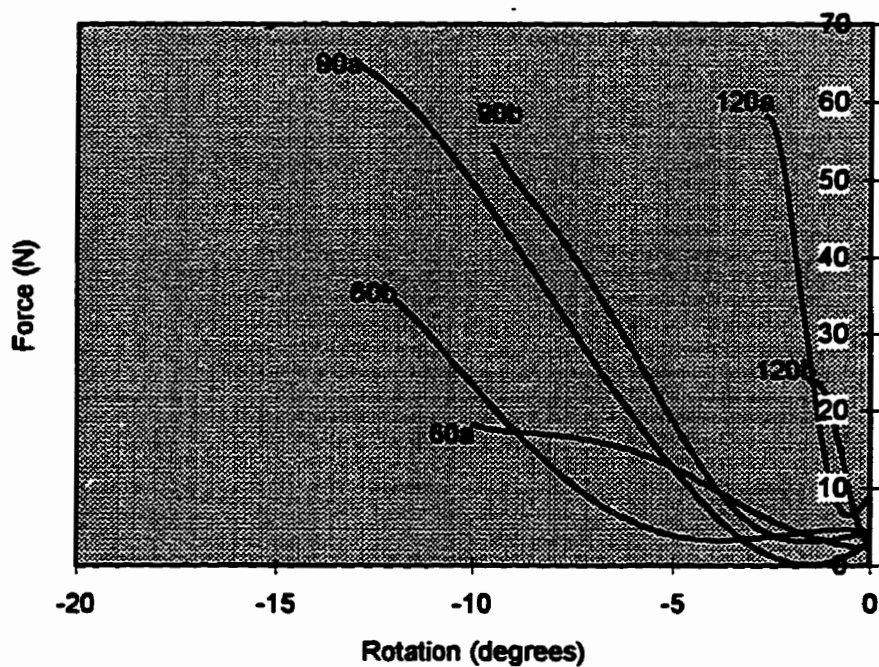
Figure 6.9: Non-Random (a) and Random (b) Force
Versus External Tibial Rotation Curves for Rabbit #5
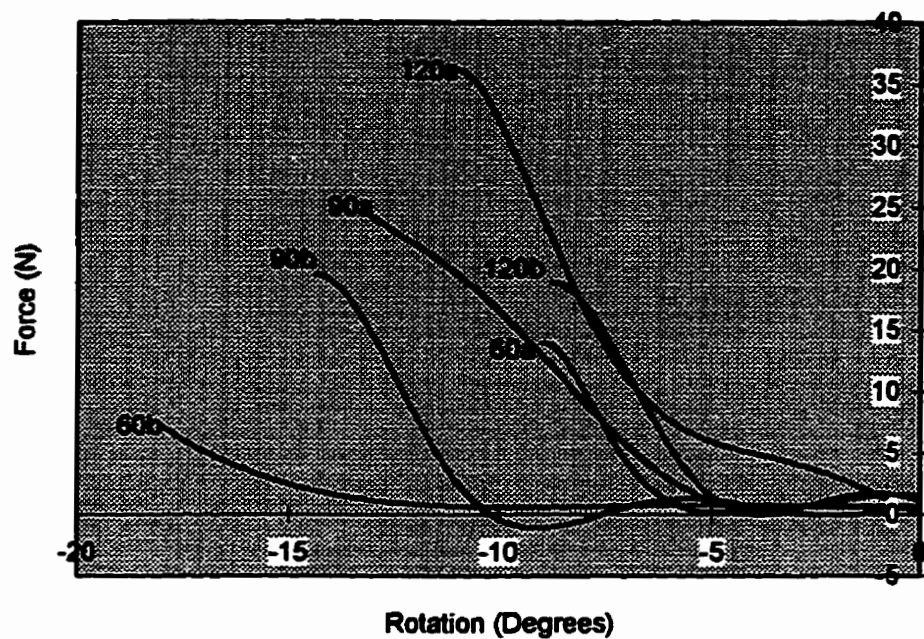
Rotation (Degrees)

Figure 6.10: Force Versus External Tibial Rotation
Curves for all Rabbits at 60 Degrees of Flexion

Rotation (degrees)
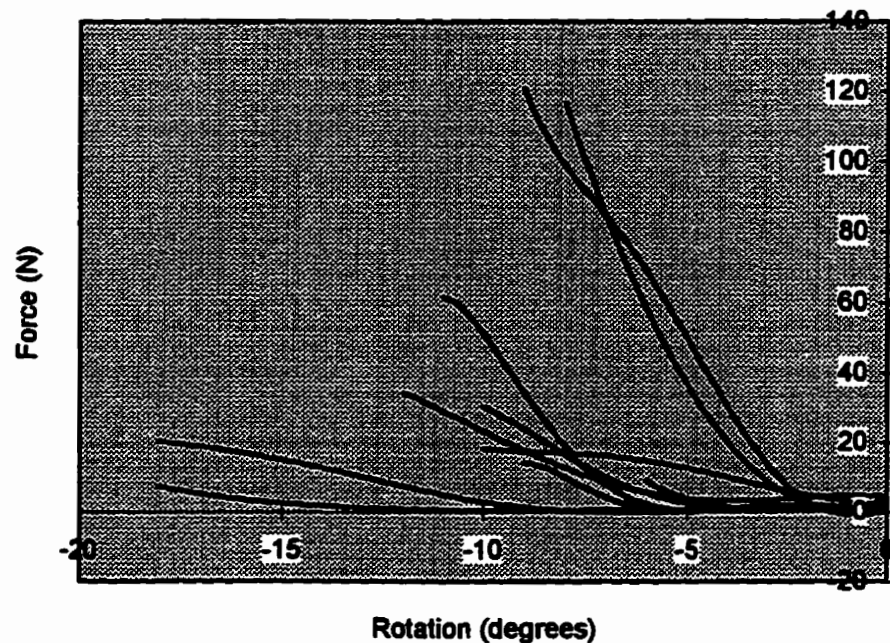
Figures 6.10–6.12 show the random and non-random force versus rotation curves for all rabbits at each joint angle.

The internal rotation tests were only performed on two rabbits, as a negligible change in force (less than 5 N) was measured on the MCL for all tests, at all joint angles. There was also an additional problem of the internal rotation causing the proximal end of the load cell to contact the muscles surrounding the femur, producing false force readings.

6.4 Discussion

The high R^2 values for all of the polynomial regressions show that both the load cell and goniometer are capable of producing consistent test results. This is supported by the consistency of the random and non-random test data at each joint angle, for each individual rabbit, as demonstrated in Figure 6.4.

Figures 6.5–6.9 indicate that the MCL is recruited earlier, and is stiffer, with increasing joint angle. This seems intuitively correct, based on the geometry of the knee joint. Figures 6.13a and b show a sketch of the femur-MCL-tibia complex at approximately full extension and full flexion respectively. The change in orientation of the MCL is caused by the femoral condyles posterior translation, relative to the tibial plateau, during flexion. By comparing the two figures it is evident that an equal amount of rotation will cause a greater relative change in the length of the MCL at full flexion versus full extension. Hence, at full flexion, the greater change in length versus rotation will cause the MCL to be loaded earlier and at a higher rate than at full extension.

In Figures 6.7 and 6.9 it is interesting to note that the series of random tests (labeled 60b, 90b, and 120b) display the pattern of earlier recruitment of the MCL with increasing joint angle. However, for the non-random series of tests the pattern is skewed. This could be caused by the difference between how the random and non-random data are collected. During the random testing the initial alignment of the foot will

Figure 6.11: Force Versus External Tibial Rotation
Curves for all Rabbits at 90 Degrees of Flexion
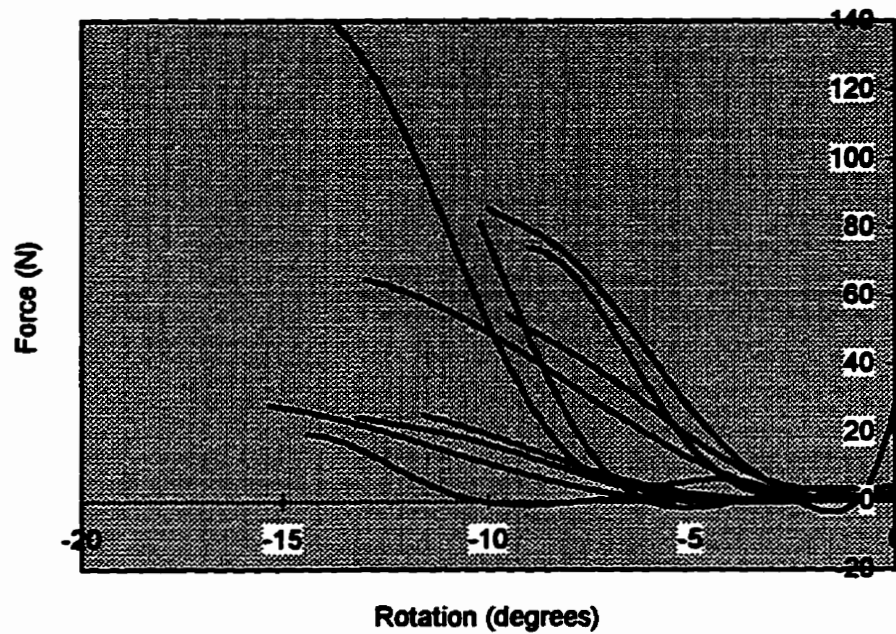
Rotation (degrees)

Figure 6.12: Force Versus External Tibial Rotation
Curves for all Rabbits at 120 Degrees of Flexion

Rotation (degrees)
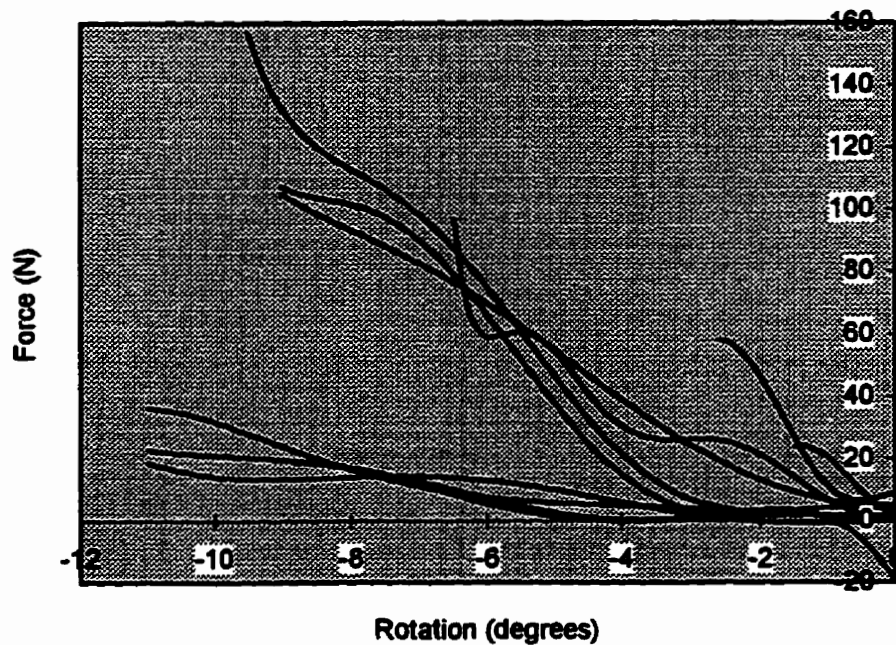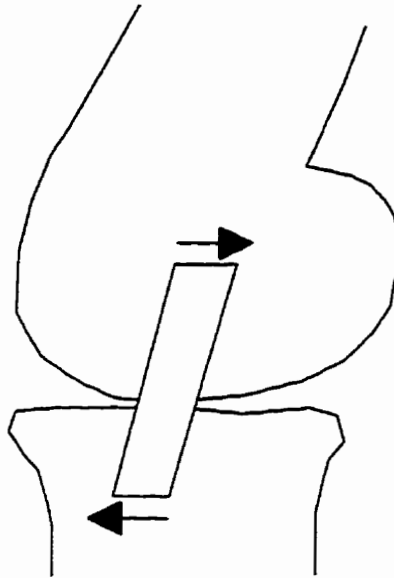
Figure 6.13a: At full extension the MCL is almost parallel to the axis of rotation and hence is extended slowly by tibial rotation.
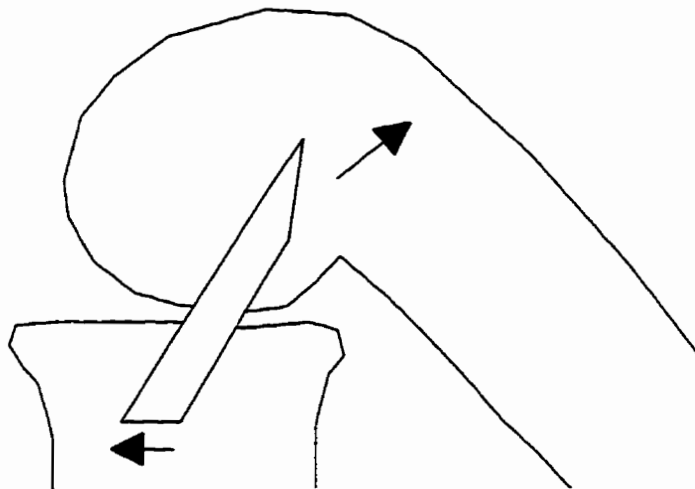
Figure 6.13b: At full flexion the MCL moves away from the axis of rotation and hence is extended quickly by tibial rotation.

be roughly consistent for all tests, and any gradual changes are averaged over tests performed at a variety of joint angles. For the non-random testing a series of rotations is performed at a single joint angle. This could allow one set of tests to be performed at a different initial rotation angle which would then shift the entire force versus rotation curve. To try and minimize this problem the initial tibial rotation data from the random and non-random testing were averaged to calculate the zero point at each joint angle. However, this problem could help to explain the discrepancies in the data shown in Figures 6.7 and 6.9.

The slopes of the load versus tibial rotation curves were calculated for some of the tests. These did help to confirm an increased stiffness in the MCL with increasing joint angle, but showed very little consistency from rabbit to rabbit at each joint angle. This, however, would be expected after examining Figures 6.10-6.12.

Figures 6.5-6.9 also show that the total amount of tibial rotation decreases with increasing joint angle. This indicates that the knee joint has a greater ability to accommodate external rotation at smaller joint angles. In addition, the maximum force on the MCL is lower at smaller joint angles. This must affect the loads carried by the other structures of the knee, as at all joint angles the force applied to the rabbit's foot was approximately equal. To have complete confidence in this result, however, a method of applying a consistent force to the foot, at each joint angle, will have to developed.

A further effect of joint angle on the loading of the MCL is the nature of the loading itself. At full extension the MCL is loaded approximately as shown in Figure 6.14a. The insertions are roughly parallel and the ligament experiences a uniform tensile load. At full flexion the insertions of the MCL are rotated relative to each other as shown in Figure 6.14b. This would appear to concentrate the load on the anterior fibers of the ligament, leaving the posterior portion unloaded. This raises several interesting questions: 1) is the ligament pre-stressed in such a way so as to maximize the average number of fibers loaded at each joint angle? 2) could this information be used to predict
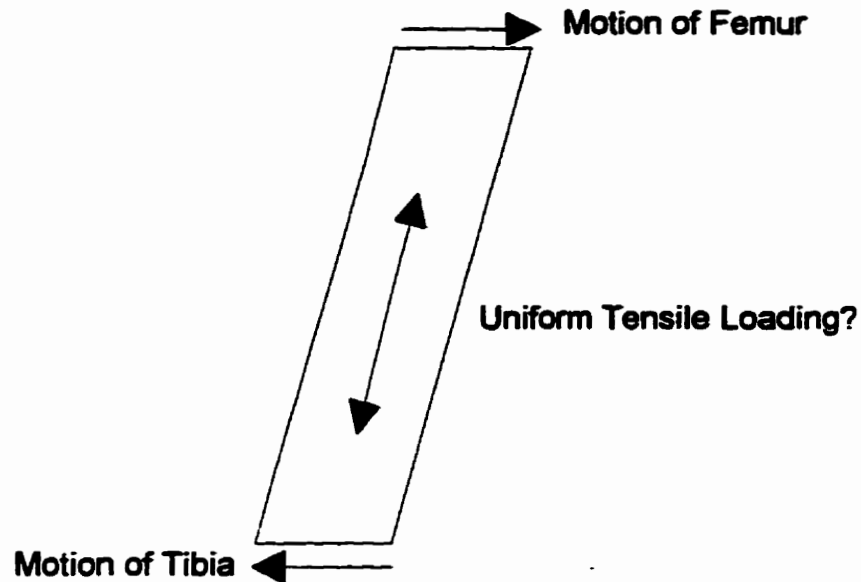
Figure 6.14a: At full extention the orientation of the femoral and tibial insertion of the MCL appears to allow the MCL to be uniformly loaded during tibial rotation.
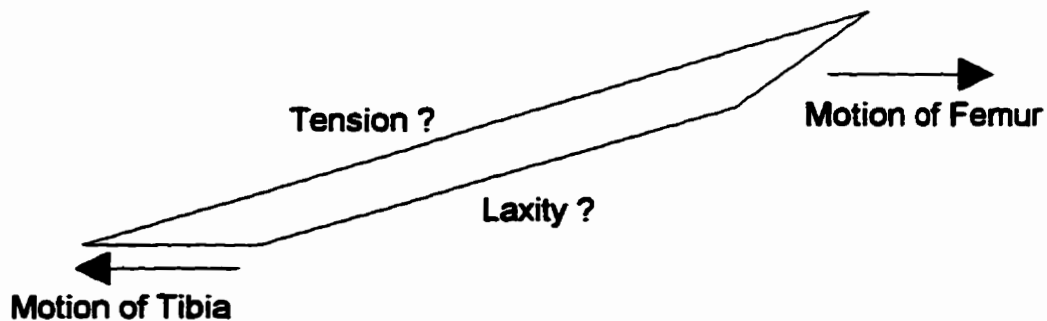
Figure 6.14b: At full flexion the geometery of the knee appears to change the orientation of the femoral and tibial insertion of the MCL sufficiently to increase the tension on the anterior side and unload the posterior side.

the location on the MCL where failure first occurs? and 3) does this cause the ultimate strength of the MCL to be affected by joint angle?

Figures 6.10-6.12 show that the force versus rotation curves, for all of the rabbits, at each joint angle are similar, but not identical. When an attempt was made to fit a single curve to all the force versus rotation data at each joint angle the R^2 value was only ~0.55. The most consistent data were generated at 90 degrees of flexion. This is also the joint angle with the highest average R^2 values, for the polynomial regressions performed on the raw force versus rotation data. This indicates that 90 degrees of flexion is the joint angle that shows the most promising for producing a reliable load versus tibial rotation curve. An additional advantage of investigating the loading of the MCL at 90 degrees is the more uniform loading of the entire ligament reported by Ahmed et al. (1987). More uniform loading should help to produce more consistent biological results across the entire MCL during loading versus healing studies.

The two key characteristics of the of the load versus rotation curves seem to be the slope, and the turning point (i.e. the rotation angle at which the load on the MCL begins to increase). The variation in the turning point of the loading curve, for each individual rabbit could be partly explained by the difficulty in defining a zero position for tibial rotation. The variation in the slope of the loading curves between the individual rabbits at a single joint angle appears to be related to the system used to control the joint angle during testing. External tibial rotation tends to cause the joint angle to increase. The curves with the steepest slope at each joint angle correspond to the tests in which the variation in flexion angle was constrained most effectively. Further testing with an improved joint angle control system should improve the consistency of the slope curves from rabbit to rabbit. Improved control of the joint angle may have the additional advantage of improving the consistency in the initial tibial rotational alignment. By concentrating further testing at 90 degrees of flexion, improving the joint angle control system, and improving the consistency of the initial tibial rotation, it should be possible to generate a much more consistent set of curves. However the surgeon was able to

predict the laxity of an individual rabbit's MCL, based on observations made during the attachment of the load cell. These prediction were later substantiated by the test data. These biological differences indicate that any force versus tibial rotation curve will always be subject to a reasonable amount of variability between animals.

The result that there is a negligible change in force on the MCL during internal tibial rotation seems to be intuitively correct from observations made during testing. Figure 6.15 shows a sketch of the femur-MCL-tibia complex. During external rotation the tibial insertion of the MCL moves from A to B, which increases the length of the MCL, and hence loads the ligament. Internal rotation however moves the tibial insertion from A to C, which shortens the length of the MCL, and hence generates no load on the ligament.

6.5 Conclusion

This pilot study has shown that both the load cell and the six degree of freedom goniometer are capable of producing consistent and valuable scientific data. The data show that external tibial rotation loads, and hence is constrained by, the MCL while internal rotation does not. The testing was able to show that the MCL is recruited earlier, and has a steeper loading curve, with increasing joint angle. In addition the testing shows that as the joint angle increases the total load carried by the MCL increases, and the joint laxity decreases; when a consistent, external rotational force, is applied to the foot.

There also appears to be a good potential for future testing using the goniometer, and a load versus tibial rotation curve, to apply a known load to the MCL. The results
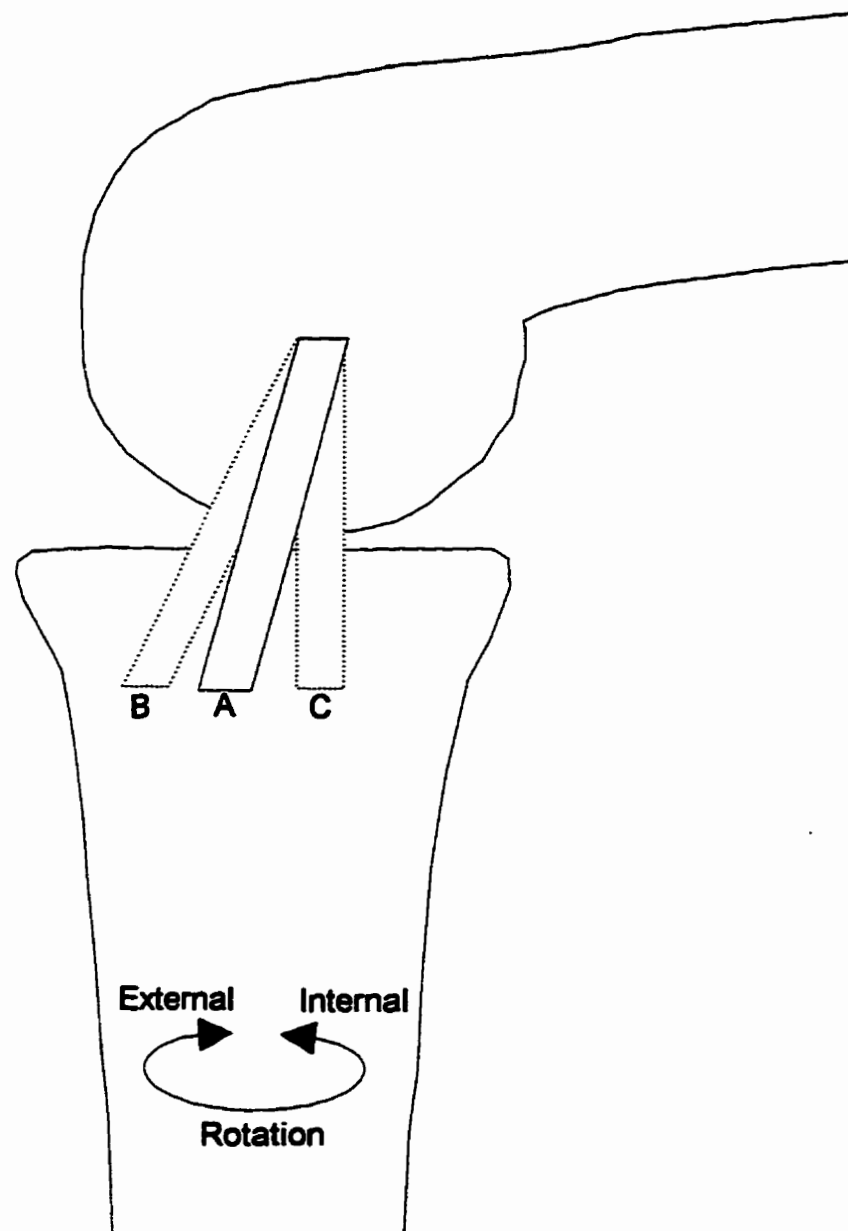
Figure 6.15: External rotation moves the tibial insertion of the MCL from A to B
which lengthens, and thus loads the ligament. Internal rotation moves the
tibial insertion from A to C shortening the MCL and thus creating no load on
the ligament.

indicates that the MCL is loaded in the most consistent fashion at 90 degrees of flexion. This will allow testing to begin into the effect on the healing, of applying a known load to a MCL injury model.

CHAPTER SEVEN: Conclusions and Recommendations

7.1 Introduction

The goniometer design process was very successful. The final design meets all of the demands listed in the design specifications, and most importantly shows distinct promise to be an effective tool for joint research. During the calibration of the goniometer, and the testing presented in Chapter Six, some areas for the possible improvement of the goniometer were noted. Having established the viability of determining the load on the MCL versus bone position, the possibilities for continued *in vivo* joint research are extremely broad.

7.2 Conclusions From Testing the Goniometer

7.2.1 Performance of the Goniometer

The goniometer should prove to be an effective research tool. Overall the potentiometers performed well within the goniometer, and as shown during calibration, were sufficiently accurate for this application.

The three rotary potentiometers worked smoothly together. One possible improvement would be half turn potentiometers (or even quarter turn units for potentiometers 2 and 3). With the full turn unit, a 10 v change represents a 360 degree rotation. With a half turn unit, 10 v would represent 180 degrees. Therefore, the half turn unit would produce a larger voltage change for the same rotation. This larger change would be easier for the data acquisition system detected, which would therefore improve the accuracy. At the time of construction, the full turn units used were the best available alternative.

The performance of the linear potentiometers is affected by the nature of the load placed upon them. When a force is applied parallel to the shaft of the potentiometer it moves smoothly under very small loads. However, when the direction of the force applied to the shaft is closer to the perpendicular, the motion can be rough and even jerky. These occasional, sudden movements of the linear potentiometers obviously compromise the goniometer's accuracy. Two potential solutions to this problem are: 1) redesign the frame connecting the linear potentiometers to include high quality linear bearings, or 2) change the goniometer design to an all rotary potentiometer unit, similar to that developed by Kinzel *et al.* (1972), which was discussed in Chapter One. Adding linear bearings should smooth out the operation of the linear potentiometers, but would increase the complexity of the frame and hence the weight of the goniometer. An all rotary potentiometer unit would operate more smoothly, but the rotary potentiometers weigh 4x as much as the linear potentiometers. This would also significantly increase the total weight of the goniometer. Hence any improvement on the functioning of the linear potentiometers, will have to be a compromise between weight and performance.

At some point the exact error in the final output from the goniometer will have to be determined. None of the other research discussed in Chapter One mentions any type of calibration beyond what has been done in Chapter Five. However, if the goniometer is to be relied upon to distinguish between increasingly smaller changes in bone alignment, then a more precise quantification of the error will be required. Quantifying the exact total error will be very difficult, as it is a combination of many different factors including: the potentiometers, deflection of the goniometer frame, movement of the bone pins, quality of the volt meter within the data acquisition system, and the measurement of the location of the bone pins relative to the bone coordinate system.

7.2.2 Performance of the Goniometer Mounting and Attachment System

There were no problems with the goniometer mounting and attachment system. Once attached, the goniometer stayed securely in place. It did not hinder the leg's

natural motion and allowed good access to most areas of the leg. The fact that the goniometer can be mounted either medially, or laterally, make it adaptable enough for most experiments.

The mounting jig was very effective for attaching the goniometer. The complex shape and slippery surface of the bone make inserting the bone pins very difficult without the aid of the mounting jig. Only a couple of practice rounds were necessary to gain the skill required to insert the bone pins quickly and accurately.

Before a set of experiments is undertaken it is important to check the adjustment of the potentiometers. All of the potentiometers, and in particular the linear potentiometers, can be adjusted relative to one another. It is important to attach the goniometers to a leg and check that the adjustment is such that the goniometer will not hinder the motion required for current testing. After adjusting the potentiometers, it is then important to ensure that all of the potentiometer shafts are at right angles. The entire series of tests described in Chapter Six were conducted without having to re adjust the goniometer, but it is foreseeable that a series of tests requiring severe joint positions could require readjustment.

7.2.3 Performance of the Data Processing System

The data processing system, including the data acquisition software, the transformation equations, and the computer program RHINO, worked well throughout the research. However, the series of calculations required to determine the location of the bone coordinate systems relative to the bone pin coordinate systems proved to be tedious. This process was greatly simplified by creating a spread sheet capable of doing almost all of the calculations. One possible improvement would be to integrate these equations into the computer program RHINO. Ideally, the user would enter two input files into the computer: the relative location of the points on the bones, and the output data from the potentiometers. The computer would then perform all the calculations and

transformations, and output the relative location of the bones, in terms of the ISB coordinate axes.

The ideal data processing system would produce a real time display of the bone's relative location in terms of the ISB coordinate axis. This would allow researchers to know where the bones were during testing. The problem with creating this type of set-up is that it is very difficult to determine the exact bone to bone pin transformations until the leg has been removed from the rabbit and cleaned of flesh. This problem could be solved by using an average location for the bone pins based on previous tests. It has been found that, with the mounting jig, the bone pins are inserted in a fairly consistent fashion. Therefore, a set of average bone to bone pin transformations could be used to provide a reasonably accurate estimation of bone location during testing. This system would not give the precise relative location of the bones, but it could increase the range of tests that the goniometer is capable of performing.

7.3 Conclusions From Experimental Results

The goniometer generally functioned very well during the testing described in Chapter Six. The load cell, however, presented some problems, that can be avoided by following the correct procedure. The calibration matrix for the load cell is not constant and hence it should be recalculated immediately before, or after, each test. It is also important to use the correct method of zeroing the load cell before each test. The load cell should be zeroed with the distal end attached to the tibia and the proximal end free. In addition, once the load cell is attached to the tibia it should be allowed to equalize in temperature with the rabbit before it is zeroed. Do not zero the load cell with both ends attached to the rabbit, either before or after the bone chip has been removed. Zeroing the load cell with the proximal end attached to the freed bone chip will eliminate the pre-load. Attaching the proximal end of the load cell to the tibia before the bone chip is removed can generate very high loads within the load cell, due to the curvature of the

bone. These loads can be in excess of 100 N. Obviously taking this large pre-load as the zero point will skew all of the test data. It is also helpful to place a small amount of methyl methacylate under each end of the load cell and then attach it to the tibia before the bone chip is removed. Once the glue is dry the load cell can be removed, and the bone chip cut free. This will create customized mounting pads for the load cell, which will ensure: 1) the secure connection of the load cell, and 2) that the orientation of the tibial insertion, of the MCL, is kept constant.

Care should also be taken when inserting the bone pins. It is important to check that the V-notch in the guide tube is centred on the bone before the pilot hole is drilled. If a hole is not drilled squarely through the bone it is possible to move the guide tube to a new location at the tibial end of the mounting jig. Additional mounting locations could also be made at femoral end of the mounting jig. However, changing the location of the guide tube will mean that the mounting bracket on the goniometer will also have to be moved. If this is not done carefully it could change the orientation of the goniometer relative to the leg. Hence, it is desirable to gain sufficient skill in mounting the goniometer to get it right the first time. The best method for this is described in Chapter Three.

A final problem area is determining the position of zero tibial rotation. This is a gray area, as no precise method exists by which this point can be defined. For the testing described in Chapter Six the zero point was defined as the average starting point for both the random and non-random testing performed at each joint angle. All efforts were made to start each test with the foot in its neutral position. Thus the zero point used to generate the final results is the average of 12 attempts to locate the foot's neutral position, at each joint angle. It is obviously very important to locate the zero point properly, as any shift in the zero point will shift the entire force versus rotation curve. One potential improvement for the testing procedure would be some sort of a pin system to hold the femur at a constant orientation, at each joint angle. This could help improve the consistency of the starting point for each test. Figure 7.1 shows one method by
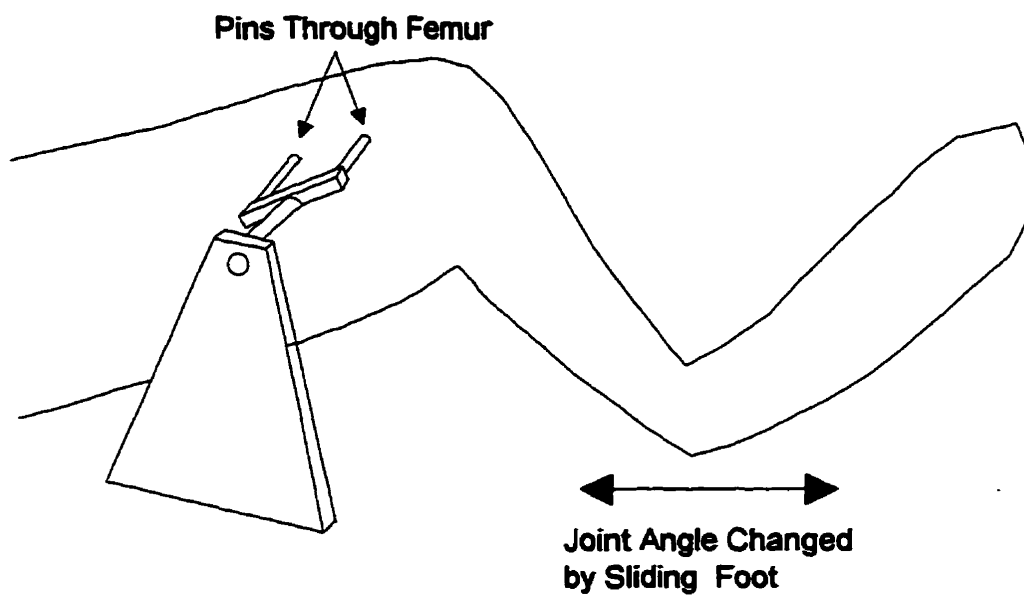
Figure 7.1: A frame, similar to the one shown above, could be used to hold the femur during testing, and thus improve the consistency of the legs alignment. Note: the pins should pass through the femur and be supported by the frame on both sides.

which the femur could be held for testing. Two pins would be drilled through the femur (these could also be used for attaching the goniometer). These pins would be attached to a single point on each side which would then be connected to a frame using some type of bearing. This would allow the femur to rotate as the foot is slide back and forth to change the joint angle. Maintaining a constant orientation of the femur should improve the consistency of the foot's location at the start of each test.

One final area of concern could be the output from the program RHINO. This will usually indicate the tibial rotation at the start of each test is approximately 15 degrees. This does not mean that the tibia has already been rotated by this amount before each test begins. This only indicates that the coordinate system imposed upon the tibia is rotated by this amount relative to the femoral coordinate system. Because the coordinate systems are imposed upon the bones, their zero point is not necessarily going to be the same as the joints natural zero point. These values should however be changed to reflect the natural zero point of the joint as described above.

7.4 Recommendations

1) The three rotary potentiometers worked very well and should continue to be used unless appropriate half or quarter turn units can be located.

2) If the linear potentiometers remain in the goniometer then they should be coupled with linear bearings to smooth out their operation. If the linear potentiometers are to be removed then they should be replaced with rotary potentiometers, in a design similar to that of Kinzel *et al.* (1972).

3) If long term testing is to be carried out using the goniometer then a removable attachment system will be required. The system developed by Korvick *et al.* (1994) looks promising.

4) The computer program RHINO could be improved by including the equations to calculate the bone to bone pin transformations.

5) To have complete confidence in the goniometer results, the exact error in the final output of the goniometer will have to be estimated accurately.

6) A possible improvement for future tibial rotation testing is the system shown in Figure 7.1. A set of pins could be inserted into the femur to maintain it at a constant alignment during testing. This system should increase the consistency of the joint alignment during testing.

7.5 Future Directions for the Goniometer

The goniometer has the potential to become a very valuable research tool as demonstrated by the testing described in Chapter Six. Some of the potential future applications of the goniometer include 1) examining the differences in how the MCL is loaded at different joint angles, 2) determining the effect of varying degrees of loading on the healing of the MCL, and 3) developing load cells for the other ligaments within the knee. The results in Chapter Six indicate that the loading on the MCL varies with joint angle. This is the type of exciting information that future *in vivo* research can expand upon. The potential to produce a load versus tibial rotation curve is also very promising. This would allow researchers to put a known load on the MCL by using the goniometer to monitor both tibial rotation and flexion angle. The success of the *in vivo* testing of the MCL, also indicates that *in vivo* testing of the other ligaments in the knee is possible.

The combination of the goniometer and the load cell for the MCL creates a powerful research system. By using these two tools together a large amount of new data about the loading of the MCL has been generated. Very little research has ever been done into the in vivo loading environment of the MCL. The simple fact that external

tibial rotation loads the MCL is a new development. The additional information into the nature of the loading of the MCL, and the possibility of generating a load versus tibial rotation curve, are further testimony to the power of this combination of research tools. By following the suggestions and recommendations made in this chapter, there is a wide range of exciting applications for the goniometer as a biomechanical research tool.

REFERENCES

Anderson DR, Weiss JA, Takai S, Ohland KJ, Woo SL-Y. Healing of the Medial Collateral Ligament Following a Triad Injury: A Biomechanical and Histological Study of the Knee in Rabbits. *J. Orthop Res.*, 1992, 10(4):485-494.

Ahmed AM, Hyder A, Burke DL, Chan KH. *In Vitro* Ligament Tension Pattern in the Flexed Knee in Passive Loading. *J. Orthop Res.*, 1987, 5:217-230.

Beasley. Theory and Design for Mechanical Measurements.

Engle CP, Noguchi M, Ohland KJ, Shelley FJ, Woo SL-Y. Healing of the Rabbit Medial Collateral Ligament Following an O'Donoghue Triad Injury: Effects of Anterior Cruciate Ligament Reconstruction. *J. Orthop Res.*, 1994, 12:357-364.

Evans M, Gardner TN, Kyberd PJ. Externally Fixated Fractures-A Non-Invasive Method of Measuring Linear and Rotational Fracture Displacements, for the Six Degrees of Freedom. Unpublished.

Goodfellow JW, O'Connor JJ. The Mechanics of the Knee and Prosthesis Design. *Journal of Bone and Joint Surgery*, 1978, 60-B(3):358-369.

Grood ES, Suntay WJ. A Joint Coordinate System for the Clinical Description of Three-Dimensional Motions: Application to the Knee. *J. Biomech. Engng*, 1983, 105:136-144.

Hartenberg RS, Denavit J. *Kinematic Synthesis of Linkages*. New York, N.Y., McGraw-Hill, 1964.

Hiromichi F, Mabuchi K, Woo SL-Y, Livesay GA, Arai S, Tsukamoto Y. The Use of Robotics Technology to Study Human Joint Kinematics: A New Methodology. *J. Biomech. Engng*, 1993, 115:211-217.

Hollis JM, Takai S, Adams DJ, Horbie S, Woo SL-Y. The Effects of Knee Motion and External Loading on the Length of the Anterior Cruciate Ligament (ACL): A Kinematic Study. *J. Biomech. Engng*, 1991, 113:208-214.

Huizer A, Day RL. Engineering Drawing with Computer Applications, Department of Civil Engineering, University of Calgary, 1988.

ISB Standardization and Terminology Committee. Recommendations for Standardization in the Reporting of Kinematic Data. Sept. 1, 1994.

Kinzel GL, Hall AS, Hillberry BM. Measurement of Total Motion Between Two Body Segments-I: Analytical Development. *J. Biomechanics*, 1971, 5:93-105.

Kinzel GL, Hillberry BM, Hall AS, Van Sickle DC, Harvey WM. Measurement of Total Motion Between Two Body Segments-II: Description of Application. *J. Biomechanics*, 1971, 5:283-293.

Korvick DL, Pijanowski GJ, Schaefer DJ. Three-Dimensional Kinematics of the Intact and Cranial Cruciate Ligament-Deficient Stifle of Dogs. *J. Biomechanics*, 1994, 27(1):77-87.

Lam TC, Frank CB, Shrive NG. Calibration Characteristics of a Video Dimension Analyzer (VDA) System. *J. Biomechanics*, 1992, 25(10):1227-1231.

Marans HJ, Jackson RW, Glossop ND, Young MC. Anterior Cruciate Ligament
Insufficiency: A Dynamic Three-Dimensional Motion Analysis. *Am J. Sports Med.*, 1989, 17(3):325-332.

Norrie D. *ENME 551: Instructors Notes*, Department of Mechanical Engineering,
University of Calgary, 1994.

O'Connor JJ, Goodfellow JW, Bradley JA. Quadriceps Forces Following Meniscal
Knee Arthroplasty-an in Vitro Study. *34th Annual Meeting, Orthopedic Research Society*, Feb. 1-4, 1988, Atlanta, Georgia.

Pahl G, Beitz W: *Engineering Design: A Systematic Approach*; in Wallace K (ed.):
The Design Council, Springer-Verlag, London, UK, 1988.

Pearcy MJ, Hindle RJ. New Method for the Non-Invasive Three-Dimensional
Measurement of Human Back Movement. *Clinical Biomechanics*, 1989, 4:73-79.

Schildt H. *Teach Yourself C 2 ed.*, Berkeley, California, Osborne McGraw Hill, 1994.

Sommer HJ, Miller NR. A Technique for the Calibration of Instrumented Spatial
Linkages used for Biomechanical Kinematic Measurements. *J. Biomechanics*, 1981, 14:91-98.

Suntay WJ, Grood ES, Hefzy MS, Butler DJ, Noyes FR. Error Analysis of a System
for Measuring Three-Dimensional Joint Motion. *J. Biomech. Engng*, 1983, 105:127-135.

Swokowski EW: *Calculus with Analytic Geometry, 2nd Alternate Edition*, Boston, PWS-Kent, 1988.

Townsend MA, Izak M, Jackson RW. Total Motion Knee Goniometry. *J. Biomechanics*, 1977, 10:183-193.

Van De Graaff KM. Human Anatomy 2ed., Dubuque, Iowa, Wm. C. Brown, College Division, 1988.

Weiss JA, Woo SL-Y, Ohland KJ, Horibe S, Newton PO. Evaluation of a New Injury Model to Study Medial Collateral Ligament Healing: Primary Repair Versus Nonoperative Treatment. *J. Orthop Res.*, 1991, 9(4):516-528.

Wu G, Ladin Z. The Kinematometer-An Integrated Kinematic Sensor for Kinesiological Measurements. *J. Biomech. Engng*, 1993, 115:53-61.

Appendix A: Preliminary Transformation Equations.

This set of transformation equations is based on the work of Evans *et al.* (1994). This style of transformation equations is derived in three steps based on the geometry of the goniometer. The first step is to calculate a set of equations which reflect how the geometry of the goniometer will affect the orientation of the potentiometers. The second step is to calculate how the goniometer's remote location from the knee will affect the magnitude of the displacements measured by the goniometer. The final step is to combine the first two sets of equations into a single set of transformation equations. For this project this style of transformation equations was never derived beyond step one. The increasing complexity, compared to the system of transformation equations described in Chapter Four, made the equations too cumbersome. This initial set of equations was, however, useful in calibrating the goniometer.

For the calibration of the goniometer described in Chapter Five the change in position of the pointer attached to the goniometer (see Figure 5.4) was calculated using the following equations. It is not recommended to attempt to use these equations to translate the output data of the goniometer. They are only included for completeness as they were used during the calibration of the goniometer. The purpose of the equations is to account for the additional displacement of the pointer caused by the rotational potentiometers. The magnitude of these additional displacements is proportional to the length of the pointer, and the offset of the shaft of R3 compared to R1 and R2. R1, R2, and R3 represent rotational potentiometers one, two, and three, and L1, L2, and L3 represent linear potentiometers one, two, and three.

$$\Delta X = \Delta L1 + \Delta X_R$$
$$\Delta Y = \Delta L2 + \Delta Y_R$$
$$\Delta Z = \Delta L3 + \Delta Z_R$$

where: $\Delta X, \Delta Y,$ and ΔZ = The change in the x, y, and z location of the pointer.

$\Delta L1, \Delta L2,$ and $\Delta L3$ = The change in linear potentiometers one, two, and three.

$\Delta X_R, \Delta Y_R,$ and ΔZ_R = The change in x, y, and z caused by the rotary potentiometers.

$\Delta X_R =$ $K((\cos((7.855-R2_f)(C_{R2}))*\sin((4.900-R3_f)(C_{R3}))) -$
$(\cos((7.855-R2_i)(C_{R2}))*\sin((4.900-R3_i)(C_{R3})))) +$
$(S(\cos((4.900-R3_f)(C_{R3})) - \cos((4.900-R3_i)(C_{R3}))))$

$\Delta Y_R =$ $K((\cos((7.855-R2_i)(C_{R2}))*\cos((4.900-R3_i)(C_{R3}))) -$
$(\cos((7.855-R2_f)(C_{R2}))*\cos((4.900-R3_f)(C_{R3})))) +$
$(S(\sin((4.900-R3_f)(C_{R3})) - \sin((4.900-R3_i)(C_{R3}))))$

$\Delta Z_R =$ $K(\sin((R2_f-7.855)(C_{R2})) - \sin((R3_i-7.855)(C_{R2})))$

where: K = The length of the pointer.

S = The distance from the shaft if R3, to the shaft of R1, along the shaft of R2.

C_{R2}, C_{R3} = The calibration factors of R2 and R3.

$R2_i, R2_f$ = The initial and final value of R2 in volts.

$R3_i, R3_f$ = The initial and final value of R3 in volts.

As mentioned in Chapter Five a set of right hand coordinate axes is attached to the base shown in Figure 5.4. The x-axis is parallel to L1, the y-axis parallel to L2, and the z-axis is parallel to L3.

Appendix B: Source code for RHINO

```c
/*  program to translate goniometer data into rotations  */
/*  about the ISB coordinate axes  */
/*  by Daren Tremaine  */

#include "math.h"
#include "stdio.h"
#define PMAX 3100


main()
{

        void rotate();
        void gon();

/*  utilities  */
        void mult4();
        void writ_data();
        int read_data();

        float frot[4][4], unit[4][4];

/*  Enter the femoral bone pin to bone transformation matrix Here!!!  */

        frot[0][0]=.99949;     frot[0][1]=.006767; frot[0][2]=.03112;  frot[0][3]=0;
        frot[1][0]=-.001313; frot[1][1]=.98509;   frot[1][2]=-.17203; frot[1][3]=0;
        frot[2][0]=-.03182;  frot[2][1]=.1719;    frot[2][2]=.9846;   frot[2][3]=0;
        frot[3][0]=0;          frot[3][1]=0;          frot[3][2]=0;        frot[3][3]=1;

/*  Enter the unit vectors representing the tibial coordinate system  */
/*  interms of the tibial bone pin doordinate system Here!!!  */

        unit[0][0]=0; unit[0][1]=.96262;  unit[0][2]=-.007647; unit[0][3]=-.27073;
        unit[1][0]=0; unit[1][1]=.02134;  unit[1][2]=.99863;   unit[1][3]=.04765;
        unit[2][0]=0; unit[2][1]=.27;     unit[2][2]=-.05164;  unit[2][3]=.96146;
        unit[3][0]=1; unit[3][1]=1;       unit[3][2]=1;        unit[3][3]=1;

/*  gon is used to multiply tunit by goniometer rotations, then frot, for each time  */

        gon (unit,frot);
}
```

```
/*_____ function rotate _____*/

void rotate (za,ya,xa,rot)
float za,ya,xa;
float rot[4][4];
{

        void mult4();
        float dott[4][4];
        float z[4][4], y[4][4], x[4][4];
        int i, j;
        za = 3.1416/180*za;
        ya = 3.1416/180*ya;
        xa = 3.1416/180*xa;

        z[0][0]= cos(za);  z[0][1]= -sin(za);  z[0][2]= 0;  z[0][3]=0;
        z[1][0]= sin(za);  z[1][1]= cos(za);   z[1][2]= 0;  z[1][3]=0;
        z[2][0]= 0;        z[2][1]= 0;         z[2][2]= 1;  z[2][3]=0;
        z[3][0]= 0;        z[3][1]= 0;         z[3][2]= 0;  z[3][3]=1;

        y[0][0]= cos(ya);  y[0][1]= 0;   y[0][2]= sin(ya);  y[0][3]=0;
        y[1][0]= 0;        y[1][1]= 1;   y[1][2]= 0;        y[1][3]=0;
        y[2][0]= -sin(ya); y[2][1]= 0;   y[2][2]= cos(ya);  y[2][3]=0;
        y[3][0]= 0;        y[3][1]= 0;   y[3][2]= 0;        y[3][3]=1;

        x[0][0]= 1;   x[0][1]= 0;        x[0][2]= 0;        x[0][3]=0;
        x[1][0]= 0;   x[1][1]= cos(xa);  x[1][2]= -sin(xa); x[1][3]=0;
        x[2][0]= 0;   x[2][1]= sin(xa);  x[2][2]= cos(xa);  x[2][3]=0;
        x[3][0]= 0;   x[3][1]= 0;        x[3][2]= 0;        x[3][3]=1;

        mult4 (x,y,dott);
        for (i=0;i<=3;i++)
                for (j=0;j<=3;j++) rot[i][j] = dott[i][j];

        mult4 (z,rot,dott);
        for (i=0;i<=3;i++)
                for (j=0;j<=3;j++) rot[i][j] = dott[i][j];

}
```

```
/*_____ function gon _____*/

void gon(tibu,femur)
float tibu[4][4], femur[4][4];
{
        void rotate();
        void mult4();
        void writ_data();
        int read_data();
        static float raw[PMAX][3];
        float cooked[PMAX][3];
        float xx, yy, zz;
        float giga[4][4], dot[4][4];
        float f[2], alpha, beta, gamma;
        int nump=0, j, i, k;
        char name[15];

        /* get file name */
        printf ("\nPlease enter the name of your raw data file: ");
        scanf ("%14s", name);

        /* call read_data to open file */
        nump = read_data(raw, name);

        for (k=0;k<=nump-1;k++)
        {

                zz = raw[k][0];
                xx = raw[k][1];
                yy = raw[k][2];

                rotate(zz,yy,xx,giga);

                mult4 (giga,tibu,dot);
                for (i=0;i<=3;i++)
                        for (j=0;j<=3;j++) giga[i][j] = dot[i][j];

                mult4 (femur,giga,dot);
                for (i=0;i<=3;i++)
                        for (j=0;j<=3;j++) giga[i][j] = dot[i][j];
```

```
                    /*  use direction cosines to get angles from giga  */

                    f[0] = giga[1][2]/(sqrt((giga[1][2]*giga[1][2])+(giga[0][2]*giga[0][2])));
                    f[1] = -
giga[0][2]/(sqrt((giga[1][2]*giga[1][2])+(giga[0][2]*giga[0][2])));

                    alpha = asin(f[1]);
                    beta = acos(giga[2][2]);
                    beta = -(beta-(3.1416/2));
                    gamma = asin((f[0]*giga[0][3]) + (f[1]*giga[1][3]));

                    alpha = 180/3.1416*alpha;
                    beta = 180/3.1416*beta;
                    gamma = 180/3.1416*gamma;


                    for (i=0;i<=2;i++)
                            cooked[k][i] = 0;

                    cooked[k][0] = alpha;
                    cooked[k][1] = beta;
                    cooked[k][2] = gamma;

            }

            writ_data (cooked, nump);
}
/*_____ function to read data in from file _____*/

int read_data(raww, namee)
float raww[PMAX][3];
char namee[];
{

            int i, j, fsv, nump=0;
            FILE *fp;
            fp=fopen(namee,"r");

            for (i=0;i<=PMAX-1;i++)
            {
                    for (j=0;j<=2;j++)
                    {
                            fsv = fscanf (fp, "%f",&raww[i][j]);
```

```
                        if (fsv==EOF) break;
                }
                if (fsv==EOF) break;
                nump++;
        }
        fclose (fp);
        return nump;
}
```

/*_____ function to write output data _____*/

```
void writ_data (cook, num)
float cook[PMAX][3];
int num;
{
        int i, j;
        char fname[15];
        FILE *fpp;

        printf ("\nPlease enter the name of your output file: ");
        scanf ("%14s", fname);
        fpp = fopen (fname, "w");

        for (i=0; i<=num-1; i++)
        {
                for (j=0; j<=2; j++)
                {
                        fprintf (fpp,"%9.4f",cook[i][j]);
                }
                fprintf (fpp,"\n");
        }
        fclose (fpp);
}
```

/*_____ funtion mult4 _____*/

```
void mult4(xx,yy,ddot)
float xx[4][4], yy[4][4], ddot[4][4];
{
        int i, j, k;

        for (i=0; i<=3; i++)
                for (j=0; j<=3; j++) ddot[i][j]=0;
```

```
for (i=0; i<=3; i++)
{
        for (j=0; j<=3; j++)
        {
                for (k=0; k<=3; k++)
                {
                        ddot [i][j] += xx[i][k] * yy[k][j];
                }
        }
}
```